ADVANCING PHOTOSYNTHETICALLY DRIVEN MICROBIAL CO-COCULTURES FOR SUSTAINABLE BIOPRODUCTION

By

Lisa Yun

A DISSERTATION

Submitted to
Michigan State University
in partial fulfillment of the requirements
for the degree of

Biochemistry and Molecular Biology – Doctor of Philosophy

2024

ABSTRACT

As carbon emissions reach record levels annually, the allure of cyanobacterial biotechnology becomes increasingly desirable. The technology to receive a variety of renewable chemicals in exchange for CO_2 and light is available, but many advancements are required before it can be commercially applicable. The focus of this dissertation is to improve the potential of cyanobacterial co-culture systems for photosynthetic bioproduction. The co-culture approach offers a degree of flexibility in output products that is difficult to match using other metabolic engineering approaches, and the overall sucrose production from cyanobacteria is promising relative to other carbohydrate feedstocks. Nonetheless, at this time, any attempts to scale cyanobacterial co-culture to industrially relevant volumes are likely to encounter various challenges. My dissertation research focused on two potential weaknesses of cyanobacterial co-culture. In Chapter 2, I describe my research to maximize the output of sucrose by modulating the cultivation conditions for sucrose-secreting strains of *Synechococcus elongatus* PCC 7942. Maximization of heterotrophic yield in co-culture is directly linked to the amount of fixed carbon that can be supplied by the cyanobacterial partner, and I interrogated a number of different illumination conditions and methods for providing inorganic CO_2 to cyanobacterial strains. In Chapter 3, I describe my efforts to rationally design co-cultures for higher resilience and productivity through engineering in a system for physical attachment between the heterotroph and cyanobacterial partner. Specifically, I expanded upon prior work on a cyanobacterial surface display system with the long-range goal of installing extracellular binding domains on the surface of *S. elongatus* that could be used to mediate direct physical attachments with other proteins displayed on the surface of an engineered heterotrophic partner. Finally, in Chapter 4, I review the outcomes and conclusions of my research program and reflect upon both my experience and future prospects for the topic areas central to my dissertation.

ACKNOWLEDGEMENTS

I would like to take this opportunity to express my appreciation and gratitude to everyone who has supported me up to and throughout my PhD. There are too many to name individually, and for that, I am blessed.

First and foremost, I would like to thank my advisor, Dr. Daniel C. Ducat, who has been unfailingly supportive academically and personally. Your compassion has been the foundation of my PhD experience, which I could not have weathered the storms of without. Your patience has not gone without notice, and I am deeply grateful for it. Thank you for guiding me through the twists and turns of my research, and helping me see the possibilities where I could not before. I am forever grateful for your mentorship and belief in me.

The members of the Ducat Lab have been a joy to work with. I thank postdoctoral researchers Dr. María Santos-Merino and Dr. Jonathan Sakkos for sharing their wealth of knowledge with me. Dr. Sreeahila Retnadhas, Dr. Amit Singh, and Dr. Joshua MacCready have answered my questions, large and small. Graduate students Rees Rillema, M.S. and Emmanuel Kokarakis, M.S. have been comrades-in-arms; there is nothing like the solidarity that comes from working together in the odd hours of the day.

Heartfelt appreciation is extended to my committee members: Dr. Robert Hausinger, Dr. Michaela TerAvest, Dr. Gregory Bonito, and Dr. Beronda Montgomery. Your guidance and support have been instrumental in my academic growth, and I deeply value your contributions to my success. Special thanks to Dr. TerAvest for introducing me to Michigan State University during my undergraduate years.

I am grateful to the departments and programs at the University that have fostered my academic and personal development. In the Department of Biochemistry and Molecular Biology, Dr. David Arnosti fosters an environment of safety and support for all graduate students. I am grateful for the opportunity you provided me to begin an outreach program with the Greer Outreach Center; it was a learning and healing experience to introduce young minds to the joys of science. Your compassion and curiosity remind me to keep mine alive. The Plant Biotechnology for Health and Sustainability training program, helmed by Dr. Robert Last and Dr. Jyothi Kumar, afforded me the opportunity to undertake an industrial internship. Jessica Lawrence, who supports both the department and program, helped me navigate the intricacies of the University. There are many to thank within the collaborative environment of the Plant Research Laboratory as well. The

leadership and staff that kept us steadfast during the uncertainty of the pandemic, the camaraderie of my friends and colleagues in other labs kept me going, and the invisible work performed by Linda Danhof, Melissa Borrusch, Heather Sharick, Adam Goetschy, and Jacob Hicks kept the place running smoothly. I am very lucky to have worked here.

Graduate school is not for the faint of heart, and I am forever grateful for those who have supported me personally through the highs and lows of the journey. To the many graduate students who I have befriended in my time: it has been an honor to have walked through the crucible with you. Deanna, I value your perspective; thank you for helping keep my head on straight. Diego, I am deeply grateful for your companionship, and I look forward to its continuance. Hannah, Bianca, Aiko, and Emily – thank you for your friendship and support; some hard things can be made easier with good company. I sincerely wish you all the best in your individual pursuits. I would also like to thank those who have supported me before and during graduate school. Ron – you began my scientific career, and I could not be where I am today without you. I am forever indebted to your wisdom, kindness, and mentorship; thank you for believing me. Alec, you are my biggest hype man. Thank you for your love and energy; it will always inspire me. Frankie, Virginia, Nicole, Angela, and Erick – thank you for being present in my times of need and for your loving support. Mr. McCullough, thank you for providing a space to explore my academic aptitude; your classes were the framework of critical thinking and writing that so much of my life today rests upon. You encouraged me to reach beyond what I thought was possible – of what I thought I was capable – and I would not have pursued a PhD or met the wonderful people in my journey without you igniting the first spark. Finally, I would like to acknowledge my families, found and inherited. I am grateful to my parents for raising me with the qualities of hard work and perseverance, which have served as a foundation in my every endeavor. I give boundless thanks to my partner, Cort, for support and solidarity in the pursuits of love, life, and one of our biggest achievements thus far. And finally, to Cassy, the kitten I adopted a month before the pandemic who has welcomed me home after every long experiment and has kept me company throughout every all-nighter.

TABLE OF CONTENTS

CHAPTER 1:

INTRODUCTION TO SUCROSE IN CYANOBACTERIA

This chapter was adapted from text originally published in:

Santos-Merino, M., Yun, L. and Ducat, D.C. (2023) Cyanobacteria as cell factories for the photosynthetic production of sucrose. *Front. Microbiol*, 14, p.1126032.

Sucrose in cyanobacteria

Cyanobacteria are ancient photosynthetic prokaryotes that date back as far as 3.5 billion years ago, and have since significantly diversified, enabling them to colonize terrestrial, aquatic, and benthic habitats (Gaysina et al., 2019). Through the development of mechanisms to withstand harsh conditions including UV rays, salt concentrations, temperatures, and irradiances, cyanobacteria have not only survived but thrived in the face of the unique challenges of each habitat, becoming arguably one of the most important and abundant taxa in existence (Rosic, 2021; Crockford et al., 2023). Their remarkable success led to the Great Oxidation Event approximately 2.5 billion years ago, causing a rapid and significant rise in atmospheric oxygen levels (Crockford et al., 2023). This shift from a reduced to an oxidized state transformed biogeochemical cycles, facilitating in the evolution of complex oxygen-dependent life (Pathak et al., 2021).

Apart from adapting to ecological niches, cyanobacteria have also forged various symbiotic relationships with prokaryotes and eukaryotes. By providing essential services like carbon and nitrogen fixation, cyanobacteria are key players with associated and neighboring organisms, even becoming so integral that they are the origin of chloroplasts (Falcón et al., 2010). The advantageous combination of oxygenic photosynthesis and ecological, biological, bioproductive, and symbiotic flexibility position cyanobacteria as attractive candidates for diverse biotechnological applications. Efforts are underway to enhance the synthesis of primary and secondary metabolites (*e.g.*, carbohydrates, fatty acids, amino acids, antioxidants, phycobiliproteins, bioplastics, biofuels), and to explore their use as a carbon source for bioproductive heterotrophs in engineered microbial communities (Zhang et al., 2021; Bakku and Rakwal, 2022; Kariyazono et al., 2022). Moreover, there is interest in employing cyanobacteria for tasks like wastewater treatment, carbon capture and sequestration, enhancing agricultural output, and more (Kroumov et al., 2021; Singh et al., 2021; Bakku and Rakwal, 2022). Despite their ancestral lineage, cyanobacteria remain a subject of ongoing study as they continue to contribute to the planetary ecosystem and a growing circular economy.

Biological applications of sucrose

Like in all photosynthetic organisms, sucrose [α-d-glucopyranosyl (1→2) β-d-fructofuranoside] metabolism is an integral component connected to central carbon metabolism in cyanobacteria. Sucrose is utilized by a number of cyanobacterial species as a protective metabolite, or so called “compatible solute,” that can be hyperaccumulated in the cell without ill effect. Unlike

other compatible solutes like glucoglycerol (GG) or glycine betaine (GB), sucrose is believed to have direct interactions with macromolecules (Hagemann, 2011). The arrangement of hydroxyl groups allow disaccharides like sucrose and trehalose to interact with the water-soluble portion of glycerolipids, enabling them to replace some water in the membrane hydration shells without altering the water structure, as observed with other compatible solutes (Potts et al., 2005; Hagemann, 2011). It is hypothesized that sucrose was the first compatible solute to emerge in cyanobacteria; the capacity for sucrose biosynthesis appears to be widespread, as shown by the presence of at least one sucrose-synthesizing enzyme found in nearly all known genome sequences (Blank, 2013).

Studies on numerous cyanobacterial strains have revealed at least 60 species accumulate sucrose under high-salt conditions, with a consistent pattern of strains that accumulate sucrose as the primary compatible solute to have relatively low salt tolerances (*e.g.*, *Synechoccocus elongatus* PCC 7942, *Microcystis aeruginosa* PCC 7806, etc) (Hagemann, 2011). While sucrose is considered to be somewhat weak as an osmoprotectant, conferring protection up to only 50-100% that of seawater salinity in such strains, it has been found in minor or transient portions of the total compatible solute pool in halotolerant species that accumulate other solutes as primary osmoprotectants (Reed and Stewart, 1985; Hagemann, 2011). In these cases, sucrose can be utilized as a secondary osmoprotectant to enhance salt tolerance, and is employed in combating general stresses such as desiccation, heat, and cold. In addition to its accumulation in the cytoplasm for osmotic stress, sucrose also concentrates in the extracellular matrix during drought conditions to create a protective glass-like shell to reduce water loss and molecular diffusion in preparation for dormancy (Waditee-Sirisattha and Kageyama, 2022). Elevated temperatures induce sucrose biosynthesis, likely due to its superior ability to bolster membrane stability at higher temperatures compared to GG or GB (Hincha and Hagemann, 2004). Sucrose biosynthesis is crucial for cyanobacterial acclimation to environmental stresses, but its biological utility extends beyond the producing organism.

As a sugar, sucrose is a versatile carbon source for cells that cannot produce their own. For example, *Anabaena* sp. PCC 7120, a diazotrophic filamentous cyanobacterium partitions photosynthetic vegetative cells apart from heterocysts performing oxygen-sensitive nitrogen fixation, all while facilitating carbon and nitrogen exchange between the two cell types (Herrero et al., 2016). Cyanobacteria also supply sucrose and other sugars to heterotrophs, fostering

multitrophic associations. A notable example are cyanolichens, which are composite organisms consisting of obligately symbiotic fungi and cyanobacteria (Rikkinen, 2015). While each lichen is unique in species composition, generally, the cyanobacteria provide fixed carbon and/or nitrogen to the fungi in exchange for minerals, nutrients, secondary metabolites, CO_2, and protection from the external environment (Rikkinen, 2017). An engineered lichen consisting of a sucrose-secreting *S. elongatus* PCC 7942 co-cultured with either *Rhodotorula glutinis* or *Cryptococcus curvatus* exhibited enhanced lipid yields from cyanobacteria compared to when they were grown axenically, indicating that the benefits of co-cultivation exceed the nutritional value of mutualistic exchange (Li et al., 2017). Likewise, symbiotic relationships with plants, mosses, diatoms, and prokaryotes have been identified, further highlighting the adaptable and advantageous nature of cyanobacterial primary production (Rai et al., 2002).

Enzymes responsible for sucrose biosynthesis

The primary enzymes involved in sucrose biosynthesis are sucrose phosphate synthase (SPS) and sucrose phosphate phosphatase (SPP). Briefly, the glucosyltransferase domain (GTD) of SPS transfers a glycosyl group from NDP-glucose to fructose-6-phosphate to produce sucrose-6-phosphate; SPP then hydrolyzes the intermediate product with the phosphohydrolyase domain (PHD) to create sucrose. Cyanobacterial SPS is the rate-limiting enzyme in sucrose biosynthesis; it most often accepts UDP-glucose, but can also utilize GDP-, TDP-, and ADP-glucose, a substrate flexibility not observed in plant SPS proteins (Porchia and Salerno, 1996; Curatti et al., 1998). Additionally, there are two types of cyanobacterial SPS proteins: one which contains only the SPS domain, and another that is fused with a SPP domain (Santos-Merino et al., 2023). The SPS-SPP fusion proteins are similar to those found in plants, but cyanobacterial SPP domains often exhibit little or no SPP activity, raising questions regarding their function in such instances (Lunn et al., 2000). It is hypothesized that the SPP domain may bind to newly formed sucrose-6-phosphate from SPS for metabolite channeling (Fieulaine et al., 2005) or function as a regulator (Albi et al., 2016). Unidomainal SPS is the most prevalent form, and SPP is encoded separately to perform the reversible dephosphorylation of sucrose-6-phosphate (Santos-Merino et al., 2023). Despite sharing little sequence similarity, these proteins exhibit three conserved motifs in the active site of the phosphohydrolase domain, which are structurally consistent across photosynthetic organisms (Fieulaine et al., 2005). However, some cyanobacterial strains code for the bidomainal SPS and no separate SPP; in these cases, SPP-like proteins, which do not contain the motifs that define SPP,

may be utilized instead (Santos-Merino et al., 2023). Interestingly, they are also they are present in strains with SPP, prompting inquiries to their role in such cases (Santos-Merino et al., 2023). There is significantly less research regarding the function of cyanobacterial SPP-like proteins relative to SPP, and their functions remain unknown.

Cyanobacterial sucrose catabolism pathways

While sucrose is required to acclimate to environmental stresses, it must be degraded once it is no longer required to mitigate carbon and energy loss (Baran et al., 2017). Invertases are a large and diverse group of sucrose-cleaving enzymes, and are the most broadly encoded pathway for cyanobacterial sucrose degradation in which this enzyme performs the irreversible hydrolysis of sucrose into glucose and fructose. In some cases, such as in *Synechocystis* sp. PCC 6803, invertases are the only enzyme responsible for *in vivo* degradation of sucrose (Kirsch et al., 2018). Only alkaline/neutral invertases (A/N-invertases; preferring pH of 6.5 to 8) are found in cyanobacteria, and they have a high specificity for the α-1,2-glycosidic linkage of sucrose (Vargas et al., 2003; Vargas and Salerno, 2010; Xie et al., 2016; Wan et al., 2018; Liang et al., 2020). In the filamentous *Anabaena* sp. PCC 7120, A/N-invertases are encoded by the genes *invA* and *invB* (Page-Sharp et al., 1999; Vargas et al., 2003). InvA regulates the carbon flux from vegetative cells to heterocysts (López-Igual et al., 2010), whereas InvB coordinates sucrose and glycogen metabolism exclusively in heterocysts (Vargas et al., 2011).

Sucrose synthase (SuS) is a glucosyltransferase that performs the reversible hydrolysis of sucrose to U/ADP-glucose and fructose, though it is believed to primarily degrade sucrose *in vivo* (Porchia and Salerno, 1996; Curatti et al., 2002). SuS is not ubiquitous among cyanobacteria, and is most often found in heterocyst-forming strains, though there have been reports of its presence in unicellular cyanobacteria (Koleman et al., 2012; Hagemann, 2013). It appears to play a vital role in nitrogen fixation by controlling the flux of carbon from vegetative cells and possibly producing precursors for cell wall synthesis (Porchia et al., 1999; Curatti et al., 2000, 2002, 2006, 2008; Cumino et al., 2007). In addition to regulating sucrose degradation, SuS may also be involved in recycling sucrose into glycogen as it as it generates U/ADP-glucose that can be reverted to glucose-1-phosphate by UDP-glucose pyrophosphorylase (UGP), a building block of glycogen (Cumino et al., 2002, 2007).

The rarest sucrose-degrading enzyme in cyanobacteria is amylosucrase, a glucosyltransferase that hydrolyzes the glycosidic bond to produce glucose and fructose; the

resulting glucose is then used to form maltooligosaccharides (Potocki de Montalk et al., 2000). It was first discovered in *Synechococcus* sp. PCC 7002 in the same transcriptional unit with *sps*, *spp*, and fructokinase (Perez-Cenci and Salerno, 2014).

Engineering cyanobacteria to produce sucrose

Innovations in biotechnology have taken advantage of aquatic photosynthetic organisms' ability to create valuable products (*e.g.*, lipids, antioxidants, pigments) to cope with environmental stressors (Chen et al., 2017; Morone et al., 2019). As a bioproduct naturally synthesized at high levels by some species of cyanobacteria in response to salt stress, sucrose has garnered attention for its potential as an alternative carbohydrate feedstock for higher-value goods (Hays and Ducat, 2015; Zhang et al., 2021). Sucrose generated by cyanobacteria could offer a number of advantages relative to plant-based feedstock crops, including potentially higher photosynthetic efficiencies and reduced requirements for potable water or arable land. Here, I review recent strategies employed to make cyanobacterial bioproduction of sucrose more productive and affordable.

Engineered heterologous transporters for sucrose export

As discussed above, cyanobacteria can accumulate osmoprotectants up to hundreds-of-millimolar concentrations when exposed to hypersaline conditions (*e.g.*, sucrose, trehalose, GG) (Hagemann, 2011; Klähn and Hagemann, 2011). For instance, under moderate salt stress (200 mM NaCl), the common freshwater model cyanobacterium *S. elongatus* PCC 7942 accumulates nearly 300 mM intracellular sucrose, representing a significant portion of the cell biomass (Suzuki et al., 2010). Although this degree of metabolite production presents an industrial and agricultural opportunity, cytosolic volume constrains how much sucrose can be accumulated: the costs associated with cyanobacterial cell recovery, lysis, and processing would likely exceed the economic value of the commodity products contained in the cytosol (Prabha et al., 2022). Therefore, secreting sugars into the supernatant for collection has been proposed as a more financially viable strategy. For this purpose, cyanobacteria have been engineered to express heterologous transporters capable of exporting lactate and hexoses (Niederholtmeyer et al., 2010; Angermayr et al., 2012).

Similarly, *S. elongatus* PCC 7942 was originally engineered to export sucrose by expressing sucrose permease (*cscB*) from *Escherichia coli* ATCC 700927 (Ducat et al., 2012), and multiple cyanobacterial species have since been similarly modified by different research teams (Table 1.1). In its native host, CscB is a sucrose/proton symporter that typically operates by

utilizing the free energy of the proton gradient to import both molecules (Vadyvaloo et al., 2006). By contrast, during periods of cyanobacterial sucrose synthesis, internal sucrose concentrations greatly exceed external levels causing reversal of chemical gradients and driving sucrose export through CscB instead. CscB-expressing, sucrose-exporting *S. elongatus* PCC 7942 strains can secrete up to 80% of photosynthetically fixed carbon as sucrose, diverting these resources away from the accumulation of cellular biomass (Ducat et al., 2012). Although efforts to scale-up cyanobacterial sucrose production have not yet come to fruition (*e.g.*, Proterro; Aikens and Turner, 2013), it has been estimated that such cyanobacterial strains have the potential to produce comparable amounts of sugar to traditional plant-based carbohydrate feedstocks. Realizing the promise of cyanobacterial sucrose is likely to require efforts to address problems of cyanobacterial/microalgal cultivation (beyond the scope of my dissertation, but see (Su et al., 2017; Khan et al., 2018) as well as strategies to maximize bioproduction rates.

Increasing metabolic flux to sucrose pathways

Published strategies for improving rates of cyanobacterial sucrose productivity generally fall into two related strategies: increasing carbon flux towards the synthesis of sucrose through the upregulation of relevant biosynthetic activities, or by reducing the loss of carbon to competing pathways or sucrose reuptake. Perhaps the most straightforward approach for improving sucrose titers has been the overexpression of genes related to sucrose biosynthesis. Several studies have now found that flux leading to sucrose production can be most impacted by increasing the activity of SPS (Du et al., 2013; Duan et al., 2016; Lin et al., 2020a), which is largely intuitive given that this enzyme catalyzes a commitment step to sucrose biosynthesis. Significant increases in sucrose production can be found in strains overexpressing SPS, even without allowing for sucrose export. First reported in *Synechocystis* sp. PCC 6803, a strain engineered to overexpress its native SPS (SPS_{6803}) accumulated nearly twice as much intracellular sucrose than its wild-type counterpart (Du et al., 2013). Likewise, when the native SPS in *S. elongatus* PCC 7942 was overexpressed, internal sucrose concentrations were 93% higher than in wild-type (Duan et al., 2016). In addition, pairing SPS overexpression with sucrose export further increases total sucrose yields. When SPS_{7942} and CscB were co-overexpressed in *S. elongatus* PCC 7942, there was a 74% increase in sucrose compared to the CscB-only strain (Table 1.1) (Duan et al., 2016), yet the nature of the SPS homolog that is overexpressed can strongly influence the degree to which sucrose production is improved. SPS_{7942} is bidomainal and bifunctional (*i.e.*, possessing active GTD and PHD domains),

in contrast to SPS_{6803} which is also bidomainal, but has a non-functional PHD domain and is regulated distinctly from SPS_{7942} (Curatti et al., 1998; Lunn et al., 1999; Gibson et al., 2002). However, the partial functionality of SPS_{6803} does not mean it is less effective, as heterologous co-overexpression of SPS_{6803} and CscB in *S. elongatus* PCC 7942 increases sucrose production relative to overexpression of the native SPS_{7942} (Abramson et al., 2016; Dan et al., 2022) (Table 1.1). It is curious that SPS_{6803} is a more effective enzyme for rerouting carbon flux towards sucrose bioproduction, given that it lacks a functional SPP domain (*S. elongatus* PCC 7942 encodes other endogenous SPP proteins in the examples above), so it is possible that this observation is related either to the manner in which salt-ions can regulate the function of some SPS domains (Liang et al., 2020), or to other unknown functions for SPP and/or SPP-like domains other than sucrose-6-phosphate phosphatase activity.

While the overexpression of SPS has yielded substantial improvements, this strategy has not been equally successful with other proteins in the sucrose biosynthetic pathway. Overexpression of SPP from *Synechocystis* sp. PCC 6803 (SPP_{6803}) either had no effect on, or decreased sucrose productivity in *S. elongatus* PCC 7942 or *Synechococcus elongatus* UTEX 2973 (Du et al., 2013; Lin et al., 2020a). Similarly, overexpression of UGP, the protein producing UDP-glucose as a substrate for SPS, led to less sucrose secretion (Ducat et al., 2012; Du et al., 2013). Only when these three enzymes were overexpressed simultaneously (*i.e.*, SPS_{6803}, SPP_{6803}, and UGP) were sucrose levels increased in comparison with SPS_{6803}-only strain, albeit marginally (Du et al., 2013) (Table 1.1).

Another successful approach for improving the flux of carbon to sucrose biosynthesis is to accelerate the rate of the upstream carbon supply from the Calvin Benson cycle. Multiple strains of cyanobacteria have been engineered to secrete sucrose through the heterologous expression of *cscB*, but the highest yields to-date have been obtained from strains with a more rapid metabolism and higher light tolerance relative to classic laboratory models (Table 1.1). *S. elongatus* UTEX 2973 is a recently re-characterized species that is 99.99% identical to *S. elongatus* PCC 7942, but has a doubling time of ~2 h (compared to ~5–9 h for *S. elongatus* PCC 7942), and is more tolerant of high-light and high temperature conditions (Kratz and Meyers, 1955; Yu et al., 2015; Adomako et al., 2022). Expression of *cscB* in *S. elongatus* UTEX 2973 led to the development of strains with relatively high sucrose productivities (Song et al., 2016; Lin et al., 2020a). A high sucrose titer was originally reported in such strains when exposed to 150 mM NaCl, reaching approximately

80 mg L^{-1} (Song et al., 2016). Lin et al. also created a *S. elongatus* UTEX 2973-*cscB* strain, and observed an even greater sucrose titer at 8 g L^{-1} at 150 mM NaCl, averaging out to 1.9 g L^{-1} day^{-1}, over 2-fold higher than the productivities of *S. elongatus* PCC 7942, representing the highest sucrose titer published thus far (Lin et al., 2020a), and illustrating the potential benefits of utilizing fast-growing strains that can reach higher densities.

Somewhat surprisingly, activation of the sucrose export pathway itself has been reported to increase the overall photosynthetic flux in some cyanobacterial strains. In *S. elongatus* PCC 7942, when sucrose synthesis pathways are placed under inducible promoters, a variety of enhancements in features related to photosynthesis have been reported in the hours following activation of the pathway (Ducat et al., 2012; Abramson et al., 2016; Santos-Merino et al., 2021; Singh et al., 2022). The quantum efficiency of photosystem II, rate of oxygen evolution, relative rate of electron flux through the photosynthetic electron transport chain, oxidation status of the photosystem, and rate of carbon fixation are all increased (Ducat et al., 2012; Abramson et al., 2016; Santos-Merino et al., 2021). The latter observation is correlated with an increase in Rubisco abundance that was revealed by proteomic analysis >24 h following induction of sucrose export, and a concomitant increase in carboxysome number (Singh et al., 2022). While the mechanisms underlying these changes in photosynthetic performance are not well understood, it has been hypothesized that they arise from a relaxation in "sink limitations" on photosynthesis that can occur when the downstream consumption of products of photosynthesis (*e.g.*, ATP, NADPH, Calvin Benson cycle outputs) is insufficient to keep up with the supply (Santos-Merino et al., 2021). Stated differently, when carbon fixation is not the rate-limiting step of cell metabolism (*e.g.*, under enriched CO_2 atmospheres commonly used in laboratory conditions), the expression of a heterologous pathway may act as an additional "sink" and bypass downstream limitations of cell growth and division. While this remains a speculative possibility, the relaxation of acceptor-side limitations on photosystem I suggests that sucrose secretion pathways (or other heterologous metabolic sinks) may utilize "excess" light energy that might otherwise be lost to photosynthetic inefficiencies under certain conditions (Abramson et al., 2016; Santos-Merino et al., 2021). Uncovering the mechanisms underlying the photosynthetic phenotypes coupled to sucrose export might allow even greater improvements in photosynthesis and/or sucrose bioproduction.

Reducing metabolic flux to competing pathways

The alternative strategy to boost sucrose production is to improve the pool of sucrose or

sucrose precursors by reducing flux to pathways that compete with sucrose biosynthesis for either substrates or total carbon pools. A straightforward example is to eliminate the dominant route for sucrose breakdown, such as the Inv proteins that are a dominant route of sucrose hydrolysis in many cyanobacterial models. In a recent report, inactivation of the *Synechocystis* sp. PCC 6803 invertase increased accumulated sucrose by 10-fold in both salt and salt-free conditions (Kirsch et al., 2018). These results were of higher magnitude, but similar trajectory to reports in other cyanobacteria, such as in sucrose-exporting *S. elongatus* PCC 7942 where a Δ*invA* background exhibited a 15% increase in extracellular sucrose (Ducat et al., 2012).

Glycogen is a storage molecule of cyanobacteria that is a significant alternative carbon sink, yet inhibiting glycogen synthesis has yielded variable results on sucrose secretion. For example, knockout of the two glycogen synthase genes (*glgA-I* and *glgA-II*) of *Synechococcus* sp. PCC 7002 led to an accumulation of three times more sucrose than wild-type under hypersaline conditions (Xu et al., 2013) (Table 1.1). However, when another glycogen synthesis gene, ADP-glucose pyrophosphorylase (*glgC*), was downregulated in sucrose-secreting *S. elongatus* PCC 7942, there was only a minor or insignificant increase in sucrose (Qiao et al., 2018). GlgP is responsible for hydrolyzing glycosidic bonds in glycogen to release glucose-1-phosphate, so it was theorized that increasing GlgP activity would mobilize carbon from the glycogen pool for sucrose biosynthesis. However, when GlgP was overexpressed in sucrose-secreting strains of *S. elongatus* PCC 7942 with its native SPS, there were no changes in glycogen content and a decrease in sucrose was observed (Ducat et al., 2012; Dan et al., 2022), while heterologous overexpression of both SPS_{6803} and GlgP reduced glycogen content while increasing sucrose secretion by 2.4-fold (Dan et al., 2022). The variability in sucrose production of glycogen-deficient strains might be related to the pleiotropic cellular deficiencies of these strains, including reduced growth, reduced O_2 evolution and consumption, abnormal pigmentation, and light sensitivity (Suzuki et al., 2010; Ducat et al., 2012; Gründel et al., 2012; Xu et al., 2013; Qiao et al., 2018). These phenotypes align with a potential broader role for glycogen beyond carbon storage, which may include buffering against periods of starvation, oxygenic stress, high-light stress, salt stress, or diurnal/transient changes in light availability (Luan et al., 2019; Shinde et al., 2020). Given the increasing recognition of regulatory roles of glycogen, more nuanced strategies may be required to regulate the flux of carbon towards glycogen synthesis in order to reliably improve sucrose bioproduction (Huang et al., 2016).

Table 1.1. Productivity and genetic modifications of sucrose-producing cyanobacteria.

Species[a]	**Over-expressed**[b*]	**Down-regulated**[c]	**Maximum Productivity**[d]	**Salt for SPS**	**Sucrose promoter**	**Ref.**
*Syn*7002	–	–	24 mol 10^{-17} cells[e]	1 M NaCl	–	(Xu et al., 2013)
	–	*glgA-I, glgA-II*	71 mol 10^{-17} cells[e]	1 M NaCl	–	
*Syn*6803	*cscB, sps*$_{6803}$, *spp*$_{6803}$, *ugp*	*ggpS, ggtCD*	0.69 mg L^{-1} h^{-1} [f]	400 mM NaCl	P_{petE}	(Du et al., 2013)
	sps$_{6803}$, *spp*$_{6803}$, *ugp*	*ggpS*	3.1 mg L^{-1} h^{-1} [f]	600 mM NaCl	P_{petE}	
*Syn*7942	*cscB*	–	3.6 mg gDW^{-1} h^{-1}	200 mM NaCl	–	(Duan et al., 2016)
	cscB, sps$_{7942}$	–	6.2 mg gDW^{-1} h^{-1}	200 mM NaCl	P_{trc}	
*Syn*7942	–	Synpcc7942_1125	5.9 mg L^{-1} OD_{730}^{-1} h^{-1} [e]	150 mM NaCl	–	(Qiao et al., 2019)
	–	*manR* (Synpcc7942_1404)	6.7 mg L^{-1} OD_{730}^{-1} h^{-1} [e]	150 mM NaCl	–	
*Syn*7942	*cscB, sps*$_{6803}$	–	5.6 mg L^{-1} h^{-1}	–	P_{cpcB}	(Dan et al., 2022)
	cscB, sps$_{6803}$, *glgP*	–	6.9 mg L^{-1} h^{-1}	–	P_{cpcB}	
*Syn*7942	*cscB, sps*$_{7942}$, *glgC*	–	8 mg L^{-1} h^{-1}	150 mM NaCl	P_{trc}	(Qiao et al., 2018)
*Syn*6803	*cscB, sps*$_{6803}$, *spp*$_{6803}$, *ugp*	*invA* (sll0626), *ggpS, ggtCD*	10.1 mg L^{-1} h^{-1}	200 mM NaCl	P_{petE}	(Kirsch et al., 2018)
*Syn*7942	*cscB*	–	10.4 mg L^{-1} h^{-1}	150 mM NaCl	–	(Löwe et al., 2017)

Table 1.1. (cont'd)

*Syn*7942	*cscB*	–	11 mg L^{-1} h^{-1}	150 mM NaCl	–	(Li et al., 2022)
*Syn*7942	*cscB*	–	16.7 mg L^{-1} h^{-1}	106 mM NaCl	–	(Hays et al., 2017)
*Syn*7942	*cscB, sps*$_{6803}$	–	30 mg L^{-1} h^{-1}	–	P_{trc}	(Abramson et al., 2016)
*Syn*2973	*cscB*	–	24.6 mg L^{-1} h^{-1}	150 mM KCl	–	(Song et al., 2016)
			35.5 mg L^{-1} h^{-1}	150 mM NaCl	–	
*Syn*7942	*cscB*	–	28 mg L^{-1} h^{-1}	150 mM NaCl	–	(Ducat et al., 2012)
	cscB	*invA, glgC*	36.1 mg L^{-1} h^{-1}	150 mM NaCl	–	
*Syn*2973	*cscB, sps*$_{6803,}$ *spp*$_{6803}$	–	22.2 mg L^{-1} h^{-1}	–	P_{trc1O}, induced	(Lin et al., 2020a)
			47.2 mg L^{-1} h^{-1}	–	P_{trc1O}, uninduced	
	cscB	–	79.2 mg L^{-1} h^{-1}	150 mM NaCl	–	

[a] *Syn7002*, *Synechococcus* sp. PCC 7002; *Syn7942*, *Synechococcus elongatus* PCC 7942; *Syn2973*, *Synechococcus elongatus* UTEX 2973; *Syn6803*, *Synechocystis* sp. PCC 6803.
[b] *cscB*, sucrose permease; *glgC*, ADP-glucose pyrophosphorylase; *glgP*, glycogen phosphorylase; *rpaB*, regulator of phycobilisome-associated B; *spp*, sucrose phosphate phosphatase; *sps*, sucrose phosphate synthase; *ugp*, UDP-glucose pyrophosphorylase.
[c] Genes are down-regulated or knocked out; *ggpS*, glucosylglycerol (GG)-phosphate synthase; *ggtCD*, GG transport system permease; *glgA-I/glgA-II*, glycogen synthase; *glgC*, ADP-glucose pyrophosphorylase; *invA*, invertase; *manR* (Synpcc7942_1404), manganese sensing response regulator; Synpcc7942_1125, histidine-containing phosphotransfer.
[d] Approximated extracellular sucrose values provided or calculated from titers.
[e] Calculated from intracellular sucrose yields.
[f] Calculated from intracellular and extracellular (total) sucrose yields.
* Subscripts in *sps* and *spp* indicate the strain that it comes from (*i.e.*, 6803 for *Synechocystis* sp. PCC 6803).

In some cyanobacterial strains that utilize other compatible solutes as the dominant metabolite for osmoprotection, synthesis of these osmoprotectant compounds may compete with sucrose biosynthesis. One example is GG, the primary solute utilized by moderately halotolerant cyanobacteria such as *Synechocystis* sp. PCC 6803 (Klähn and Hagemann, 2011). When GG-phosphate synthase (GgpS), the enzyme that generates a GG precursor, was knocked out in *Synechocystis* sp. PCC 6803, increased flux of carbon to sucrose production was reported (Du et al., 2013; Kirsch et al., 2019; Thiel et al., 2019) (Table 1.1). A GgpS variant incapable of generating GG under salt stress instead accumulated nearly 1.5-fold more sucrose than wild-type cells, although these engineered strains also exhibited growth inhibition at lower salt concentrations that would be well tolerated by wild-type lines (Du et al., 2013).

While most studies focus on restricting metabolic pathways that consume cellular carbon resources, downregulation of processes that compete for reducing equivalents may be an alternative approach to engineering strains with high-sucrose productivity. Flavodiiron proteins are part of cyanobacterial photoprotective systems that are engaged during periods of redox stress (*e.g.,* fluctuating light) and can direct electrons from an over-reduced photosynthetic electron transport chain to oxygen (Allahverdiyeva et al., 2015). The flavodiiron-catalyzed reaction is essentially a water–water cycle that dissipates potential energy from reducing equivalents generated from photosynthetic light reactions, but this reaction appears to be important for preventing photodamage under dynamic light conditions (Allahverdiyeva et al., 2013). Knockout of flavodiiron genes *flv1* and *flv3* in *S. elongatus* PCC 7942 could boost sucrose production in a *cscB/sps*6803 expressing background (Santos-Merino et al., 2021). Furthermore, activation of sucrose secretion pathways could partially compensate for the loss of Flv1/Flv3 under transient light changes, further suggesting that heterologous metabolic sinks may have some ability to utilize "overpotential" on the photosynthetic electron transport chain (Santos-Merino et al., 2021).

Altering regulatory networks to increase sucrose synthesis

Sucrose biosynthesis is a natural component of many cyanobacterial adaptive responses, so a deeper understanding of the regulatory networks that control this process could allow researchers to manipulate sucrose production in the absence of abiotic stressors. In this context, a couple of studies have reported promising improvements in sucrose secretion rates by altering cyanobacterial two-component regulatory proteins, although the specific mechanisms remain uncertain. In a screen of all two-component regulatory factors in *S. elongatus* PCC 7942, Qiao and

colleagues identified genes indirectly linked to sucrose productivity, glycogen accumulation, and photosynthetic activity (Qiao et al., 2019). The partial deletion of ManR, a protein that plays a regulatory role in Mn^{2+} uptake (Ogawa et al., 2002; Yamaguchi et al., 2002; Zorina et al., 2016), increased sucrose by 60%, a complete knockout of Synpcc7942_1125 increased sucrose by 41% (Qiao et al., 2019) (Table 1.1). In a separate study, overexpression of the two-component protein regulator of phycobilisome assembly B (*rpaB*) reproduced a growth-arrest phenotype in *S. elongatus* PCC 7942 (Moronta-Barrios et al., 2013), and increased sucrose secretion in a *cscB*-expressing background (Abramson et al., 2018) (Table 1.1). It was suggested that the growth arrest restricted carbon flux to many downstream pathways that might otherwise compete for sucrose biosynthesis, though a more specific alteration in regulatory processes controlling sucrose synthesis could not be excluded. While the number of studies is still limited, two-component signaling pathways have so far proven to be a promising strategy to improve sucrose yields, though our mechanistic understanding for these phenotypes is far from complete.

Applications of sucrose production in co-culture

While the biotechnological focus for cyanobacteria has predominantly been upon direct synthesis of high-value products (Ducat et al., 2012; Knoot et al., 2018), there is growing interest in utilizing sugar-producing cyanobacteria for indirect bioproduction. This approach involves the use of carbohydrate-secreting cyanobacteria that support the growth of co-cultivated heterotrophic microbes. Co-cultures become "one-pot" reactions where cyanobacteria specialize in photosynthetic metabolism to supply carbon to a heterotroph, which in turn performs the metabolic labor of converting the carbon to higher value goods or services (Hays and Ducat, 2015; Ortiz-Reyes and Anex, 2022). In this section, I will cover the modular nature of synthetic microbial consortia designed using sucrose-secreting cyanobacteria, their applications, and their future opportunities and challenges.

Potential advantages of modular microbial platforms

Microbial bioproduction is now a well-recognized approach that harnesses metabolic diversity for synthesis of valuable chemicals (*e.g.*, polymers, fuels, pharmaceuticals) as an alternative to traditional environmentally unsustainable processes (Tsuge et al., 2016; Wendisch et al., 2016; Liu and Nielsen, 2019; Zhong, 2020; Wu et al., 2021). Multiple decades of sustained investments in microbial research, prospecting, and genetic engineering have yielded a wealth of bacterial strains optimized to generate specific bioproducts. In some cases, efficient bioproduction

Table 1.2. Sucrose-based autotroph-heterotroph co-cultures and their products.

Sucrose Strain				Heterotroph Strain				
Species[a]	**Genotype[b]***	**Maximum productivity[c]**	**Induction**	**Species[d]**	**Genotype[e]**	**Product[f]**	**Maximum productivity[g]**	**Reference**
*Syn*7942	*cscB*	400 mg L^{-1} d^{-1}	106 mM NaCl	*B. subtilis*	–	α-amylase	not quantified	(Hays et al., 2017)†
				E. coli W	*phaCAB* Δ*cscR*	PHB	0.04 mg L^{-1} d^{-1}	
*Syn*7942	*cscB*	34.2 mg L^{-1} d^{-1}	N/A; physical encapsulation	*A. vinelandii*	Δ*nifL*	PHB	8 mg L^{-1} d^{-1}	(Smith and Francis, 2017)‡
*Syn*7942	*cscB*	27.4 mg L^{-1} d^{-1}	150 mM NaCl	*A. vinelandii*	Δ*nifL*	PHB	3.8% DW d^{-1}	(Smith and Francis, 2016)†
*Syn*7942	*cscB*	0.5 mg L^{-1} d^{-1}	170 mM NaCl	*H. boliviensis*	–	PHB	28.3 mg L^{-1} d^{-1}	(Weiss et al., 2017)‡
*Syn*7942	*cscB*	102 mg L^{-1} d^{-1}	150 mM NaCl	*P. putida* EM178	*cscRABY* Δ*nasT*	PHA	2.3 mg L^{-1} d^{-1}	(Hobmeier et al., 2020)†
*Syn*7942	*cscB*	250 mg L^{-1} d^{-1}	150 mM NaCl	*P. putida* EM178	*cscAB*	PHA	23.8 mg L^{-1} d^{-1}	(Löwe et al., 2017)
*Syn*7942	*cscB*	108 mg L^{-1} d^{-1}**	150 mM NaCl	*P. putida* EM178	*cscRABY* Δ*nasT*	PHA	42.1 mg L^{-1} d^{-1}	(Kratzl et al., 2022)
*Syn*7942	*cscB*	45 mg L^{-1} d^{-1}	100 mM NaCl	*R. glutinis*	–	DW	24.8 mg L^{-1} DW^{-1} d^{-1}	(Li et al., 2017)†
						TFA	1.2 mg L^{-1} d^{-1}	

Table 1.2. (cont'd)

*Syn*2973	*cscB*	96 mg L^{-1} d^{-1}	150 mM NaCl	*E. coli* BL21(DE3)	*cscA, cscB, cscK, mcr*	3-HP	9.8 mg L^{-1} d^{-1}	(Ma et al., 2022)†
Therm PKUAC	*cscB*	18.1 mg L^{-1} d^{-1}	150 mM NaCl	*E. coli* BL21(DE3)	*efe*	ethylene	0.74 mg L^{-1} d^{-1}	(Cui et al., 2022)
*Syn*7942	*cscB*	10 mg L^{-1} d^{-1}			*ispS*	isoprene	0.03 mg L^{-1} d^{-1}	
*Cup*H16	sps_{6803}, spp_{6803}, *scrY*	18.1 mg L^{-1} d^{-1}	0.3% arabinose	*E. coli* W	*vioABCDE, cscABK* Δ*cscR*	violacein	4.5 mg L^{-1} d^{-1}	(Nangle et al., 2020)
					crtEBIY, cscABK ΔcscR	β-carotene	4.8 mg L^{-1} d^{-1}	
*Syn*2973	*cscB*	0.7 mg L^{-1} d^{-1}**	150 mM NaCl	*Y. lipolytica*	*carB, carRP*	β-carotene	325 mg L^{-1} d^{-1}	(Zhao et al., 2022)‡
				P. putida KT2440	*sfp, bpsA*	indigoidine	1.9 g L^{-1} d^{-1}	
*Syn*7942	*cscB*	263.5 mg L^{-1} d^{-1}	150 mM NaCl	*V. natriegens*	*tyr*	melanin	1.56 mg L^{-1} d^{-1}	(Li et al., 2022)†
					tal	*p*-coumaric acid	8.75 mg L^{-1} d^{-1}	
					budABC	2,3-butanediol	60 mg L^{-1} d^{-1}	
					ldh	lactate	100 mg L^{-1} d^{-1}	

Table 1.2. (cont'd)

*Syn*7942	*cscB, sh3l*	108 mg L^{-1} d^{-1}	50 mM NaCl	*P. putida* S12	*cscA, hmfH, sh3d*	FDCA	~100% in 4 d	(Lin et al., 2020b)†‡
*Syn*7942	*cscB*	240 mg L^{-1} d^{-1}	100 mM NaCl	*P. putida* EM173	*cscRABY, dnt*	2,4-DNT degradation	22.7 mg L^{-1} d^{-1}	(Fedeson et al., 2020)‡
						PHA	5.1 mg L^{-1} d^{-1}	

[a] *Cup*H16, *Cupriavidus necator* H16; *Syn*7942, *Synechococcus elongatus* PCC 7942; *Syn*2973, *Synechococcus elongatus* UTEX 2973; *Syn*6803, *Synechocystis* sp. PCC 6803; *Therm*PKUAC, *Thermosynechococcus elongatus* PKUAC-SCTE542.
[b] *cscB*, sucrose permease; *scrY*, sucrose porin; *sh3l*, SH3 ligand; *sps*, sucrose phosphate synthase; *spp*, sucrose phosphate phosphatase.
[c] Approximated values from axenic cultivations in conditions most similar to co-culture conditions.
[d] *A. vinelandii*, *Azotobacter vinelandii* AV3; *B. subtilis*, *Bacillus subtilis* 168; *E. coli*, *Escherichia coli*; *G. sulfurreducens*, *Geobacter sulfurrenducens* PCA; *H. boliviensis*, *Halomonas boliviensis*; *P. putida*, *Pseudomonas putida*; *R. glutinis*, *Rhodotorula glutinis*; *S. onedensis*, *Shewanella onedensis* MR-1; *Y. lipolytica*, *Yarrowia lipolytica* CLIB138; *V. natriegens*, *Vibrio natriegens*.
[e] *bpsA*, non-ribosomal peptide synthetase; *budABC*, 2,3-butanediol gene cluster; *carB*, phytoene dehydrogenase; *carRP*, bifunctional lycopene cyclase/phytoene synthase; *crtEBIY*, β-carotene biosynthesis cassette; *cscA*, sucrose hydrolase; *cscB*, sucrose permease; *cscK*, fructokinase; *cscR*, sucrose operon repressor; *cscY*, sucrose porin; *dnt*, dinitrotoluence degradation gene cluster; *efe*, ethylene-forming protein; *frdABCD*, operon encoding fumarate reductase; *glk*, glucokinase; *gtfA*, sucrose phosphorylase; *hmfH*, HMF/furfural oxidoreductase; Inv, *cscA* invertase gene with an N-terminal *pelB* leader sequence; *ispS*, isoprene synthase; *ldh*, D-lactate dehydrogenase; *mcr*, malonyl-CoA reductase; *mgsA*, methylglyoxal synthase; *narG*, *napA*, and *narZ*, nitrate reductases; *nasT*, nitrate response regulator; *nifL*, negative regulator of nitrogen fixation; Parvi, synthetic Baeyer–Villiger monooxygenase; *pflB*, pyruvate formate-lyase B; *phaCAB*, polyhydroxybutyrate synthesis operon; *sfp*, phosphopantetheinyl transferase; *sh3d*, SH3 domain; *tal*, tyrosine ammonia lyase; *tyr*, tyrosinase; *vioABCDE*, violacein biosynthesis cassette. Unless otherwise denoted by "Δ," genes are heterologously expressed.
[f] 3-HP, 3-hydroxypropionic acid; DNT, dinitrotoluene; DW, cyanobacterial biomass dry weight; FDCA, 2,5-furandicarboxylic acid; PHA, polyhydroxyalkanoate; PHB, polyhydroxybutyrate; TFA, cyanobacterial total fatty acids.
[g] Approximated values provided or calculated from titers.
† Enhanced photoautotroph growth in co-culture.
‡ Implemented spatial control of co-culture.
* Subscript in *sps* and *spp* indicates the strain that it comes from (i.e., 6803 for *Synechocystis* sp. PCC 6803).
** Values from axenic cultivation prior to the introduction of heterotroph.
*** Maximum power output reported for the four-species consortium.

of a target compound can be achieved by expressing relevant metabolic pathways in different microbial species. But there are also many examples where heterologously expressed metabolic pathways perform poorly due to other physiological features of a microbe that make it a non-optimal chassis (Calero and Nikel, 2019). For this reason, it is often non-trivial to re-engineer cyanobacterial metabolism for direct synthesis of a desired compound, which may stubbornly resist efforts to improve product titer (Savakis and Hellingwerf, 2015; Nagarajan et al., 2017; Lin and Pakrasi, 2019).

A modular approach for multi-species product synthesis offers the capacity to leverage species with the most compatible physiology and desirable endogenous pathways for a given biochemical transformation, thus bypassing metabolic limitations of one biological chassis. At least in theory, each member of a synthetic microbial consortium can be conceptualized as a "module" selected specifically to perform functions well-suited with organism's abilities. In this context, cyanobacteria-heterotroph co-cultures can be rationally designed to retain the advantages of cyanobacterial metabolism (*i.e.*, use of light/ CO_2 inputs, efficient carbon fixation) and paired with other microbes that have demonstrated efficiency in transforming simple carbohydrates into a desired end product. Additionally, because the co-culture output can be changed by swapping the "heterotrophic module" (*i.e.*, organism), some steps to optimize synthesis for one product (*e.g.*, improving cyanobacterial sucrose production) may be transferable to achieve enhanced synthesis across many distinct cyanobacteria-heterotroph pairings. In practice, sucrose-secreting cyanobacteria have already been used as the basis for engineered microbial communities with numerous heterotrophic species and for a variety of end products (Table 1.2), although a number of improvements will be required to make these co-cultures feasible for scaled application.

Cyanobacterial co-culture as a flexible platform for value-added products

At the time of this writing, the most common metabolic output reported from cyanobacteria-heterotroph co-cultures are polyhydroxyalkanoates (PHAs), a class of biological polymers with comparative qualities to petroleum-based plastics. PHAs have the advantage of being both compatible in blends with commonly used petroleum-based polymers while also exhibiting superior biodegradation properties (Boey et al., 2021; Mezzina et al., 2021). Additionally, some heterotrophic microbes utilize PHAs as an intracellular storage polymer and under stress, conditions can naturally hyperaccumulate PHAs in excess of 80% of their dry cell mass (Leong et al., 2014; Lee et al., 2021), making these compounds an ideal test case for the

division of labor between metabolic specialists, as outlined above. Polyhydroxybutyrate (PHB) is a PHA polymer that has been produced in cyanobacterial co-culture with three different heterotrophic species: *Azotobacter vinelandii*, *Halomonas boliviensis*, and *E. coli* W (Hays et al., 2017; Smith and Francis, 2017; Weiss et al., 2017) (Table 1.2). PHB is a natural storage polymer for both *A. vinelandii* and *H. boliviensis*, while heterologous expression of the *phaCAB* operon in *E. coli* will confer PHB synthesis capability. The most productive co-cultures reported included a heterotrophic partner species that was naturally capable of PHB synthesis. Notably, the co-cultivation of *S. elongatus* PCC 7942 *cscB* with *H. boliviensis* was extended over 6 months with no organic carbon input, demonstrating that these synthetic consortia can be stable and productive over long time periods (Weiss et al., 2017).

Pseudomonas putida is a model organism that naturally accumulates medium chain length PHAs (mcl-PHAs) granules in response to starvation, primarily under low-nitrogen and high-carbon conditions (Hoffmann and Rehm, 2004). While sucrose is not naturally consumed by *P. putida*, expression of heterologous sucrose transporters and sucrose hydrolyzing enzymes allows it to grow on sucrose as the sole carbon source (Sabri et al., 2013; Löwe et al., 2020), a strategy that has been used to enable other microbial species without native pathways to consume cyanobacterially secreted sucrose (Sabri et al., 2013; Hobmeier et al., 2020; Zhang et al., 2020). Indeed, initial reports demonstrated that *P. putida* expressing *cscAB* was capable of growing solely on sucrose provided by *S. elongatus* PCC 7942 and accumulated PHA in co-culture, though sucrose utilization was incomplete and productivities were modest (Löwe et al., 2017; Fedeson et al., 2020). Additional expression of a sucrose porin (*cscY*) and a sucrose operon repressor (*cscR*) further improved sucrose utilization (Löwe et al., 2020), while further optimization of the nitrogen-deficiency response pathway (Hobmeier et al., 2020) and culture conditions could boost PHA titer further (Kratzl et al., 2022) (Table 1.2).

Other co-culture products include the metabolites ethylene, isoprene, 3-hydroxypropionic acid (3-HP), and 2,3-butanediol (Table 1.2), which are compounds in a broader class of industrially relevant precursors widely used for chemical synthesis (*e.g.*, diols, organic acids, gaseous alkenes) (Cui et al., 2022; Li et al., 2022; Ma et al., 2022). In most of these reports, the heterotrophic microbe utilized were *E. coli* substrains, although the rapidly growing halophile *Vibrio natriegens* was able to produce a relatively high amount of 2,3-butanediol in co-culture (Li et al., 2022). Interestingly, co-cultures of *S. elongatus* PCC 7942 and *P. putida* designed to convert 5-

hydroxymethylfurfural to 2,5-furandicarboxylic acid (FDCA), a common precursor molecule, exhibited higher efficiency when the two species were engineered to display complementary surface proteins (Lin et al., 2020b). The authors suggest that physical binding between the two species could improve metabolic exchange (Lin et al., 2020b), an intriguing strategy that may be valuable to develop further.

Beyond commodity products, several higher-value chemicals expand the metabolic repertoire of cyanobacteria-heterotroph co-cultures. The pigment industry routinely uses a number of compounds that generate significant environmental hazards when chemically synthesized (Pereira and Alves, 2012). Biosynthetic pathways for pigment derivatives (*e.g.*, indigoidine for the popular pigment, indigo) are being explored for more environmentally conscious pigment synthesis (Celedón and Díaz, 2021). Recently, co-cultures have been reported for the synthesis of indigoidine using the heterotroph *P. putida*, β-carotene with *E. coli* or the yeast *Yarrowia lipolytica*, and violacein by *E. coli* (Nangle et al., 2020; Zhao et al., 2022). Although most cyanobacteria-heterotroph co-cultures make use of the model laboratory strain *S. elongatus* PCC 7942, Zhao and colleagues used a sucrose-secreting variant of the fast-growing and high-light tolerant relative, *S. elongatus* UTEX 2973, in their co-culture experiments to produce indigoidine and β-carotene (Zhao et al., 2022). The cosmetic *p*-coumaric acid, is another higher value compound useful for its antioxidant and antimicrobial properties (Boz, 2015; Boo, 2019). The biosynthetic pathway for *p*-coumaric acid was introduced into *V. natriegens* and co-cultures of these engineered strains with *S. elongatus* PCC 7942 allowed for photosynthetically driven *p*-coumaric acid production (Li et al., 2022). Other recent reports provide further evidence of the flexibility of this cyanobacterial co-cultivation system (Table 1.2), including bioproduction of fatty acids (Li et al., 2022), ε-caprolactone (Tóth et al., 2022), lactate (Li et al., 2022), and secreted enzymes (Hays et al., 2017). Additionally, some products can be used to feed downstream bacteria and develop more complex systems. A four-species consortium utilized lactate-consuming *Shewanella oneidensis* to generate electricity and acetate, in which the latter was consumed by *Geobacter sulfurreducens* to produce CO_2 for *S. elongatus* PCC 7942 (Zhu et al., 2022).

Co-culture as a platform to study microbial communities

Phototrophs and heterotrophs are often metabolically intertwined in natural contexts (Morris, 2015; Henry et al., 2016). For example, many marine *Prochlorococcus* species secrete organic carbon to neighboring heterotrophic partners that perform functions in detoxifying reactive

oxygen species present in the open ocean (Morris et al., 2011; Braakman et al., 2017). It has been hypothesized that the natural export of sugars from *Prochlorococcus* and other cyanobacteria may prime them to engage with surrounding heterotrophs *via* cross-feeding, and potentially "outsource" the metabolic burden of synthesizing some nutritional requirements to other organisms (Werner et al., 2014; Henry et al., 2016; Braakman et al., 2017). Natural microbial communities and symbiotic relationships usually develop over evolutionary time scales and may exhibit numerous and complex cross-feeding patterns and other self-stabilizing interactions (Konopka et al., 2015). Yet, these important dynamics can be challenging to study due to the difficulty of disentangling specific mechanisms from the complex interaction networks (Ponomarova and Patil, 2015). The fact that many natural symbioses also have cyanobacterial partners that exchange fixed carbon for other microbial partner(s) has led some groups to explore synthetic cyanobacteria/heterotroph co-cultures as a possible "bottom-up" system to gain insight into complex microbial consortia.

Synthetic phototroph-heterotroph microbial consortia may represent a complementary system to study natural consortia in parallel, as they present a platform for interrogating microbial interactions that is relatively simple, genetically tractable, and experimentally tunable (De Roy et al., 2014; Song et al., 2015) (Table 1.3). One intriguing phenomenon that recurs across several synthetic cyanobacteria/ heterotroph co-cultures is an increase in the vigor or productivity of one or both partners relative to axenic controls. For instance, cyanobacterial growth was enhanced in mixed culture with several heterotrophic species (Hays et al., 2017; Li et al., 2017; Hobmeier et al., 2020; Ma et al., 2022), although the partner species were evolutionarily "naïve" to one another. Similarly, heterotrophic productivity in co-culture can be significantly higher than can be attributed to the cyanobacterially secreted sucrose (Hays et al., 2017; Cui et al., 2022; Ma et al., 2022). Conversely, when cyanobacteria are allowed to overpopulate a synthetic co-culture, heterotrophic partners may exhibit reduced viability (Hays et al., 2017). It is highly likely that some of these effects arise due to unprogrammed metabolic interactions and emergent behaviors of division of labor (Rafieenia et al., 2022), such as the generation of damaging reactive oxygen species (Hays et al., 2017; Ma et al., 2022).

Our current understanding of the emergent properties of mixed microbial communities is limited and cannot fully explain observed phenomena. Preliminary analyses and multi-omics approaches have been used to predict hidden interactions within synthetic consortia, providing insight on areas of cooperation and competition that could be validated and exploited to design

Table 1.3. Synthetic cyanobacteria-heterotroph microbial consortia used as a platform to study microbial interactions.

Sucrose strain[a]	Genotype[b]	Heterotroph strain[c]	Genotype[d]	Notes	Reference
*Syn*7942	*cscB*	*E. coli* K-12	AA knockouts	Utilizes metabolic modeling and experimental validation to predict co-cultivation outcomes and identify optimizable parameters.	(Zuñiga et al., 2020)
		E. coli W	–		
		Y. lipolytica	SUC2		
		B. subtilis	–		
*Syn*7942	*cscB*, sps_{6803}	*A. vinelandii*	Δ*nifL*	Develops tripartite consortium with carbon-providing *S. elongatus* PCC 7942 and nitrogen-providing *A. vinelandii* to support a third microbe. Performed computational analyses to identify bottlenecks to improve cultivation conditions.	(Carruthers, 2020)
		E. coli K-12 MG1655	*cscABK*		
		C. glutamicum	–		
		B. subtilis 168	–		
*Syn*2973	*cscB*	*E. coli* BL21(DE3)	*cscABK*, *mcr*	Utilizes transcriptomic, proteomic, and metabolomic analyses to reveal differentially regulated pathways during co-cultivation to identify optimizable parameters to improve stability and 3-hydroxypropionic productivity.	(Ma et al., 2022)
*Syn*7942	*cscB*	*E. coli* MG1655	*cscABK*	Spatially separates subpopulations with encapsulation to impart species stability while still allowing the transport of small molecules.	(Wang et al., 2022)

Table 1.3 (cont'd)

*Syn*7942	*cscB*, sps_{6803}	*E. coli* W	Δ*cscR*	Utilizes individual-based modeling in spatial context to predict colony fitness.	(Sakkos et al., 2022)
*Syn*7942	*cscB*, sps_{6803}	*E. coli* W	Δ*cscR*	Integrates quorum sensing modules for cross-species communication.	(Kokarakis et al., 2022)

[a] *Syn*7942, *Synechococcus elongatus* PCC 7942; *Syn*2973, *Synechococcus elongatus* UTEX 2973.
[b] AA knockouts, multiple one-way amino acid auxotrophs were generated; *cscB*, sucrose permease; *sps6803*, sucrose phosphate synthase from *Synechocystis* sp. PCC 6803.
[c] *A. vinelandii*, *Azotobacter vinelandii* AZBB163; *B. subtilis*, *Bacillus subtilis* 168; *C. glutamicum*, *Corynebacterium glutamicum* 13032; *E. coli*, *Escherichia coli*, *Y. lipolytica*, *Yarrowia lipolytica* Po1g. d*cscABK*, sucrose utilization operon; *cscR*, sucrose operon repressor; *mcr*, malonyl-CoA reductase; *nifL*, negative regulator of nitrogen fixation; SUC2, cassette for internal and external invertases.

more robust co-cultures (Carruthers, 2020; Zuñiga et al., 2020; Ma et al., 2022). Synthetic co-cultures also present a simpler set of variables in comparison to natural communities which may be more amenable to simulations, such as agent-based modeling, for predicting emergent behaviors in a population (Sakkos et al., 2023). Finally, additional layers of metabolic exchange can be designed into the synthetic co-culture system to experimentally probe and validate hypotheses of interspecies exchange. A notable example in this regard is multiple groups' use of the diazotroph, *A. vinelandii,* to fix atmospheric nitrogen and secrete ammonia, effectively creating a carbon-for-nitrogen exchange in co-culture with sucrose-secreting cyanobacteria (Smith and Francis, 2017; Carruthers, 2020). Taken together, the computational, systems, and genetic toolkits available for synthetic microbial consortia may lead to important insights on the dynamics of microbial exchange that would be difficult to probe in natural microbiomes.

Organizational structure of dissertation

In my dissertation, I focused upon improving the potential of the aforementioned co-culture system of photosynthetic bioproduction. The co-culture approach offers a degree of flexibility in output products that is difficult to match using other metabolic engineering approaches, and the overall sucrose production from cyanobacteria is promising relative to terrestrial plant carbohydrate feedstocks. Nonetheless, at this time, any attempts to scale cyanobacterial co-culture to industrially relevant volumes would surely run into a number of problems. My dissertation research focused on two potential weaknesses of cyanobacterial co-culture. In Chapter 2, I describe my research to maximize the output of sucrose by modulating the cultivation conditions for sucrose-secreting strains of *S. elongatus*. Maximizing heterotrophic yield in co-culture is directly related to the amount of fixed carbon that can be supplied by the cyanobacterial partner, and I interrogated a number of different conditions of illumination as well as ways to supply inorganic CO_2 to cyanobacterial cultures. In Chapter 3, I describe my efforts to rationally design co-cultures for higher resilience and productivity through engineering in a system for physical attachment between the heterotroph and cyanobacterial partner. Specifically, I expanded upon prior work on a cyanobacterial surface display system with the long-range goal of installing extracellular binding domains on the surface of *S. elongatus* that could be used to mediate direct physical attachments with other proteins displayed on the surface of an engineered heterotrophic partner. Finally, in Chapter 4, I review the outcomes and conclusions of my research program and reflect upon both my experience and future prospects for the topic areas central to my dissertation.

REFERENCES

Abramson, B. W., Kachel, B., Kramer, D. M., and Ducat, D. C. (2016). Increased photochemical efficiency in cyanobacteria via an engineered sucrose sink. *Plant Cell Physiol.* 57, 2451–2460. doi: 10.1093/pcp/pcw169

Abramson, B. W., Lensmire, J., Lin, Y. T., Jennings, E., and Ducat, D. C. (2018). Redirecting carbon to bioproduction via a growth arrest switch in a sucrose-secreting cyanobacterium. *Algal Res.* 33, 248–255. doi: 10.1016/j.algal.2018.05.013

Adomako, M., Ernst, D., Simkovsky, R., Chao, Y.-Y., Wang, J., Fang, M., et al. (2022). comparative genomics of *Synechococcus elongatus* explains the phenotypic diversity of the strains. *mBio* 13, e00862-22. doi: 10.1128/mbio.00862-22

Aikens, J. and Turner, R.J., PROTERRO Inc (2013). Method of producing a fermentable sugar. U.S. Patent 8,597,914.

Albi, T., Ruiz, M. T., Reyes, P. de los, Valverde, F., and Romero, J. M. (2016). Characterization of the sucrose phosphate phosphatase (SPP) isoforms from *Arabidopsis thaliana* and role of the S6PPc domain in dimerization. *PLOS ONE* 11, e0166308. doi: 10.1371/journal.pone.0166308

Allahverdiyeva, Y., Isojärvi, J., Zhang, P., and Aro, E.-M. (2015). Cyanobacterial oxygenic photosynthesis is protected by flavodiiron proteins. *Life* 5, 716–743. doi: 10.3390/life5010716

Allahverdiyeva, Y., Mustila, H., Ermakova, M., Bersanini, L., Richaud, P., Ajlani, G., et al. (2013). Flavodiiron proteins Flv1 and Flv3 enable cyanobacterial growth and photosynthesis under fluctuating light. *Proc. Natl. Acad. Sci.* 110, 4111–4116. doi: 10.1073/pnas.1221194110

Angermayr, S. A., Paszota, M., and Hellingwerf, K. J. (2012). Engineering a cyanobacterial cell factory for production of lactic acid. *Appl. Environ. Microbiol.* 78, 7098–7106. doi: 10.1128/AEM.01587-12

Bakku, R. K., and Rakwal, R. (2022). "Applications of cyanobacterial compounds in the energy, health, value-added product, and agricultural sectors: A perspective," in *Cyanobacterial Physiology*, eds. H. Kageyama and R. Waditee-Sirisattha (Academic Press), 149–164. doi: 10.1016/B978-0-323-96106-6.00009-5

Baran, R., Lau, R., Bowen, B. P., Diamond, S., Jose, N., Garcia-Pichel, F., et al. (2017). Extensive turnover of compatible solutes in cyanobacteria revealed by deuterium oxide (D_2O) stable isotope probing. *ACS Chem. Biol.* 12, 674–681. doi: 10.1021/acschembio.6b00890

Blank, C. E. (2013). Phylogenetic distribution of compatible solute synthesis genes support a freshwater origin for cyanobacteria. *J. Phycol.* 49, 880–895. doi: 10.1111/jpy.12098

Boey, J. Y., Mohamad, L., Khok, Y. S., Tay, G. S., and Baidurah, S. (2021). A review of the applications and biodegradation of polyhydroxyalkanoates and poly(lactic acid) and its composites. *Polymers* 13, 1544. doi: 10.3390/polym13101544

Boo, Y. C. (2019). p-Coumaric acid as an active ingredient in cosmetics: a review focusing on its antimelanogenic effects. *Antioxidants* 8, 275. doi: 10.3390/antiox8080275

Boz, H. (2015). p-Coumaric acid in cereals: presence, antioxidant and antimicrobial effects. *Int. J. Food Sci. Technol.* 50, 2323–2328. doi: 10.1111/ijfs.12898

Braakman, R., Follows, M. J., and Chisholm, S. W. (2017). Metabolic evolution and the self-organization of ecosystems. *Proc. Natl. Acad. Sci. U. S. A.* 114, E3091–E3100. doi: 10.1073/pnas.1619573114

Calero, P., and Nikel, P. I. (2019). Chasing bacterial chassis for metabolic engineering: a perspective review from classical to non-traditional microorganisms. *Microb. Biotechnol.* 12, 98–124. doi: 10.1111/1751-7915.13292

Carruthers, D. (2020). Engineering modular synthetic microbial consortia for sustainable bioproduction from CO_2. University of Michigan, Horace H. Rackham School of Graduate Studies.

Celedón, R. S., and Díaz, L. B. (2021). Natural pigments of bacterial origin and their possible biomedical applications. *Microorganisms* 9, 739. doi: 10.3390/microorganisms9040739

Chen, B., Wan, C., Mehmood, M. A., Chang, J.-S., Bai, F., and Zhao, X. (2017). Manipulating environmental stresses and stress tolerance of microalgae for enhanced production of lipids and value-added products–a review. *Bioresour. Technol.* 244, 1198–1206. doi: 10.1016/j.biortech.2017.05.170

Crockford, P. W., Bar On, Y. M., Ward, L. M., Milo, R., and Halevy, I. (2023). The geologic history of primary productivity. *Curr. Biol.* 33, 4741-4750.e5. doi: 10.1016/j.cub.2023.09.040

Cui, Y., Rasul, F., Jiang, Y., Zhong, Y., Zhang, S., Boruta, T., et al. (2022). Construction of an artifcial consortium of *Escherichia coli* and cyanobacteria for clean indirect production of volatile platform hydrocarbons from CO_2. *Front. Microbiol.* 13, 965968. doi: 10.3389/fmicb.2022.965968

Cumino, A. C., Marcozzi, C., Barreiro, R., and Salerno, G. L. (2007). Carbon cycling in *Anabaena* sp. PCC 7120. sucrose synthesis in the heterocysts and possible role in nitrogen fixation. *Plant Physiol.* 143, 1385–1397. doi: 10.1104/pp.106.091736

Cumino, A., Curatti, L., Giarrocco, L., and Salerno, G. L. (2002). Sucrose metabolism: *Anabaena* sucrose-phosphate synthase and sucrose-phosphate phosphatase define minimal functional domains shuffled during evolution. *FEBS Lett.* 517, 19–23. doi: 10.1016/S0014-5793(02)02516-4

Curatti, L., Flores, E., and Salerno, G. (2002). Sucrose is involved in the diazotrophic metabolism of the heterocyst-forming cyanobacterium Anabaena sp. *FEBS Lett.* 513, 175–178. doi: 10.1016/S0014-5793(02)02283-4

Curatti, L., Folco, E., Desplats, P., Abratti, G., Limones, V., Herrera-Estrella, L., et al. (1998b). Sucrose-phosphate synthase from *Synechocystis* sp. strain PCC 6803: identification of the spsa gene and characterization of the enzyme expressed in *Escherichia coli. J. Bacteriol.* 180, 6776–6779. doi: 10.1128/jb.180.24.6776-6779.1998

Curatti, L., Giarrocco, L. E., Cumino, A. C., and Salerno, G. L. (2008). Sucrose synthase is involved in the conversion of sucrose to polysaccharides in filamentous nitrogen-fixing

cyanobacteria. *Planta* 228, 617–625. doi: 10.1007/s00425-008-0764-7

Curatti, L., Giarrocco, L., and Salerno, G. L. (2006). Sucrose synthase and RuBisCo expression is similarly regulated by the nitrogen source in the nitrogen-fixing cyanobacterium *Anabaena* sp. *Planta* 223, 891–900. doi: 10.1007/s00425-005-0142-7

Curatti, L., Porchia, A. C., Herrera-Estrella, L., and Salerno, G. L. (2000). A prokaryotic sucrose synthase gene (*susA*) isolated from a filamentous nitrogen-fixing cyanobacterium encodes a protein similar to those of plants. *Planta* 211, 729–735. doi: 10.1007/s004250000343

Dan, Y., Sun, J., Zhang, S., Wu, Y., Mao, S., Luan, G., et al. (2022). Manipulating the expression of glycogen phosphorylase in *Synechococcus elongatus* PCC 7942 to mobilize glycogen storage for sucrose synthesis. *Front. Bioeng. Biotechnol.* 10, 925311. doi: 10.3389/fbioe.2022.925311

De Roy, K., Marzorati, M., Van den Abbeele, P., Van de Wiele, T., and Boon, N. (2014). Synthetic microbial ecosystems: an exciting tool to understand and apply microbial communities. *Environ. Microbiol.* 16, 1472–1481. doi: 10.1111/1462-2920.12343

Du, W., Liang, F., Duan, Y., Tan, X., and Lu, X. (2013). Exploring the photosynthetic production capacity of sucrose by cyanobacteria. *Metab. Eng.* 19, 17–25. doi: 10.1016/j.ymben.2013.05.001

Duan, Y., Luo, Q., Liang, F., and Lu, X. (2016). Sucrose secreted by the engineered cyanobacterium and its fermentability. *J. Ocean Univ. China* 15, 890–896. doi: 10.1007/s11802-016-3007-8

Ducat, D. C., Avelar-Rivas, J. A., Way, J. C., and Silvera, P. A. (2012). Rerouting carbon flux to enhance photosynthetic productivity. *Appl. Environ. Microbiol.* 78, 2660–2668. doi: 10.1128/AEM.07901-11

Falcón, L. I., Magallón, S., and Castillo, A. (2010). Dating the cyanobacterial ancestor of the chloroplast. *ISME J.* 4, 777–783. doi: 10.1038/ismej.2010.2

Fedeson, D. T., Saake, P., Calero, P., Nikel, P. I., and Ducat, D. C. (2020). Biotransformation of 2,4-dinitrotoluene in a phototrophic co-culture of engineered *Synechococcus elongatus* and *Pseudomonas putida*. *Microb. Biotechnol.* 13, 997–1011. doi: 10.1111/1751-7915.13544

Fieulaine, S., Lunn, J. E., Borel, F., and Ferrer, J.-L. (2005). The structure of a cyanobacterial sucrose-phosphatase reveals the sugar tongs that release free sucrose in the cell. *Plant Cell* 17, 2049–2058. doi: 10.1105/tpc.105.031229

Gaysina, L. A., Saraf, A., and Singh, P. (2019). "Cyanobacteria in diverse habitats," in *Cyanobacteria*, eds. A. K. Mishra, D. N. Tiwari, and A. N. Rai (Academic Press), 1–28. doi: 10.1016/B978-0-12-814667-5.00001-5

Gibson, R. P., Turkenburg, J. P., Charnock, S. J., Lloyd, R., and Davies, G. J. (2002). Insights into trehalose synthesis provided by the structure of the retaining glucosyltransferase OtsA. *Chem. Biol.* 9, 1337–46. doi: 10.1016/s1074-5521(02)00292-2

Gründel, M., Scheunemann, R., Lockau, W., and Zilliges, Y. (2012). Impaired glycogen synthesis causes metabolic overflow reactions and affects stress responses in the cyanobacterium *Synechocystis* sp. PCC 6803. *Microbiology* 158, 3032–3043. doi: 10.1099/mic.0.062950-0

Hagemann, M. (2011). Molecular biology of cyanobacterial salt acclimation. *FEMS Microbiol. Rev.* 35, 87–123. doi: 10.1111/j.1574-6976.2010.00234.x

Hagemann, M. (2013). "Genomics of salt acclimation: Synthesis of compatible solutes among cyanobacteria," in *Advances in Botanical Research*, eds. F. Chauvat and C. Cassier-Chauvat (Academic Press), 27–55. doi: 10.1016/B978-0-12-394313-2.00002-0

Hays, S. G., and Ducat, D. C. (2015). Engineering cyanobacteria as photosynthetic feedstock factories. *Photosynth. Res.* 123, 285–295. doi: 10.1007/s11120-014-9980-0

Hays, S. G., Yan, L. L. W., Silver, P. A., and Ducat, D. C. (2017). Synthetic photosynthetic consortia define interactions leading to robustness and photoproduction. *J. Biol. Eng.* 11, 1-4. doi: 10.1186/s13036-017-0048-5

Henry, C. S., Bernstein, H. C., Weisenhorn, P., Taylor, R. C., Lee, J., Zucker, J., et al. (2016). Microbial community metabolic modeling: a community data-driven network reconstruction. *J. Cell. Physiol.* 231, 2339–2345. doi: 10.1002/jcp.25428

Herrero, A., Stavans, J., and Flores, E. (2016). The multicellular nature of filamentous heterocyst-forming cyanobacteria. *FEMS Microbiol. Rev.* 40, 831–854. doi: 10.1093/femsre/fuw029

Hincha, D. K., and Hagemann, M. (2004). Stabilization of model membranes during drying by compatible solutes involved in the stress tolerance of plants and microorganisms. *Biochem. J.* 383, 277–283. doi: 10.1042/BJ20040746

Hobmeier, K., Lowe, H., Liefeldt, S., Kremling, A., and Pfluger-Grau, K. (2020). A nitrate-blind *P. putida* strain boosts PHA production in a synthetic mixed culture. *Front. Bioeng. Biotechnol.* 8, 486. doi: 10.3389/fbioe.2020.00486

Hoffmann, N., and Rehm, B. H. A. (2004). Regulation of polyhydroxyalkanoate biosynthesis in *Pseudomonas putida* and *Pseudomonas aeruginosa*. *FEMS Microbiol. Lett.* 237, 1–7. doi: 10.1111/j.1574-6968.2004.tb09671.x

Huang, C.-H., Shen, C. R., Li, H., Sung, L.-Y., Wu, M.-Y., and Hu, Y.-C. (2016). CRISPR interference (CRISPRi) for gene regulation and succinate production in cyanobacterium *S. elongatus* PCC 7942. *Microb. Cell Fact.* 15, 1–11. doi: 10.1186/s12934-016-0595-3

Kariyazono, R., Ito, S., and Osanai, T. (2022). "Carbon metabolism of great biotechnological interest: Metabolic engineering and synthetic biology of cyanobacteria," in *Cyanobacterial Physiology*, eds. H. Kageyama and R. Waditee-Sirisattha (Academic Press), 189–200. doi: 10.1016/B978-0-323-96106-6.00003-4

Khan, M., Shin, J., and Kim, J. (2018). The promising future of microalgae: current status, challenges, and optimization of a sustainable and renewable industry for biofuels, feed, and other products. *Microb. Cell Fact.*, 17, 1-21. doi: 10.1186/s12934-018-0879-x

Kirsch, F., Klähn, S., and Hagemann, M. (2019). Salt-regulated accumulation of the compatible solutes sucrose and glucosylglycerol in cyanobacteria and its biotechnological potential. *Front. Microbiol.* 10, 482569. doi: 10.3389/fmicb.2019.02139

Kirsch, F., Luo, Q., Lu, X., and Hagemann, M. (2018). Inactivation of invertase enhances sucrose production in the cyanobacterium *Synechocystis* sp. PCC 6803. *Microbiology* 164, 1220–1228. doi: 10.1099/mic.0.000708

Klähn, S., and Hagemann, M. (2011). Compatible solute biosynthesis in cyanobacteria. *Environ. Microbiol.* 13, 551–562. doi: 10.1111/j.1462-2920.2010.02366.x

Knoot, C. J., Ungerer, J., Wangikar, P. P., and Pakrasi, H. B. (2018). Cyanobacteria: promising biocatalysts for sustainable chemical production. *J. Biol. Chem.* 293, 5044–5052. doi: 10.1074/jbc.R117.815886

Konopka, A., Lindemann, S., and Fredrickson, J. (2015). Dynamics in microbial communities: Unraveling mechanisms to identify principles. *ISME J.* 9, 1488–1495. doi: 10.1038/ismej.2014.251

Kratz, W. A., and Meyers, J. (1955). Nutrition and Growth of Several Blue-Green Algae. *Am. J. Bot.* 42, 282–287. doi: 10.2307/2438564

Kratzl, F., Kremling, A., and Pflüger-Grau, K. (2022). Streamlining of a synthetic co-culture towards an individually controllable one-pot process for polyhydroxyalkanoate production from light and CO2. *Eng. Life Sci.* 21, e2100156. doi: 10.1002/elsc.202100156

Kroumov, A. D., Zaharieva, M. M., Scheufele, F. B., Balabanova, V., and Najdenski, H. (2021). "Engineering challenges of carbon dioxide capture and sequestration by cyanobacteria," in *Ecophysiology and Biochemistry of Cyanobacteria*, ed. R. P. Rastogi (Singapore: Springer Nature), 351–372. doi: 10.1007/978-981-16-4873-1_16

Lee, J., Park, H. J., Moon, M., Lee, J.-S., and Min, K. (2021). Recent progress and challenges in microbial polyhydroxybutyrate (PHB) production from CO_2 as a sustainable feedstock: A state-of-the-art review. *Bioresour. Technol.* 339, 125616. doi: 10.1016/j.biortech.2021.125616

Leong, Y. K., Show, P. L., Ooi, C. W., Ling, T. C., and Lan, J. C.-W. (2014). Current trends in polyhydroxyalkanoates (PHAs) biosynthesis: Insights from the recombinant *Escherichia coli*. *J. Biotechnol.* 180, 52–65. doi: 10.1016/j.jbiotec.2014.03.020

Li, C., Wang, R., Wang, J., Liu, L., Li, H., Zheng, H., et al. (2022). A highly compatible phototrophic community for carbon-negative biosynthesis. *Angew. Chem. Int. Ed.* 62, e202215013. doi: 10.1002/anie.202215013

Li, T., Li, C. T., Butler, K., Hays, S. G., Guarnieri, M. T., Oyler, G. A., et al. (2017). Mimicking lichens: Incorporation of yeast strains together with sucrose-secreting cyanobacteria improves survival, growth, ROS removal, and lipid production in a stable mutualistic co-culture production platform. *Biotechnol. Biofuels* 10, 1-11. doi: 10.1186/s13068-017-0736-x

Liang, Y., Zhang, M., Wang, M., Zhang, W., Qiao, C., Luo, Q., et al. (2020). Freshwater cyanobacterium *Synechococcus elongatus* PCC 7942 adapts to an environment with salt stress via ion-induced enzymatic balance of compatible solutes. *Appl. Environ. Microbiol.* 86, 2904–2923. doi: 10.1128/AEM

Lin, P. C., Zhang, F., and Pakrasi, H. B. (2020a). Enhanced production of sucrose in the fast-growing cyanobacterium *Synechococcus elongatus* UTEX 2973. *Sci. Rep.* 10, 390. doi: 10.1038/s41598-019-57319-5

Lin, P. C., and Pakrasi, H. B. (2019). Engineering cyanobacteria for production of terpenoids.

Planta 249, 145–154. doi: 10.1007/s00425-018-3047-y

Lin, T. Y., Wen, R. C., Shen, C. R., and Tsai, S. L. (2020b). Biotransformation of 5-Hydroxymethylfurfural to 2,5-Furandicarboxylic Acid by a Syntrophic Consortium of Engineered Synechococcus elongatus and Pseudomonas putida. *Biotechnol J* 15, e1900357. doi: 10.1002/biot.201900357

Liu, Y., and Nielsen, J. (2019). Recent trends in metabolic engineering of microbial chemical factories. *Curr. Opin. Biotechnol.* 60, 188–197. doi: 10.1016/j.copbio.2019.05.010

López-Igual, R., Flores, E., and Herrero, A. (2010). Inactivation of a heterocyst-specific invertase indicates a principal role of sucrose catabolism in heterocysts of *Anabaena* sp. *J. Bacteriol.* 192, 5526–5533. doi: 10.1128/jb.00776-10

Löwe, H., Hobmeier, K., Moos, M., Kremling, A., and Pfluger-Grau, K. (2017). Photoautotrophic production of polyhydroxyalkanoates in a synthetic mixed culture of *Synechococcus elongatus* cscB and *Pseudomonas putida* cscAB. *Biotechnol. Biofuels* 10, 190. doi: 10.1186/s13068-017-0875-0

Löwe, H., Sinner, P., Kremling, A., and Pflüger-Grau, K. (2020). Engineering sucrose metabolism in Pseudomonas putida highlights the importance of porins. *Microb. Biotechnol.* 13, 97–106. doi: 10.1111/1751-7915.13283

Luan, G., Zhang, S., Wang, M., and Lu, X. (2019). Progress and perspective on cyanobacterial glycogen metabolism engineering. *Biotechnol. Adv.* 37, 771–786. doi: 10.1016/j.biotechadv.2019.04.005

Lunn, J. E., Ashton, A. R., Hatch, M. D., and Heldt, H. W. (2000). Purification, molecular cloning, and sequence analysis of sucrose-6F-phosphate phosphohydrolase from plants. *Proc. Natl. Acad. Sci.* 97, 12914–12919. doi: 10.1073/pnas.230430197

Lunn, J. E., Price, G. D., and Furbank, R. T. (1999). Cloning and expression of a prokaryotic sucrose-phosphate synthase gene from the cyanobacterium *Synechocystis* sp. PCC 6803. *Plant Mol. Biol.* 40, 297–305. doi: 10.1023/a:1006130802706

Ma, J., Guo, T., Ren, M., Chen, L., Song, X., and Zhang, W. (2022). Cross-feeding between cyanobacterium *Synechococcus* and *Escherichia coli* in an artificial autotrophic-heterotrophic coculture system revealed by integrated omics analysis. *Biotechnol. Biofuels Bioprod.* 15, 69. doi: 10.1186/s13068-022-02163-5

Mezzina, M. P., Manoli, M. T., Prieto, M. A., and Nikel, P. I. (2021). Engineering native and synthetic pathways in *Pseudomonas putida* for the production of tailored polyhydroxyalkanoates. *Biotechnol. J.* 16, 2000165. doi: 10.1002/biot.202000165

Morone, J., Alfeus, A., Vasconcelos, V., and Martins, R. (2019). Revealing the potential of cyanobacteria in cosmetics and cosmeceuticals — A new bioactive approach. *Algal Res.* 41, 101541. doi: 10.1016/j.algal.2019.101541

Moronta-Barrios, F., Espinosa, J., and Contreras, A. (2013). Negative control of cell size in the cyanobacterium *Synechococcus elongatus* PCC 7942 by the essential response regulator RpaB. *FEBS Lett.* 587, 504–509. doi: 10.1016/j.febslet.2013.01.023

Morris, J. J. (2015). Black Queen evolution: The role of leakiness in structuring microbial

communities. *Trends Genet.* 31, 475–482. doi: 10.1016/j.tig.2015.05.004

Morris, J. J., Johnson, Z. I., Szul, M. J., Keller, M., and Zinser, E. R. (2011). Dependence of the cyanobacterium *Prochlorococcus* on hydrogen peroxide scavenging microbes for growth at the ocean's surface. *PloS One* 6, e16805. doi: 10.1371/journal.pone.0016805

Nagarajan, D., Lee, D.-J., Kondo, A., and Chang, J.-S. (2017). Recent insights into biohydrogen production by microalgae–From biophotolysis to dark fermentation. *Bioresour. Technol.* 227, 373–387. doi: j.biortech.2016.12.104

Nangle, S. N., Ziesack, M., Buckley, S., Trivedi, D., Loh, D. M., Nocera, D. G., et al. (2020). Valorization of CO_2 through lithoautotrophic production of sustainable chemicals in Cupriavidus necator. *Metab Eng* 62, 207–220. doi: 10.1016/j.ymben.2020.09.002

Niederholtmeyer, H., Wolfstadter, B. T., Savage, D. F., Silver, P. A., and Way, J. C. (2010). Engineering cyanobacteria to synthesize and export hydrophilic products. *Appl Env. Microbiol* 76, 3462–6. doi: 10.1128/AEM.00202-10

Ogawa, T., Bao, D. H., Katoh, H., Shibata, M., Pakrasi, H. B., and Bhattacharyya-Pakrasi, M. (2002). A two-component signal transduction pathway regulates manganese homeostasis in *Synechocystis* 6803, a photosynthetic organism. *J. Biol. Chem.* 277, 28981–28986. doi: 10.1074/jbc.M204175200

Ortiz-Reyes, E., and Anex, R. P. (2022). Economic and environmental performance of non-cellulosic fermentable carbohydrates production for biofuels and chemicals. *J. Clean. Prod.* 353, 131526. doi: 10.1016/j.jclepro.2022.131526

Page-Sharp, M., Behm, C. A., and Smith, G. D. (1999). Involvement of the compatible solutes trehalose and sucrose in the response to salt stress of a cyanobacterial *Scytonema* species isolated from desert soils. *Biochim. Biophys. Acta BBA - Gen. Subj.* 1472, 519–528. doi: 10.1016/S0304-4165(99)00155-5

Pathak, J., Singh, P. R., Sinha, R. P., and Rastogi, R. P. (2021). "Evolution and distribution of cyanobacteria," in *Ecophysiology and Biochemistry of Cyanobacteria*, ed. R. P. Rastogi (Singapore: Springer Nature), 1–30. doi: 10.1007/978-981-16-4873-1_1

Pereira, L., and Alves, M. (2012). "Dyes—Environmental impact and remediation," in *Environmental Protection Strategies for Sustainable Development*, eds. A. Malik and E. Grohmann (Dordrecht: Springer Netherlands), 111–162. doi: 10.1007/978-94-007-1591-2_4

Perez-Cenci, M., and Salerno, G. L. (2014). Functional characterization of *Synechococcus* amylosucrase and fructokinase encoding genes discovers two novel actors on the stage of cyanobacterial sucrose metabolism. *Plant Sci.* 224, 95–102. doi: 10.1016/j.plantsci.2014.04.003

Ponomarova, O., and Patil, K. R. (2015). Metabolic interactions in microbial communities: untangling the Gordian knot. *Curr. Opin. Microbiol.* 27, 37–44. doi: 10.1016/j.mib.2015.06.014

Porchia, A. C., Curatti, L., and Salerno, G. L. (1999). Sucrose metabolism in cyanobacteria: sucrose synthase from *Anabaena* sp. strain PCC 7119 is remarkably different from the plant

enzymes with respect to substrate affinity and amino-terminal sequence. *Planta* 210, 34–40. doi: 10.1007/s004250050651

Porchia, A. C., and Salerno, G. L. (1996). Sucrose biosynthesis in a prokaryotic organism: presence of two sucrose-phosphate synthases in *Anabaena* with remarkable differences compared with the plant enzymes. *Proc. Natl. Acad. Sci.* 93, 13600–13604. doi: 10.1073/pnas.93.24.13600

Potocki de Montalk, G., Remaud-Simeon, M., Willemot, R.-M., Sarçabal, P., Planchot, V., and Monsan, P. (2000). Amylosucrase from *Neisseria polysaccharea*: novel catalytic properties. *FEBS Lett.* 471, 219–223. doi: 10.1016/S0014-5793(00)01406-X

Potts, M., Slaughter, S. M., Hunneke, F.-U., Garst, J. F., and Helm, R. F. (2005). Desiccation tolerance of prokaryotes: Application of principles to human cells. *Integr. Comp. Biol.* 45, 800–809. doi: 10.1093/icb/45.5.800

Prabha, S., Vijay, A. K., Paul, R. R., and George, B. (2022). Cyanobacterial biorefinery: Towards economic feasibility through the maximum valorization of biomass. *Sci. Total Environ.* 814, 152795. doi: 10.1016/j.scitotenv.2021.152795

Qiao, C., Duan, Y., Zhang, M., Hagemann, M., Luo, Q., and Lu, X. (2018). Effects of reduced and enhanced glycogen pools on salt-induced sucrose production in a sucrose-secreting strain of *Synechococcus elongatus* PCC 7942. *Appl. Environ. Microbiol.* 84. doi: 10.1128/AEM.02023-17

Qiao, C., Zhang, M., Luo, Q., and Lu, X. (2019). Identification of two two-component signal transduction mutants with enhanced sucrose biosynthesis in *Synechococcus elongatus* PCC 7942. *J. Basic Microbiol.* 59, 465–476. doi: 10.1002/jobm.201800676

Rafieenia, R., Atkinson, E., and Ledesma-Amaro, R. (2022). Division of labor for substrate utilization in natural and synthetic microbial communities. *Curr. Opin. Biotechnol.* 75, 102706. doi: 10.1016/j.copbio.2022.102706

Rai, A. N., Bergman, B., and Rasmussen, U. (2002). *Cyanobacteria in symbiosis*. Springer.

Reed, R. H., and Stewart, W. D. P. (1985). Osmotic adjustment and organic solute accumulation in unicellular cyanobacteria from freshwater and marine habitats. *Mar. Biol.* 88, 1–9. doi: 10.1007/BF00393037

Rikkinen, J. (2015). Cyanolichens. *Biodivers. Conserv.* 24, 973–993. doi: 10.1007/s10531-015-0906-8

Rikkinen, J. (2017). "Symbiotic Cyanobacteria in lichens," in *Algal and Cyanobacteria Symbioses*, (World Scientific), 147–167. doi: 10.1142/9781786340580_0005

Rosic, N. (2021). "Molecular mechanisms of stress tolerance in cyanobacteria," in *Ecophysiology and Biochemistry of Cyanobacteria*, ed. R. P. Rastogi (Singapore: Springer Nature), 131–153. doi: 10.1007/978-981-16-4873-1_7

Sabri, S., Nielsen, L. K., and Vickers, C. E. (2013). Molecular control of sucrose utilization in *Escherichia coli* W, an efficient sucrose-utilizing strain. *Appl. Environ. Microbiol.* 79, 478–487. doi: 10.1128/AEM.02544-12

Sakkos, J. K., Santos-Merino, M., Kokarakis, E. J., Li, B., Fuentes-Cabrera, M., Zuliani, P., et al. (2023). Predicting partner fitness based on spatial structuring in a light-driven microbial community. *PLOS Comput. Biol.* 19, e1011045. doi: 10.1371/journal.pcbi.1011045

Santos-Merino, M., Singh, A. K., and Ducat, D. C. (2021). "Sink engineering in photosynthetic microbes," in *Cyanobacteria Biotechnology*, eds. J. Nielsen, S. Lee, G. Stephanopoulos, and P. Hudson (Wiley-VCH), 171–209. doi: 10.1002/9783527824908.ch6

Santos-Merino, M., Torrado, A., Davis, G. A., Röttig, A., Bibby, T. S., Kramer, D. M., et al. (2021). Improved photosynthetic capacity and photosystem I oxidation via heterologous metabolism engineering in cyanobacteria. *Proc. Natl. Acad. Sci.* 118, e2021523118. doi: 10.1073/pnas.2021523118

Santos-Merino, M., Yun, L., and Ducat, D. C. (2023). Cyanobacteria as cell factories for the photosynthetic production of sucrose. *Front. Microbiol.* 14, 1126032. doi: 10.3389/fmicb.2023.1126032

Savakis, P., and Hellingwerf, K. J. (2015). Engineering cyanobacteria for direct biofuel production from CO_2. *Curr. Opin. Biotechnol.* 33, 8–14. doi: 10.1016/j.copbio.2014.09.007

Shinde, S., Zhang, X., Singapuri, S. P., Kalra, I., Liu, X., Morgan-Kiss, R. M., et al. (2020). Glycogen metabolism supports photosynthesis start through the oxidative pentose phosphate pathway in cyanobacteria. *Plant Physiol.* 182, 507–517. doi: 10.1104/pp.19.01184

Singh, A. K., Santos-Merino, M., Sakkos, J. K., Walker, B. J., and Ducat, D. C. (2022). Rubisco regulation in response to altered carbon status in the cyanobacterium *Synechococcus elongatus* PCC 7942. *Plant Physiol.* 189, 874–888. doi: 10.1093/plphys/kiac065

Singh, S., Kumar, V., Shekar, S., Kapoor, D., Bhatia, D., Dhanjal, D. S., et al. (2021). "Phycoremediation of wastewater," in *Ecophysiology and Biochemistry of Cyanobacteria*, ed. R. P. Rastogi (Singapore: Springer Nature), 269–289. doi: 10.1007/978-981-16-4873-1_13

Smith, M. J., and Francis, M. B. (2017). Improving metabolite production in microbial co-cultures using a spatially constrained hydrogel. *Biotechnol Bioeng* 114, 1195–1200. doi: 10.1002/bit.26235

Song, H. S., Renslow, R. S., Fredrickson, J. K., and Lindemann, S. R. (2015). Integrating ecological and engineering concepts of resilience in microbial communities. *Front. Microbiol.* 6. doi: 10.3389/fmicb.2015.01298

Song, K., Tan, X., Liang, Y., and Lu, X. (2016). The potential of *Synechococcus elongatus* UTEX 2973 for sugar feedstock production. *Appl. Microbiol. Biotechnol.* 100, 7865–7875. doi: 10.1007/s00253-016-7510-z

Su, Y., Song, K., Zhang, P., Su, Y., Cheng, J., and Chen, X. (2017). Progress of microalgae biofuel's commercialization. *Renew. Sustain. Energy Rev.* 74, 402–411. doi: 10.1016/j.rser.2016.12.078

Suzuki, E., Ohkawa, H., Moriya, K., Matsubara, T., Nagaike, Y., Iwasaki, I., et al. (2010). Carbohydrate metabolism in mutants of the cyanobacterium *Synechococcus elongatus*

PCC 7942 defective in glycogen synthesis. *Appl Env. Microbiol* 76, 3153–9. doi: 10.1128/AEM.00397-08

Thiel, K., Patrikainen, P., Nagy, C., Fitzpatrick, D., Pope, N., Aro, E.-M., et al. (2019). Redirecting photosynthetic electron flux in the cyanobacterium *Synechocystis* sp. PCC 6803 by the deletion of flavodiiron protein Flv3. *Microb. Cell Factories* 18, 189. doi: 10.1186/s12934-019-1238-2

Tóth, G. S., Siitonen, V., Nikkanen, L., Sovic, L., Kallio, P., Kourist, R., et al. (2022). Photosynthetically produced sucrose by immobilized *Synechocystis* sp. PCC 6803 drives biotransformation in *E. coli*. *Biotechnol. Biofuels Bioprod.* 15, 146. doi: 10.1186/s13068-022-02248-1

Tsuge, Y., Kawaguchi, H., Sasaki, K., and Kondo, A. (2016). Engineering cell factories for producing building block chemicals for bio-polymer synthesis. *Microb. Cell Factories* 15, 1–12. doi: 10.1186/s12934-016-0411-0

Vadyvaloo, V., Smirnova, I. N., Kasho, V. N., and Kaback, H. R. (2006). Conservation of residues involved in sugar/H^+ symport by the sucrose permease of *Escherichia coli* relative to lactose permease. *J Mol Biol* 358, 1051–9. doi: 10.1016/j.jmb.2006.02.050

Vargas, W. A., Nishi, C. N., Giarrocco, L. E., and Salerno, G. L. (2011). Differential roles of alkaline/neutral invertases in *Nostoc* sp. PCC 7120: Inv-B isoform is essential for diazotrophic growth. *Planta* 233, 153–162. doi: 10.1007/s00425-010-1288-5

Vargas, W. A., and Salerno, G. L. (2010). The Cinderella story of sucrose hydrolysis: Alkaline/neutral invertases, from cyanobacteria to unforeseen roles in plant cytosol and organelles. *Plant Sci.* 178, 1–8. doi: 10.1016/j.plantsci.2009.09.015

Vargas, W., Cumino, A., and Salerno, G. L. (2003). Cyanobacterial alkaline/neutral invertases. Origin of sucrose hydrolysis in the plant cytosol? *Planta* 216, 951–960. doi: 10.1007/s00425-002-0943-x

Waditee-Sirisattha, R., and Kageyama, H. (2022). "Extremophilic cyanobacteria," in *Cyanobacterial Physiology*, eds. H. Kageyama and R. Waditee-Sirisattha (Academic Press), 85–99. doi: 10.1016/B978-0-323-96106-6.00012-5

Wan, H., Wu, L., Yang, Y., Zhou, G., and Ruan, Y.-L. (2018). Evolution of sucrose metabolism: The dichotomy of invertases and beyond. *Trends Plant Sci.* 23, 163–177. doi: 10.1016/j.tplants.2017.11.001

Weiss, T. L., Young, E. J., and Ducat, D. C. (2017). A synthetic, light-driven consortium of cyanobacteria and heterotrophic bacteria enables stable polyhydroxybutyrate production. *Metab. Eng.* 44, 236–245. doi: 10.1016/j.ymben.2017.10.009

Wendisch, V. F., Jorge, J. M., Pérez-García, F., and Sgobba, E. (2016). Updates on industrial production of amino acids using *Corynebacterium glutamicum*. *World J. Microbiol. Biotechnol.* 32, 1–10. doi: 10.1007/s11274-016-2060-1

Werner, G. D. A., Strassmann, J. E., Ivens, A. B. F., Engelmoer, D. J. P., Verbruggen, E., Queller, D. C., et al. (2014). Evolution of microbial markets. *Proc. Natl. Acad. Sci. U. S. A.* 111, 1237–1244. doi: 10.1073/pnas.1315980111

Wu, S., Snajdrova, R., Moore, J. C., Baldenius, K., and Bornscheuer, U. T. (2021). Biocatalysis: enzymatic synthesis for industrial applications. *Angew. Chem. Int. Ed.* 60, 88–119. doi: 10.1002/anie.202006648

Xie, J., Cai, K., Hu, H.X., Jiang, Y.L., Yang, F., Hu, P.F., Cao, D.D., Li, W.F., Chen, Y. and Zhou, C.Z (2016). Structural analysis of the catalytic mechanism and substrate specificity of Anabaena alkaline invertase InvA reveals a novel glucosidase. *J. Biol. Chem.* 291, 25667–25677. doi: 10.1074/jbc.M116.759290

Xu, Y., Tiago Guerra, L., Li, Z., Ludwig, M., Charles Dismukes, G., and Bryant, D. A. (2013). Altered carbohydrate metabolism in glycogen synthase mutants of *Synechococcus* sp. strain PCC 7002: Cell factories for soluble sugars. *Metab. Eng.* 16, 56–67. doi: 10.1016/j.ymben.2012.12.002

Yamaguchi, K., Suzuki, I., Yamamoto, H., Lyukevich, A., Bodrova, I., Los, D. A., et al. (2002). A two-component Mn^{2+}-sensing system negatively regulates expression of the mntCAB operon in *Synechocystis*. *Plant Cell* 14, 2901–2913. doi: 10.1105/tpc.006262

Yu, J., Liberton, M., Cliften, P. F., Head, R. D., Jacobs, J. M., Smith, R. D., et al. (2015). *Synechococcus elongatus* UTEX 2973, a fast-growing cyanobacterial chassis for biosynthesis using light and CO_2. *Sci. Rep.* 5, 8132. doi: 10.1038/srep08132

Zhang, L., Chen, L., Diao, J., Song, X., Shi, M., and Zhang, W. (2020). Construction and analysis of an artificial consortium based on the fast-growing cyanobacterium *Synechococcus elongatus* UTEX 2973 to produce the platform chemical 3-hydroxypropionic acid from CO_2. *Biotechnol. Biofuels* 13. doi: 10.1186/s13068-020-01720-0

Zhang, S., Sun, H., Sun, J., Luo, Q., Luan, G., and Lu, X. (2021). "Engineering cyanobacteria cell factories for photosynthetic production of sucrose," in *Ecophysiology and Biochemistry of Cyanobacteria*, ed. R. P. Rastogi (Singapore: Springer Nature), 373–399. doi: 10.1007/978-981-16-4873-1_17

Zhao, R., Sengupta, A., Whelan, R., Pinkerton, T., Menasalvas, J., Eng, T., et al. (2022). Photobiological production of high-value pigments via compartmentalized co-cultures using Ca-alginate hydrogels. *Sci. Rep.* 12, 22163. doi: 10.1038/s41598-022-26437-y

Zhong, C. (2020). Industrial-scale production and applications of bacterial cellulose. *Front. Bioeng. Biotechnol.* 8, 605374. doi: 10.3389/fbioe.2020.605374

Zhu, H., Xu, L., Luan, G., Zhan, T., Kang, Z., Li, C., et al. (2022). A miniaturized bionic ocean-battery mimicking the structure of marine microbial ecosystems. *Nat. Commun.* 13, 5608. doi: 10.1038/s41467-022-33358-x

Zorina, A., Sinetova, M. A., Kupriyanova, E. V., Mironov, K. S., Molkova, I., Nazarenko, L. V., et al. (2016). *Synechocystis* mutants defective in manganese uptake regulatory system, ManSR, are hypersensitive to strong light. *Photosynth. Res.* 130, 11–17. doi: 10.1007/s11120-015-0214-x

Zuñiga, C., Li, T., Guarnieri, M. T., Jenkins, J. P., Li, C. T., Bingol, K., et al. (2020). Synthetic microbial communities of heterotrophs and phototrophs facilitate sustainable growth. *Nat. Commun.* 11. doi: 10.1038/s41467-020-17612-8

CHAPTER 2:

ENHANCEMENT OF CYANOBACTERIAL SUCROSE BIOSYNTHESIS THROUGH CULTIVATION METHODS

This chapter was adapted from text originally published in:

Yun, L. Zegarac, R., and Ducat, D.C. (2024) Impact of irradiance and inorganic carbon availability on heterologous sucrose production in *Synechococcus elongatus* PCC 7942. *Front. Plant Sci*. 15: 1378573. doi: 10.3389/fpls.2024.1378573

Introduction

There is a need for sustainable carbohydrate feedstocks as we increasingly look to biotechnology and green chemistry approaches for energy and other commodity chemicals. Sucrose is one significant feedstock for bio-ethanol (Balat and Balat, 2009) and is a promising building block for many value-added chemicals (Peters et al., 2010). However, sucrose is typically produced by plant crop species (*e.g.*, sugar beet and sugar cane) (Peters et al., 2010), giving rise to ethical concerns about diverting arable land and potable water from food production to fuel and chemicals (Graham-Rowe, 2011; Lang et al., 2017). Cellulosic biomass is another promising alternative source of fermentable carbohydrates that is under active study, yet the high costs of converting lignocellulosic materials into simple carbohydrates suitable for fermentation is currently prohibitive (Graham-Rowe, 2011; Ziolkowska, 2014). For these reasons, an alternative source for sucrose that circumvents the controversies and complexities of plants is desirable.

Cyanobacteria are a diverse phylum of photosynthetic prokaryotes that are under consideration as an alternative carbohydrate feedstock species due to their ability to hyperaccumulate soluble sugars under certain growth conditions (Hays and Ducat, 2015). Moreover, cyanobacteria are less likely to compete for land and water resources with food crops, are faster growing, relatively easier to genetically engineer, and have a higher photosynthetic efficiency than land plant sources of carbohydrate feedstocks (Parmar et al., 2011; Satta et al., 2023). One promising approach for cyanobacterial sucrose production involves the heterologous expression of sucrose permease (*cscB*), which was originally reported to allow up to ~80% of fixed carbon to be exported in the form of sucrose when expressed in the model cyanobacterium, *Synechococcus elongatus* PCC 7942 (Ducat et al., 2012). The high productivity of such strains is in part due to an emergent property whereby photosynthetic activity is increased: exporting sucrose increases the quantum efficiency of photosystem II, rate of photosystem II oxygen evolution, and carbon fixation rate (Ducat et al., 2012; Abramson et al., 2016; Santos-Merino et al., 2021, 2023; Wang et al., 2023). Additional genetic modifications have been employed to increase sucrose export by increasing carbon flux to the sucrose synthesis pathway and/or decreasing flux to potential competing pathways, with mixed success (Santos-Merino et al., 2023). For example, multiple groups have shown that sucrose productivity can be enhanced by artificially over-expressing sucrose phosphate synthase (*sps*), an enzyme involved in a rate-limiting step of sucrose synthesis, in the background of sucrose exporting lines (Ducat et al., 2012; Duan et al., 2016; Hays

et al., 2017; Qiao et al., 2018).

Similar strategies to enable sucrose export have been used across a variety of cyanobacterial species; *cscB* has been expressed in *S. elongatus* UTEX 2973 (Lin et al., 2020; Zhang et al., 2020), *Synechococcus* sp. PCC 7002 (Xu et al., 2013; Han et al., 2023), and *Synechocystis* sp. PCC 6803 (Du et al., 2013; Thiel et al., 2019). Different cyanobacterial species exhibit varying rates of sucrose productivity (Santos-Merino et al., 2023), though it is often uncertain if inter-species differences are due to genetics, distinct conditions utilized for laboratory growth, metabolic requirements, tolerances for environmental stresses, or inherent photosynthetic capacities (Billis et al., 2014; Ungerer et al., 2018b; Cassier-Chauvat et al., 2021; Adomako et al., 2022). For instance, *S. elongatus* PCC 7942 and *S. elongatus* UTEX 2973 share 99.9% genome similarity, yet the latter has significantly faster growth rates, higher light and temperature tolerances, and has been reported to have a significantly higher sucrose productivity (Yu et al., 2015; Ungerer et al., 2018b; Lin et al., 2020; Adomako et al., 2022). A handful of single nucleotide polymorphisms appear to significantly contribute to enhanced tolerance of light and heat in *S. elongatus* UTEX 2973 (Ungerer et al., 2018b), and these strains also exhibit substantially faster growth rates (2.5 hour doubling time compared to 7-8 hours). Therefore, it is possible that the increased sucrose productivity of engineered *S. elongatus* UTEX 2973 strains may be due to an inherently improved photosynthetic capacity. Alternatively, other factors like higher routine temperature, light growth conditions or altered partitioning of fixed carbon may contribute to the productivity of *S. elongatus* UTEX 2973 (Mueller et al., 2017; Hendry et al., 2019).

In this study, we set out to systematically assess how different laboratory equipment and growth conditions impact the efficacy of sucrose production, with a particular focus on light and inorganic carbon availability as two critical factors that may impact sucrose secretion rates, and that could contribute (in part or in full) to the differences in sucrose productivity observed across different laboratories and cyanobacterial species. The interest in exploring cyanobacteria as an alternative carbohydrate feedstock has led to many recent reports documenting sucrose production, yet, as we recently reviewed (Santos-Merino et al., 2023), there can be considerable variation in productivity between different publications, even when the species and genetic modifications are identical. We explored a variety of commercial and custom-built cyanobacterial growth chambers, and report cultivation conditions and bioproduction values in standardized units to facilitate cross-comparisons between laboratories. We find a direct relationship between irradiance used for

cyanobacterial cultivation and sucrose productivity, especially when inorganic carbon availability was not limiting. Our results may be valuable for the broader community of scientists working with different strains of cyanobacteria engineered as potential alternative carbohydrate feedstocks, and especially point to limitations imposed on productivity caused by inefficient CO_2 delivery methods. Additionally, our results have implications for the degree of variation in sucrose productivity of related cyanobacterial species, which may be significantly influenced by cultivation conditions rather than solely due to inherent metabolic and physiological limitations of slower-growing species.

Results

Assessing high-light tolerance in S. elongatus

We first selected a strain of *S. elongatus* that has been engineered for sucrose secretion in a salt-independent manner. Briefly, hyperaccumulation of cytosolic sucrose is a common strategy for osmotic stress protection in many freshwater cyanobacterial species (Klähn and Hagemann, 2011), where this compatible solute can act as a counter osmoticum while also conferring other cellular protective effects. A rate-limiting step of sucrose biosynthesis occurs at the enzyme sucrose phosphate synthase (SPS), that catalyzes the condensation of NDP-glucose with fructose 6-phosphate to form sucrose 6-phosphate. SPS enzymes are frequently encoded as a bidomainal protein that also contains sucrose 6-phosphate phosphatase (SPP) activity that dephosphorylates this intermediate to sucrose. We and others have found that expression of sucrose permease (*cscB*), a symporter of sucrose and protons, will lead to the export of cytosolic sucrose to the medium (Ducat et al., 2012; Santos-Merino et al., 2023). In *S. elongatus* strains with inducible copies of both *sps* and *cscB*, sucrose synthesis and export can be achieved in the absence of external osmotic pressure (Abramson et al., 2016, 2018; Lin et al., 2020; Dan et al., 2022). We therefore selected this strain to minimize the requirement for the addition of salt to the growth medium.

We first used the MC-1000 multi-cultivator to evaluate the impact of varied light intensity (150, 250, 500, 1000, 2000 µmol photons m^{-2} s^{-1}) on growth and sucrose production of *S. elongatus* PCC 7942 *cscB*/*sps* strains and to broadly assess light tolerance. The growth of wild-type (WT) strains cultured with 150 and 1000 µmol photons m^{-2} s^{-1}, and non-exporting *cscB*/*sps* with 1000 µmol photons m^{-2} s^{-1} grew at similar rates, reaching a final density of ~2.2 OD_{750} (Figure 2.1A, left). Sucrose-exporting strains, however, can partition a large fraction of their fixed carbon to secreted sucrose, leading to less cellular growth and biomass under certain conditions (Ducat et

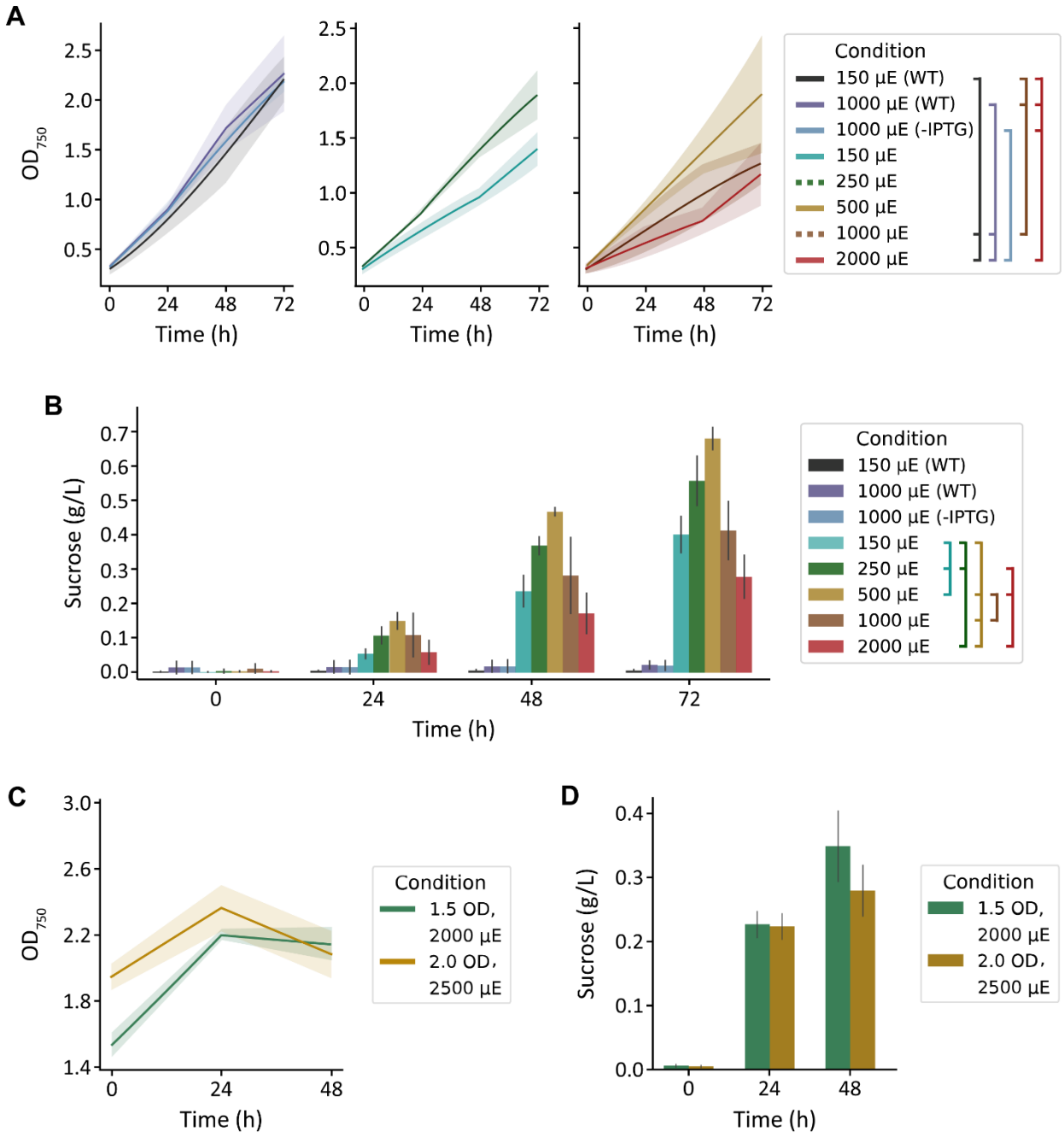

Figure 2.1. Growth and sucrose titers of MC-1000 cultures. Growth and sucrose yields of WT and cscB/sps-expressing S. elongatus grown in the MC-1000 under various light intensities. **(A)** The OD_{750} of non-sucrose exporting (left) and exporting (center and right) strains, and **(B)** sucrose production of cultures started at low cell density (~0.3 OD_{750}). Brackets in the legend denote significant differences ($p < 0.05$) at 72 h by one-way ANOVA in **(A)** all cultures and **(B)** induced cultures. **(C)** The OD_{750} and **(D)** sucrose production of cultures started at high cell densities (~1.5 and 2 OD_{750}). Error bars denote standard deviation.

al., 2012) (*see also*, Figure S2.3). The highest OD_{750} amongst sucrose exporters were from cultures grown with moderate irradiances of 250 and 500 µmol photons m^{-2} s^{-1} (Figure 2.1A, right), though differences were not statistically significant from other exporting conditions ($p > 0.05$). For sucrose-secreting lines in the MC-1000, there was a direct correlation between illumination and both cell growth and sucrose production up to 500 µmol photons m^{-2} s^{-1}; light intensities beyond this threshold led to a decline in productivity (Figure 2.1A, B). Sucrose production over 72 hours peaked at 0.56 g L^{-1} for 250 µmol photons m^{-2} s^{-1} and 0.68 g L^{-1} for 500 µmol photons m^{-2} s^{-1} ($p < 0.001$ against all other light conditions) (Figure 2.1B). The relationship between irradiance and growth, however, is abolished when strains are not induced to export sucrose, and growth rates were relatively unaffected by illumination between 150 and 1000 µmol photons m^{-2} s^{-1} (Figure 2.1A, left). These data suggest that high light may indeed be harmful, and the increased photosynthetic capacity provided by a heterologous sink (*i.e.*, sucrose export) is not protective against light stress. However, it appears that *S. elongatus* PCC 7942 can remain resilient when not imposed with the additional burden of producing and secreting sucrose.

To evaluate if the sucrose productivity in these experiments was limited by a low-starting density, we increased the starting inoculation density. Since the effects of self-shading within higher density cultures lead to an effectively lower irradiation under the same outside illumination, we utilized brighter lights for our high-density starter cultures of 1.5 and 2.0 OD_{750}, the upper range of OD_{750} the MC-1000 was able to support. To select the irradiances for these dense cultures, we revisited the most successful light intensity in our previous experiment. Cultures of 0.3 OD_{750} exposed to 500 µmol photons m^{-2} s^{-1} light receive ~300 µmol photons m^{-2} s^{-1} light when measured 1 cm from the surface (Figure S2.4). Application of 2000 and 2500 µmol photons m^{-2} s^{-1} to cultures of 1.5 and 2.0 OD_{750}, respectively, would achieve similar internal light intensities (Figure S2.4). We observed limited growth within the first 24 h of these cultures, but the density of the culture plateaued or declined in the following day to values statistically similar to starting turbidities ($p > 0.05$) (Figure 2.1C). Cultures grown with 2000 µmol photons m^{-2} s^{-1} produced 0.23 g L^{-1} sucrose within the first day, and had a final sucrose content of 0.35 g L^{-1} ($p > 0.4$); cultures grown with 2500 µmol photons m^{-2} s^{-1} produced 0.22 and 0.28 g L^{-1} sucrose at 24 and 48 h ($p = 1.0$), respectively (Figure 2.1D). Notably, the level of sucrose production from high density cultures was only marginally improved (~15%) at 48 h relative to cultures seeded at a lower density grown with 2000 µmol photons m^{-2} s^{-1} ($p = 0.002$) (Figure 2.1B, D).

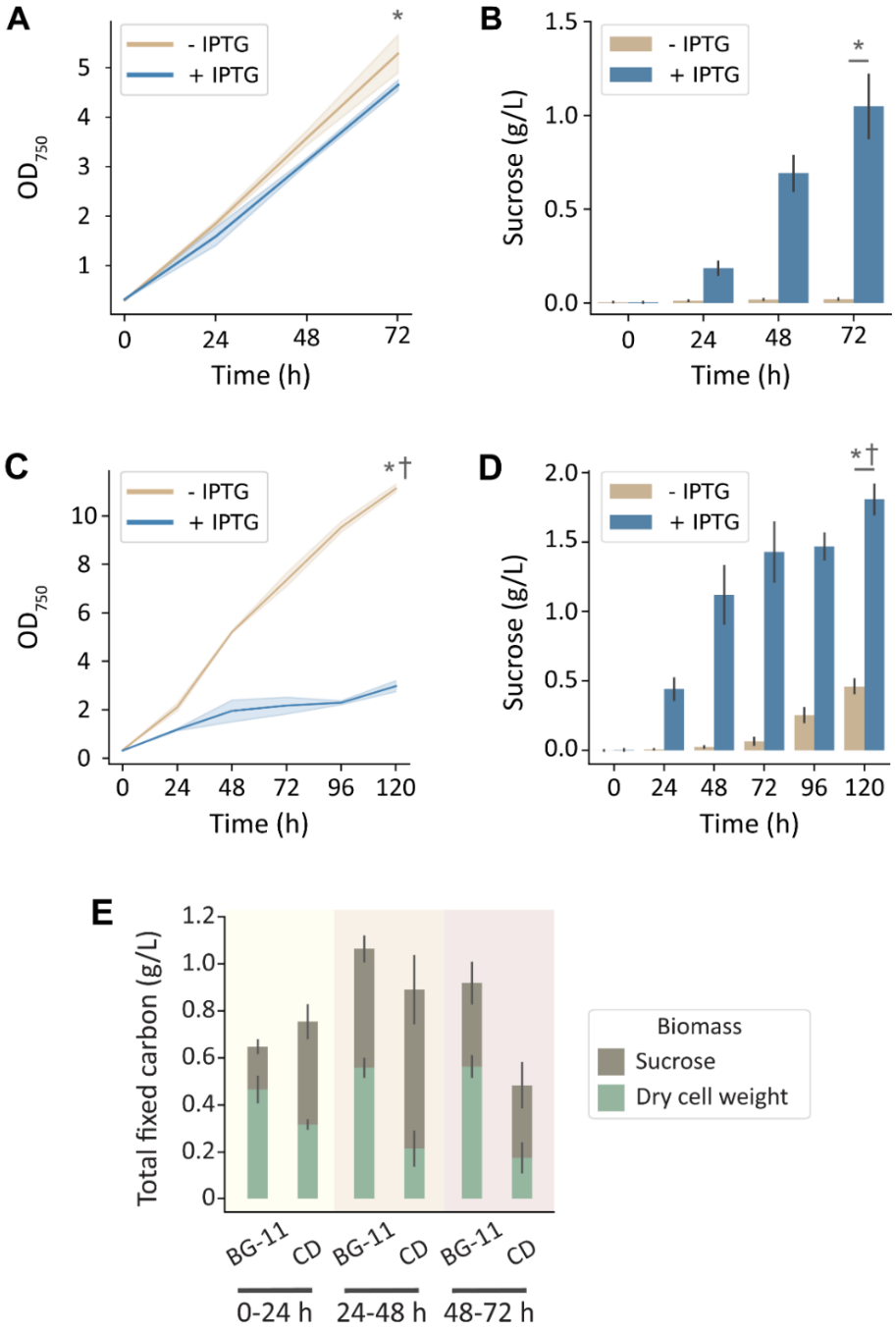

Figure 2.2. Growth and sucrose titers of HDC cultures grown with different media. Growth and sucrose production of induced and uninduced *cscB*/*sps*-expressing *S. elongatus* grown in the CellDEG HDC cultivator system at moderate light intensity (~250 µmol photons m^{-2} s^{-1}). The OD_{750} and sucrose production, respectively, of cultures grown in **(A, B)** BG-11 medium, and **(C, D)** CD medium. **(E)** Total fixed carbon for induced strains in BG-11 and CD media as shown by sucrose and dry cell weight accumulated per day. Error bars denote standard deviation. Asterisks denote significant differences between induction conditions at the indicated timepoint ($p < 0.005$)

Figure 2.2. (cont'd)
by independent samples t-test. Daggers denote significant differences in induced cultures between **(A, B)** and **(B, C)** conditions ($p < 0.001$) by independent samples t-test.

Curiously, both the cellular growth rate and sucrose productivity were relatively modest in the MC-1000 in comparison to values reported for similar strains by our group and others (Santos-Merino et al., 2023), suggesting that these cultures might be limited by another environmental variable (Figure 2.1A, B). Although 3% CO_2 was bubbled into the cultivation tubes for these experiments, the method of delivery (sparging via a large-bore needle) may not be the most efficient compared to other methods for enriching inorganic carbon. Consistent with a possible inorganic carbon limitation, sucrose productivity was slightly, but significantly, enhanced in MC-1000 cultures supplemented with 10 mM HCO_3^- (Figure 2.1B) relative to cultures without bicarbonate when grown with 500, 1000, and 2000 µmol photons m^{-2} s^{-1} ($p = 0.038$, 0.020, 0.028, respectively) (Figure S2.5). However, we were unable to overcome any potential limitation of inorganic carbon in dense cultures through the supplementation of additional HCO_3^- (Figure S2.6).

To more directly evaluate the hypothesis that carbon limitation was limiting for growth and sucrose productivity in the MC-1000, we utilized the High-Density Cultivation (HDC) system (CellDEG GmbH, Germany). These cultivation vessels are designed to deliver a saturating level of inorganic carbon through a permeable membrane with a large surface area (Lippi et al., 2018). Using an identical growth medium (BG-11), a significant enhancement of cell growth and sucrose production was observed in the CellDeg HDC system relative to the MC-1000 with comparable illumination (250 µmol photons m^{-2} s^{-1}). Strains that were not induced to export sucrose grew to 5.3 OD_{750} over 72 h while producing a marginal amount of sucrose (0.02 g L^{-1}). Strains induced to secrete sucrose grew to 4.6 OD_{750} and produced 1.0 g L^{-1} sucrose (Figure 2.2A, B). Curiously, under these conditions of high inorganic carbon availability, we observed little, but significant, difference in growth rate in the sucrose-exporting strains despite a significant rate of carbon export in the form of sucrose (Figure 2.2A, B, E).

Since nutrients in BG-11 medium can become limiting at higher density, we next evaluated an enriched medium (CD) designed to support high-density cultures, such as those achievable in the HDC system (Dienst et al., 2020). When cultures were grown in CD medium, non-exporting strains reached 11.1 OD_{750} over the course of 5 days (Figure 2.2C), while also secreting a disproportionally high level of sucrose for an uninduced culture (Figure 2.2D). Strains induced to export sucrose were significantly stunted in growth after 120 h (3 OD_{750}; Figure 2.2C) and secreted

sucrose at a higher rate.

Increasing light and CO_2 availability to enhance sucrose synthesis

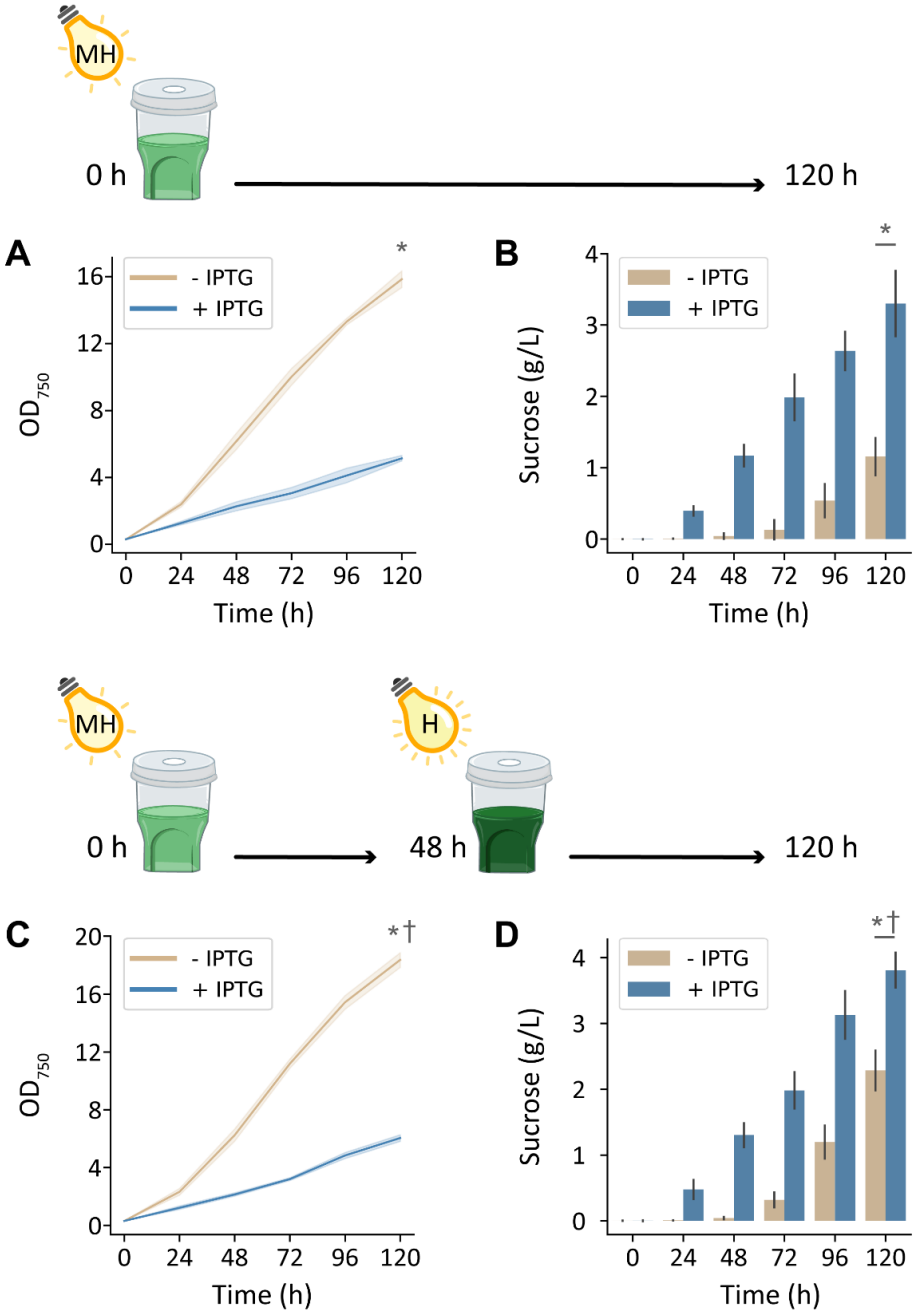

Figure 2.3. Growth and sucrose titers of HDC cultures grown with varying irradiances. Growth and sucrose production of induced and uninduced *cscB*/*sps*-expressing *S. elongatus* grown in the HDC system with moderately high and high-light intensity (MH and H, respectively) and CD medium. The OD_{750} and supernatant sucrose concentration of cultures grown with **(A, B)** 500 µmol photons m^{-2} s^{-1} for 0-120 h, and **(C, D)** 500 µmol photons m^{-2} s^{-1} for 0-48 h and 1000 µmol photons m^{-2} s^{-1} for 48-120 h. Error bars denote standard deviation. Asterisks denote significant differences between induction conditions at the indicated timepoint ($p < 0.001$) by independent

Figure 2.3 (cont'd)
samples t-test. Daggers denote significant differences in induced cultures between **(A, B)** and **(C, D)** conditions ($p < 0.005$) by independent samples t-test.

Environmental conditions enriched with nutrients and inorganic carbon supported substantially higher cyanobacterial production with increased irradiation. Cultivating *cscB*/*sps* strains with high CO_2 (HDC) and with 500 μmol photons m^{-2} s^{-1}, non-exporting and sucrose-exporting strains reached OD_{750} of 15.8 and 5.2, respectively (Figure 2.3A). Furthermore, strains induced to secrete sucrose accumulated up to 3.3 g L^{-1} over the course of 5 days, while uninduced cultures accumulated 1.15 g L^{-1} (Figure 2.3B). Further enhancements in bioproduction could be achieved by further increasing light intensity to 1000 μmol photons m^{-2} s^{-1} at 48 h when cultures were more turbid: sucrose-secreting strains reached an OD_{750} of 6.0 and sucrose yields of 3.8 g L^{-1} (Figure 2.3C, D). Uninduced strains under these growth conditions achieved 18.4 OD_{750} and secreted a surprisingly high amount of sucrose, reaching 2.3 g/L sucrose at the end of 120 h.

Discussion

Considerable variation in the productivity of cyanobacteria engineered to secrete sucrose has been reported in the literature (Table 1.1), and this variability has significant implications for the viability of biotechnological applications. Obviously, light is a crucial component of photosynthetically driven cultivation, yet it is also well-established that over-irradiation of cyanobacteria can lead to cell damage and/or death if surplus light energy is not safely dissipated (Montgomery, 2014). *S. elongatus* PCC 7942 has been often described in the literature as a strain that prefers a relatively low-light, and many groups routinely cultivate this strain ≤100 μmol photons m^{-2} s^{-1}. Our results show that light and CO_2 availability strongly impact the bioproductivity of sucrose-secreting cyanobacterial strains, independent of the genetic background. Under conditions of high nutrient and CO_2 availability, cell biomass and sucrose secretion rates are positively correlated with irradiation, up to 1000 μmol photons m^{-2} s^{-1} (Figures 2, 3): a light intensity regarded as photodamaging for *S. elognatus* in some literature. The light tolerance we observe is consistent with recent publications reporting that the maximum growth rate of *S. elongatus* PCC 7942 is achieved with 400 μmol photons m^{-2} s^{-1} (Takatani et al., 2015; Ungerer et al., 2018a). Further complication of *S. elongatus*'s light tolerance is that self-shading in dense cultures or chambers with long optical cross-sections can rapidly attenuate effective light availability (Andersson et al., 2019). Our results suggest that differences in cyanobacterial cultivation conditions likely can account for a significant portion of variability (up to 3- to 10-fold)

in reported sucrose production values, even when solely accounting for strains grown in common, commercially available photobioreactors.

We observe that the mechanism of CO_2 delivery strongly impacts the bioproduction potential for sucrose-secreting cyanobacteria at higher light intensities. In the MC-1000 cultivator, CO_2 is delivered via a bubble column-style sparging system, and we observed indications of carbon limitation despite continual sparging with 3% CO_2 gas. In the MC-1000, a positive correlation for production was observed with increasing illumination up to ≤ 500 µmol photons m^{-2} s^{-1} (Figure 2.1A, B). Interestingly, even the highest light conditions were not lethal (Figure 2.1A; 2000 µmol photos m^{-2} s^{-1} is roughly equivalent to full, midday sunlight), although *S. elongatus* PCC 7942 is frequently described in the literature as a low-light tolerant strain (*e.g.*, Ungerer et al., 2018b; Takatani et al., 2022; Walker and Pakrasi, 2022). Furthermore, the final OD_{750} and sucrose productivities of strains cultivated in the MC-1000 system were substantially lower than values reported by our group and others with the same growth medium in other bioreactor designs (Abramson et al., 2016, 2018; Qiao et al., 2018). One possible explanation may be that inorganic carbon availability could be limiting, despite the continual sparging of 3% CO_2 delivered via a stream of CO_2 bubbles through a submerged needle design (Markou et al., 2014).

When cultures were grown under conditions with greater inorganic carbon and/or nutrient availability, increasing illumination resulted in an even greater boost in productivity. The HDC system uses cultivators with a gas-permeable bottom inserted into a carrier plate that exposes it to the CO_2 headspace created by a HCO_3^- buffer reservoir; the device can generate up to 8% CO_2 under the conditions outlined in this work (CellDEG GmbH, 2020). Using the HDC system, uninduced *cscB*/*sps* strains achieved an OD_{750} of 5.3, while induced strains reached an OD_{750} of 4.6 and sucrose yield of 1.0 g L^{-1} when grown in BG-11 medium (Figure 2A, B). For sucrose-exporting strains, this amounts to 245% higher OD_{750} and 188% more sucrose than cultures grown in the MC-1000 with the same medium and irradiance (250 µmol photons m^{-2} s^{-1}). Importantly, under conditions of saturating inorganic carbon, we do not observe a "cost" for sucrose secretion, as indicated by the comparable levels of cellular biomass even when substantial sucrose is secreted (Figure 2.2E). This suggests that growth does not have to be sacrificed when inorganic carbon is not a limiting factor, assuming that the fraction of fixed carbon diverted to sucrose production does not exceed a threshold value. By comparison, when grown in CD medium, the OD_{750} of non-exporting strains rose to an average of 11.1, but the OD_{750} of sucrose-secreting strains dropped to

~3.0 at the end of the 120 h experimental period (Figure 2.2C). We attribute this loss of cell biomass in cultures induced to secrete sucrose to the higher osmotic pressure of CD medium. At ~140 mOsm, CD medium has an osmolarity that is approximately 3-fold higher than that of BG-11 alone and can provide osmotic pressure equivalent to BG-11 supplemented with ~50 mM NaCl. The strain in this study produces sucrose utilizing a heterologous salt-independent SPS; however, increased salt or osmotic stress engages the endogenous salt-dependent sucrose production pathways and has been shown to lead to a higher diversion of fixed carbon towards sucrose biosynthesis (Ducat et al., 2012; Kirsch et al., 2019; Liang et al., 2020). Sucrose exporters grown in CD medium produced 139% more sucrose than their BG-11 counterparts by 72 hours, and a total of 1.8 g L^{-1} sucrose by 120 h (Figure 2.2D). Non-exporting strains in CD medium produce more sucrose than in BG-11 as well; this can also be explained by the medium exerting osmotic stress, and thus activating the native SPS.

To potentially combine the productivity gains of cultivating with high light with those of high CO_2 availability, we required a separate light source capable of reaching intensities beyond those of most commercial photobioreactors. For this purpose, we created a custom LED light source in-house consisting of four COB LEDs used for growth of photosynthetic organisms; when placed above the HDC and shaker, there is generally an equitable distribution of light between the six cultivators. By cultivating strains in the HDC system with CD medium and 250 µmol photons m^{-2} s^{-1}, growth and sucrose yield increased in both induced and uninduced *cscB*/*sps* strains. By doubling irradiance to 500 µmol photons m^{-2} s^{-1}, OD_{750} and sucrose yield increased by 173% and 182%, respectively, in *cscB*/*sps* expressing strains (Figure 2.3A, B). Non-sucrose exporting strains underwent a 142% and 251% increase in growth and sucrose, respectively. Finally, a further increase in culture productivity could be achieved by both increasing light intensity to 1000 µmol photons m^{-2} s^{-1} while taking advantage of the self-shading of higher density cultures. By doubling the light intensity of cultures that were grown with 500 µmol photons m^{-2} s^{-1} at 48 h (average of 2.3 OD_{750}), cell growth increased by 17% ($p < 0.001$) and sucrose productivity increased by 15% ($p < 0.005$) (Figure 2.3C, D). The highest sucrose productivity we report was reached under these conditions, at 47.8 mg L^{-1} h^{-1}. Surprisingly, sucrose bioproduction was nearly as strong in strains not induced to express *cscB*/*sps* (highest productivity observed at 45.3 mg L^{-1} h^{-1}), likely due to a combination of very high cell density (OD_{750} up to 18.3) and induction of endogenous sucrose production via native osmotic-responsive pathways (Figure 2.3A, B). This latter observation may

suggest an alternative route for high sucrose production from late-phase, dense cultures with only basal levels of activation of the sucrose export pathway.

Conclusions

In this study we assessed how irradiance, inorganic carbon availability, and cultivation method affect the growth and sucrose production of *S. elongatus* PCC 7942. We found that increasing light intensity up to 1000 μmol photons m^{-2} s^{-1} has a positive effect on sucrose production, and higher irradiances can be tolerated if cultures grow into sufficient turbidity. By adjusting light regimes and increasing CO_2 availability, *S. elongatus cscB*/*sps* reached a productivity of 47.8 mg sucrose L^{-1} h^{-1}, which is comparable to or exceeds other reported strains, including some metabolic engineering interventions that can negatively affect cell health. Our survey underscores the importance of cultivation conditions on sucrose productivity and may partially explain the variability observed across different institutions using similar strains. These results may contribute insights into future optimization of cyanobacterial bioproduction efforts.

Methods and Materials

Strains and cultivation conditions

The base strain of cyanobacterium we utilize for our sucrose measurements is constructed as reported in Abramson et al., 2016. Briefly, this strain contains a copy of sucrose permease (*cscB*) under an IPTG-inducible Ptrc promoter installed into Neutral Site 3. An additional copy of sucrose phosphate synthase (*sps*) cloned from *Synechocystis sp.* PCC 6803 is also expressed under Ptrc and is integrated into the genome at Neutral Site 2. Inducible *sps* allows us to bypass the requirement for external salt for sucrose production that is in many sucrose-secreting strains. For results from WT strains, we use the ATCC strain of *S. elongatus* PCC 7942 (ATCC #33912).

S. elongatus PCC 7942 strains were routinely grown in BG-11 medium (C3061, Sigma-Aldrich, USA) supplemented with 1 g L^{-1} HEPES and set to pH 8.3 with NaOH to maintain or expand cultures. Cultures were incubated in a Multitron Infors HT incubator at 32°C with 2% CO_2, 150 rpm shaking, and ~150 μmol m^{-2} s^{-1} of continuous light from Sylvania 15 W Gro-Lux fluorescent bulbs. To standardize the growth history of strains between different experiments, all cultures were back-diluted 1:10 into BG-11 for three days prior to initiating any of the reported experiments. When needed, 1 mM IPTG was added to induce the expression of *cscB* and *sps* genes at time = 0 h. Chloramphenicol (Cm; 25 μg mL^{-1}) and kanamycin (Kn; 50 μg mL^{-1}) were used to maintain *cscB* and *sps*, respectively. Antibiotics were not added on the final day of back-dilution

to minimize confounding effects.

Examining light tolerance and sucrose production in MC-1000 multi-cultivators

The MC-1000 multi-cultivator system (Photon System Instruments, Czech Republic) was used to examine the light tolerance of *S. elongatus*; the device emits cool white light at varying light intensities (150, 250, 500, 1000, 2000, or 2500 μmol photons m^{-2} s^{-1}). MC-1000 cultures were kept at 32°C and provided with 3% CO_2. Overnight cultures were back-diluted to an OD_{750} of ~0.3 into MC-1000 vessels with fresh BG-11 medium supplemented with 10 mM HCO_3^-, and induced with 1 mM IPTG as needed for low-starting density experiments. Samples were taken at 0, 24, 48, and 72 h for OD_{750} and sucrose measurements.

For the experiments specifically evaluating high-light with high-starting density cultivation in the MC-1000 system, overnight cultures (prepared as outlined in section 2.1) were pelleted in a benchtop centrifuge. The supernatant was removed, and the cell pellet was resuspended with fresh BG-11 medium supplemented with 10 mM HCO_3^- to an OD_{750} of ~1.5 or 2.0 (provided 2000 and 2500 μmol photons m^{-2} s^{-1}, respectively). An additional 10 mM HCO_3^- was added at 24 h for vessels that were provided bicarbonate daily. Samples were taken at 0, 24, and 48 h for OD_{750} measurements and sucrose quantification.

Sucrose production in high-density multi-cultivators

The High-Density Cultivation (HDC) 6.10B starter kit (CellDEG GmbH, Germany) was used for high-CO_2 and high-density cultivation. The kit consists of a bottom base with a buffer reservoir and 10 mL cultivators with a gas permeable bottom membrane. At the start of the experiments, the reservoir was filled with 200 mL of a 3 M $KHCO_3$/ 3 M K_2CO_3 solution to provide CO_2. Cultures prepared in BG-11 were centrifuged for 10 min at 3700 xg and 22°C before removing the supernatant and resuspending to an OD_{750} of ~0.3 with CD medium. CD medium is designed to sustain extended periods of high-density cultivation of photosynthetic microbes, and has higher concentrations of macronutrients (N, P, and K) and micronutrients (Mg, S, Ca, Na, Cl, Fe, Zn, and Mo) relative to BG-11. Due to its enrichment, CD medium has a high osmolarity (~140 mOsm) that is approximately three times greater than of BG-11 (~40 mOsm); the exact composition is available on protocols.io (dx.doi.org/10.17504/protocols.io.2bxgapn). Relevant cultures were induced with 1 mM IPTG before transferring 12 mL to the HDC system cultivators. Moderate-light HDC experiments were incubated in a Multitron incubator (Infors HT, Switzerland) providing ~150 rpm shaking and ~250 μmol photons m^{-2} s^{-1} from Sylvania 15 W

Gro-Lux fluorescent bulbs. High-light HDC experiments were incubated in a growth chamber (AL-36L4, Percival Scientific, USA) with either ~500 μmol photons m^{-2} s^{-1} for 0-120 h, or ~500 μmol photons m^{-2} s^{-1} for 0-48 h and ~1000 μmol photons m^{-2} s^{-1} for 48-120 h from a light array fabricated in-house consisting of four equidistant chip-on-board (COB) LED lights (BXRA-56C5300-H, Bridgelux, USA) (Figure S2.1). Both incubators provided 2% ambient CO_2, constant illumination, and ~150 rpm shaking. Samples were taken at 0, 24, 48, 72, 96, and 120 h to measure OD_{750} and to collect supernatant for sucrose quantification.

Measuring light penetration through culture depth

The following experimental configuration was used to measure the relationship between surface irradiance, light penetration, and culture turbidity: a glass graduated cylinder with a clear bottom was clamped onto a ring stand. A Submersible Spherical Micro Quantum Sensor (US-SQS/L; WALZ, Germany) connected to a LI-250A light meter (LI-COR, USA) was clamped above and in-center of the graduated cylinder. A single COB LED from the in-house lighting device was placed below and center of the graduated cylinder. With this setup, 5 cm of liquid (BG-11 or cell culture at the indicated OD_{750}) fill the graduated cylinder, and the sensor measures the light that penetrates through the liquid when 0, 1, 2, or 3 cm away from the light interface of the culture (0 cm). A black, opaque sheet was wrapped around the graduated cylinder to cover all but the bottom 4 cm of the culture to block ambient light.

To set the desired irradiance (150, 500, 1000, 2000, 3000, or 4000 μmol photons m^{-2} s^{-1}), the graduated cylinder was filled with 5 cm of BG-11, and the sensor was placed flush to the bottom of the glass to measure the incoming light at 0 cm. WT cultures were prepared as outlined in Section 2.1, pelleted, and supernatants removed. Pellets were resuspended with fresh BG-11 to create a concentrate that was diluted with BG-11 to 0.3, 1.0, 2.0, 5.0, and 10.0 OD_{750}. Five mL of each culture filled the graduated cylinder and penetrating irradiances at 1, 2, and 3 cm were recorded at applicable light intensities. For this and setting the irradiance, the average function of the LI-250A was used in which the device averages the values recorded over a 15-second interval.

Sucrose quantification

Samples collected at the time points specified above were pelleted in a microcentrifuge; the supernatants were saved and stored at -20°C until the end of the experiment. Sucrose quantification was performed using the Sucrose/D-Glucose Assay Kit (K-SUCGL; Megazyme, USA).

Dry cell weight determination

To determine the dry cell weight of *S. elongatus* PCC 7942 strains, cultivation conditions were recreated as outlined in Section 2.2 for low-starting density experiments in the MC-1000, and Section 2.3 for moderate-light experiments in the HDC. Samples were collected at a variety of culture densities (OD_{750}) in order to generate a broad distribution for standard curves correlating OD_{750} with dry cell biomass (Figure S2.2). The OD_{750} of collected samples was determined with a visible spectrophotometer (Genesys 20; Thermo Fisher Scientific, USA), washed with Milli-Q water twice, and resuspended into the desired OD_{750} with Milli-Q water. Three to 20 mL of the prepared samples were pelleted in a Falcon tube and most of the supernatant removed; the remaining water was used to create a concentrated resuspension to transfer to a pre-weighed 3 mL glass test tube. Milli-Q water was used as needed to rinse the Falcon tube and added to the glass test tube. Samples were dried in a 90°C oven for 24 h, or until the mass remained stable. The mass of the empty glass test tube was subtracted from the final weight, and the resulting value was divided by the volume used to determine the dry cell weight (g L^{-1}) for corresponding OD_{750}. Python was used to create a linear regression model and derive the function parameters, which was then used to convert OD_{750} into dry cell weight.

ACKNOWLEDGEMENTS

We thank the Ducat Lab for their helpful comments on the manuscript, the Kerfeld Lab for the use of equipment, and the staff of the Plant Research Laboratory for their technical assistance.

The research reported in this manuscript was primarily supported by the National Science Foundation and the Division of Molecular and Cellular Bioscience (Grant: 1845463) to D.C.D. Fellowship and training support provided by a fellowship from the Plant Biotechnology for Health and Sustainability Training Program at Michigan State University (Grant: NIH T32-GM110523). Additional institutional and facilities support from the Office of Science, Office of Basic Energy Sciences of the U.S. Department of Energy (DOE) under grant DE-FG02-91ER2002.

REFERENCES

Abramson, B. W., Kachel, B., Kramer, D. M., and Ducat, D. C. (2016). Increased photochemical efficiency in cyanobacteria via an engineered sucrose sink. *Plant Cell Physiol.* 57, 2451–2460. doi: 10.1093/pcp/pcw169

Abramson, B. W., Lensmire, J., Lin, Y. T., Jennings, E., and Ducat, D. C. (2018). Redirecting carbon to bioproduction via a growth arrest switch in a sucrose-secreting cyanobacterium. *Algal Res.* 33, 248–255. doi: 10.1016/j.algal.2018.05.013

Adomako, M., Ernst, D., Simkovsky, R., Chao, Y.-Y., Wang, J., Fang, M., et al. (2022). Comparative Genomics of *Synechococcus elongatus* Explains the Phenotypic Diversity of the Strains. *mBio* 13, e00862-22. doi: 10.1128/mbio.00862-22

Andersson, B., Shen, C., Cantrell, M., Dandy, D. S., and Peers, G. (2019). The Fluctuating Cell-Specific Light Environment and Its Effects on Cyanobacterial Physiology. *Plant Physiol.* 181, 547–564. doi: 10.1104/pp.19.00480

Balat, M., and Balat, H. (2009). Recent trends in global production and utilization of bio-ethanol fuel. *Appl. Energy* 86, 2273–2282. doi: 10.1016/j.apenergy.2009.03.015

Billis, K., Billini, M., Tripp, H. J., Kyrpides, N. C., and Mavromatis, K. (2014). Comparative Transcriptomics between *Synechococcus* PCC 7942 and *Synechocystis* PCC 6803 Provide Insights into Mechanisms of Stress Acclimation. *PLoS ONE* 9. doi: 10.1371/journal.pone.0109738

Cassier-Chauvat, C., Blanc-Garin, V., and Chauvat, F. (2021). Genetic, Genomics, and Responses to Stresses in Cyanobacteria: Biotechnological Implications. *Genes* 12, 500. doi: 10.3390/genes12040500

CellDEG GmbH (2020). High-Density Cultivation System HDC 6.10B User Manual. (Berlin, Germany: CellDeg GmbH).

Dan, Y., Sun, J., Zhang, S., Wu, Y., Mao, S., Luan, G., et al. (2022). Manipulating the Expression of Glycogen Phosphorylase in *Synechococcus elongatus* PCC 7942 to Mobilize Glycogen Storage for Sucrose Synthesis. *Front. Bioeng. Biotechnol.* 10. doi: 10.3389/fbioe.2022.925311

Dienst, D., Wichmann, J., Mantovani, O., Rodrigues, J. S., and Lindberg, P. (2020). High density cultivation for efficient sesquiterpenoid biosynthesis in *Synechocystis* sp. PCC 6803. *Sci. Rep.* 10, 5932. doi: 10.1038/s41598-020-62681-w

Du, W., Liang, F., Duan, Y., Tan, X., and Lu, X. (2013). Exploring the photosynthetic production capacity of sucrose by cyanobacteria. *Metab. Eng.* 19, 17–25. doi: 10.1016/j.ymben.2013.05.001

Duan, Y., Luo, Q., Liang, F., and Lu, X. (2016). Sucrose secreted by the engineered cyanobacterium and its fermentability. *J. Ocean Univ. China* 15, 890–896. doi: 10.1007/s11802-016-3007-8

Ducat, D. C., Avelar-Rivas, J. A., Way, J. C., and Silvera, P. A. (2012). Rerouting carbon flux to enhance photosynthetic productivity. *Appl. Environ. Microbiol.* 78, 2660–2668. doi: 10.1128/AEM.07901-11

Graham-Rowe, D. (2011). Agriculture: Beyond food versus fuel. *Nature* 474, S6–S8. doi: 10.1038/474S06a

Han, X., Wang, W., and Lu, X. (2023). Engineering *Synechococcus* sp. PCC 7002 for sustainable production of sucrose. *Algal Res.* 74, 103212. doi: 10.1016/j.algal.2023.103212

Hays, S. G., and Ducat, D. C. (2015). Engineering cyanobacteria as photosynthetic feedstock factories. *Photosynth. Res.* 123, 285–295. doi: 10.1007/s11120-014-9980-0

Hays, S. G., Yan, L. L. W., Silver, P. A., and Ducat, D. C. (2017). Synthetic photosynthetic consortia define interactions leading to robustness and photoproduction. *J. Biol. Eng.* 11. doi: 10.1186/s13036-017-0048-5

Hendry, J. I., Gopalakrishnan, S., Ungerer, J., Pakrasi, H. B., Tang, Y. J., and Maranas, C. D. (2019). Genome-Scale Fluxome of *Synechococcus elongatus* UTEX 2973 Using Transient 13C-Labeling Data. *Plant Physiol.* 179, 761–769. doi: 10.1104/pp.18.01357

Kirsch, F., Klähn, S., and Hagemann, M. (2019). Salt-Regulated Accumulation of the Compatible Solutes Sucrose and Glucosylglycerol in Cyanobacteria and Its Biotechnological Potential. *Front. Microbiol.* 10. doi: 10.3389/fmicb.2019.02139

Klähn, S., and Hagemann, M. (2011). Compatible solute biosynthesis in cyanobacteria. *Environ. Microbiol.* 13, 551–562. doi: 10.1111/j.1462-2920.2010.02366.x

Lang, T., Schoen, V., Hashem, K., McDonald, L., Parker, J., and Savelyeva, A. (2017). "The Environmental, Social, and Market Sustainability of Sugar," in *Advances in Food Security and Sustainability*, ed. D. Barling (Elsevier), 115–136. doi: 10.1016/bs.af2s.2017.09.002

Liang, Y., Zhang, M., Wang, M., Zhang, W., Qiao, C., Luo, Q., et al. (2020). Freshwater Cyanobacterium *Synechococcus elongatus* PCC 7942 Adapts to an Environment with Salt Stress via Ion-Induced Enzymatic Balance of Compatible Solutes Downloaded from. *Aemasmorg 1 Appl. Environ. Microbiol.* 86, 2904–2923. doi: 10.1128/AEM

Lin, P. C., Zhang, F., and Pakrasi, H. B. (2020). Enhanced production of sucrose in the fast-growing cyanobacterium *Synechococcus elongatus* UTEX 2973. *Sci. Rep.* 10. doi: 10.1038/s41598-019-57319-5

Lippi, L., Bähr, L., Wüstenberg, A., Wilde, A., and Steuer, R. (2018). Exploring the potential of high-density cultivation of cyanobacteria for the production of cyanophycin. *Algal Res.* 31, 363–366. doi: 10.1016/j.algal.2018.02.028

Markou, G., Vandamme, D., and Muylaert, K. (2014). Microalgal and cyanobacterial cultivation: The supply of nutrients. *Water Res.* 65, 186–202. doi: 10.1016/j.watres.2014.07.025

Montgomery, B. L. (2014). The Regulation of Light Sensing and Light-Harvesting Impacts the Use of Cyanobacteria as Biotechnology Platforms. *Front. Bioeng. Biotechnol.* 2. doi: 10.3389/fbioe.2014.00022.

Mueller, T. J., Ungerer, J. L., Pakrasi, H. B., and Maranas, C. D. (2017). Identifying the Metabolic Differences of a Fast-Growth Phenotype in *Synechococcus* UTEX 2973. *Sci. Rep.* 7, 41569. doi: 10.1038/srep41569

Parmar, A., Singh, N. K., Pandey, A., Gnansounou, E., and Madamwar, D. (2011). Cyanobacteria

and microalgae: A positive prospect for biofuels. *Bioresour. Technol.* 102, 10163–10172. doi: 10.1016/j.biortech.2011.08.030

Peters, S., Rose, T., and Moser, M. (2010). "Sucrose: A Prospering and Sustainable Organic Raw Material," in *Carbohydrates in Sustainable Development I*, eds. A. P. Rauter, P. Vogel, and Y. Queneau (Berlin, Heidelberg: Springer), 1–23. doi: 10.1007/128_2010_58

Qiao, C., Duan, Y., Zhang, M., Hagemann, M., Luo, Q., and Lu, X. (2018). Effects of reduced and enhanced glycogen pools on salt-induced sucrose production in a sucrose-secreting strain of *Synechococcus elongatus* PCC 7942. *Appl. Environ. Microbiol.* 84. doi: 10.1128/AEM.02023-17

Santos-Merino, M., Torrado, A., Davis, G. A., Röttig, A., Bibby, T. S., Kramer, D. M., et al. (2021). Improved photosynthetic capacity and photosystem I oxidation via heterologous metabolism engineering in cyanobacteria. *Proc. Natl. Acad. Sci.* 118, e2021523118. doi: 10.1073/pnas.2021523118

Santos-Merino, M., Yun, L., and Ducat, D. C. (2023). Cyanobacteria as cell factories for the photosynthetic production of sucrose. *Front. Microbiol.* 14, 1126032. doi: 10.3389/fmicb.2023.1126032

Satta, A., Esquirol, L., and Ebert, B. E. (2023). Current Metabolic Engineering Strategies for Photosynthetic Bioproduction in Cyanobacteria. *Microorganisms* 11, 455. doi: 10.3390/microorganisms11020455

Takatani, N., Uenosono, M., Hara, Y., Yamakawa, H., Fujita, Y., and Omata, T. (2022). Chlorophyll and Pheophytin Dephytylating Enzymes Required for Efficient Repair of PSII in *Synechococcus elongatus* PCC 7942. *Plant Cell Physiol.* 63, 410–420. doi: 10.1093/pcp/pcac006

Takatani, N., Use, K., Kato, A., Ikeda, K., Kojima, K., Aichi, M., et al. (2015). Essential Role of Acyl-ACP Synthetase in Acclimation of the Cyanobacterium *Synechococcus elongatus* Strain PCC 7942 to High-Light Conditions. *Plant Cell Physiol.* 56, 1608–1615. doi: 10.1093/pcp/pcv086

Thiel, K., Patrikainen, P., Nagy, C., Fitzpatrick, D., Pope, N., Aro, E.-M., et al. (2019). Redirecting photosynthetic electron flux in the cyanobacterium *Synechocystis* sp. PCC 6803 by the deletion of flavodiiron protein Flv3. *Microb. Cell Factories* 18, 189. doi: 10.1186/s12934-019-1238-2

Ungerer, J., Lin, P.-C., Chen, H.-Y., and Pakrasi, H. B. (2018a). Adjustments to Photosystem Stoichiometry and Electron Transfer Proteins Are Key to the Remarkably Fast Growth of the Cyanobacterium *Synechococcus elongatus* UTEX 2973. *mBio* 9, 10.1128/mbio.02327-17. doi: 10.1128/mbio.02327-17

Ungerer, J., Wendt, K. E., Hendry, J. I., Maranas, C. D., and Pakrasi, H. B. (2018b). Comparative genomics reveals the molecular determinants of rapid growth of the cyanobacterium *Synechococcus elongatus* UTEX 2973. *Proc. Natl. Acad. Sci.* 115, E11761–E11770. doi: 10.1073/pnas.1814912115

Walker, P. L., and Pakrasi, H. B. (2022). A Ubiquitously Conserved Cyanobacterial Protein Phosphatase Essential for High Light Tolerance in a Fast-Growing Cyanobacterium.

Microbiol. Spectr. 10, e01008-22. doi: 10.1128/spectrum.01008-22

Wang, B., Zuniga, C., Guarnieri, M. T., Zengler, K., Betenbaugh, M., and Young, J. D. (2023). Metabolic engineering of *Synechococcus elongatus* 7942 for enhanced sucrose biosynthesis. *Metab. Eng.* 80, 12–24. doi: 10.1016/j.ymben.2023.09.002

Xu, Y., Tiago Guerra, L., Li, Z., Ludwig, M., Charles Dismukes, G., and Bryant, D. A. (2013). Altered carbohydrate metabolism in glycogen synthase mutants of *Synechococcus* sp. strain PCC 7002: Cell factories for soluble sugars. *Metab. Eng.* 16, 56–67. doi: 10.1016/j.ymben.2012.12.002

Yu, J., Liberton, M., Cliften, P. F., Head, R. D., Jacobs, J. M., Smith, R. D., et al. (2015). *Synechococcus elongatus* UTEX 2973, a fast-growing cyanobacterial chassis for biosynthesis using light and CO2. *Sci. Rep.* 5, 8132. doi: 10.1038/srep08132

Zhang, L., Chen, L., Diao, J., Song, X., Shi, M., and Zhang, W. (2020). Construction and analysis of an artificial consortium based on fast-growing cyanobacterium *Synechococcus elongatus* UTEX 2973 to produce platform chemical 3-hydroxypropionic acid from CO2. doi: 10.21203/rs.2.22486/v1

Ziolkowska, J. R. (2014). Prospective technologies, feedstocks and market innovations for ethanol and biodiesel production in the US. *Biotechnol. Rep.* 4, 94–98. doi: 10.1016/j.btre.2014.09.001

APPENDIX

ADDITIONAL SUPPORTING DATA FIGURES

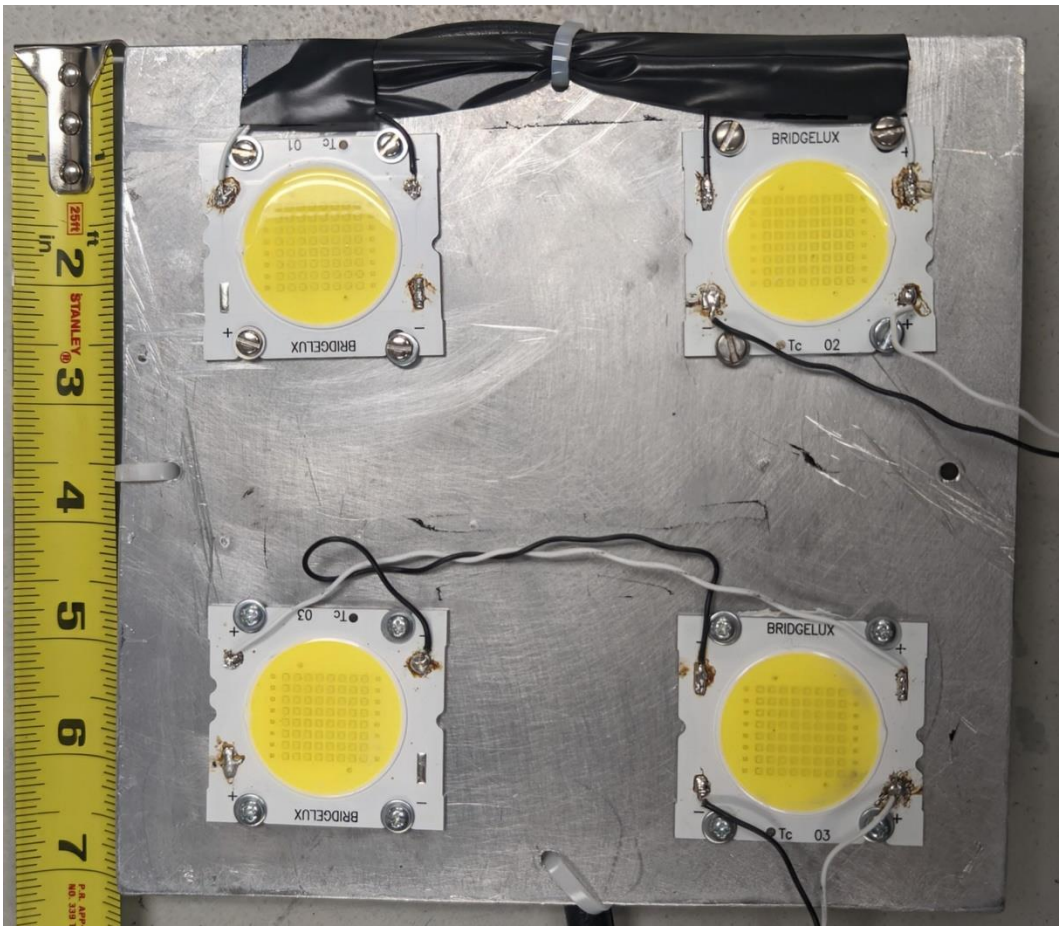

Figure S2.1. Custom lighting array consisting of four COB LED lights (BXRA-56C5300-H, Bridgelux, USA) mounted on an aluminum panel two inches apart and connected to a power supply (LS35-24, TDK-Lambda, Japan). The panel was attached to a ring clamp, and the clamp fastened to a ring stand. Light intensity can be set by adjusting the distance of the panel to the HDC, or by modulating the voltage of the power supply.

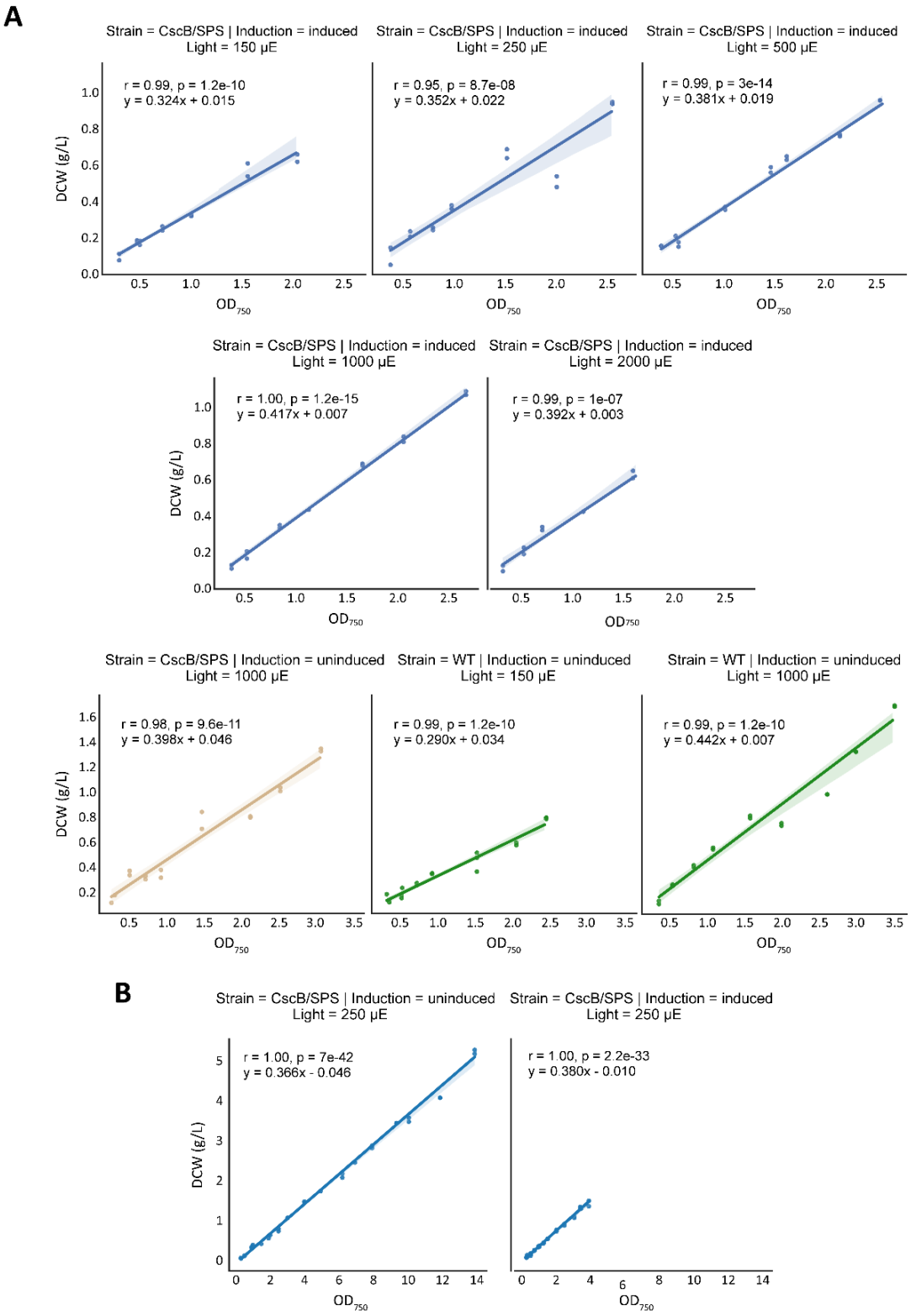

Figure S2.2. Relationship between dry cell weight (DCW, g/L) and OD_{750} in different growth conditions and cultivators. **(A)** WT, and uninduced and induced *cscB*/*sps* cultured in the MC-1000 under various light intensities. **(B)** Uninduced and induced *cscB*/*sps* grown in the CellDEG HDC system with 250 µmol photons m^{-2} s^{-1} and 2% CO_2.

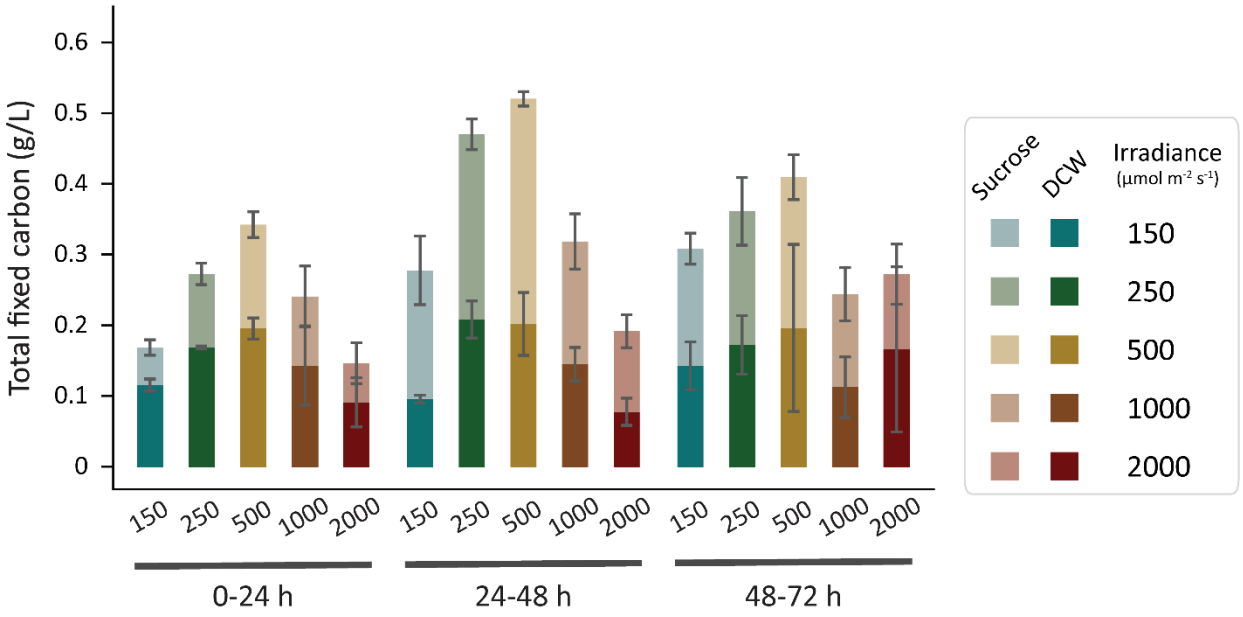

Figure S2.3. Total fixed carbon as shown by sucrose and dry cell weight accumulated per day in cultures grown in the MC-1000 under varying irradiances. Error bars denote standard deviation.

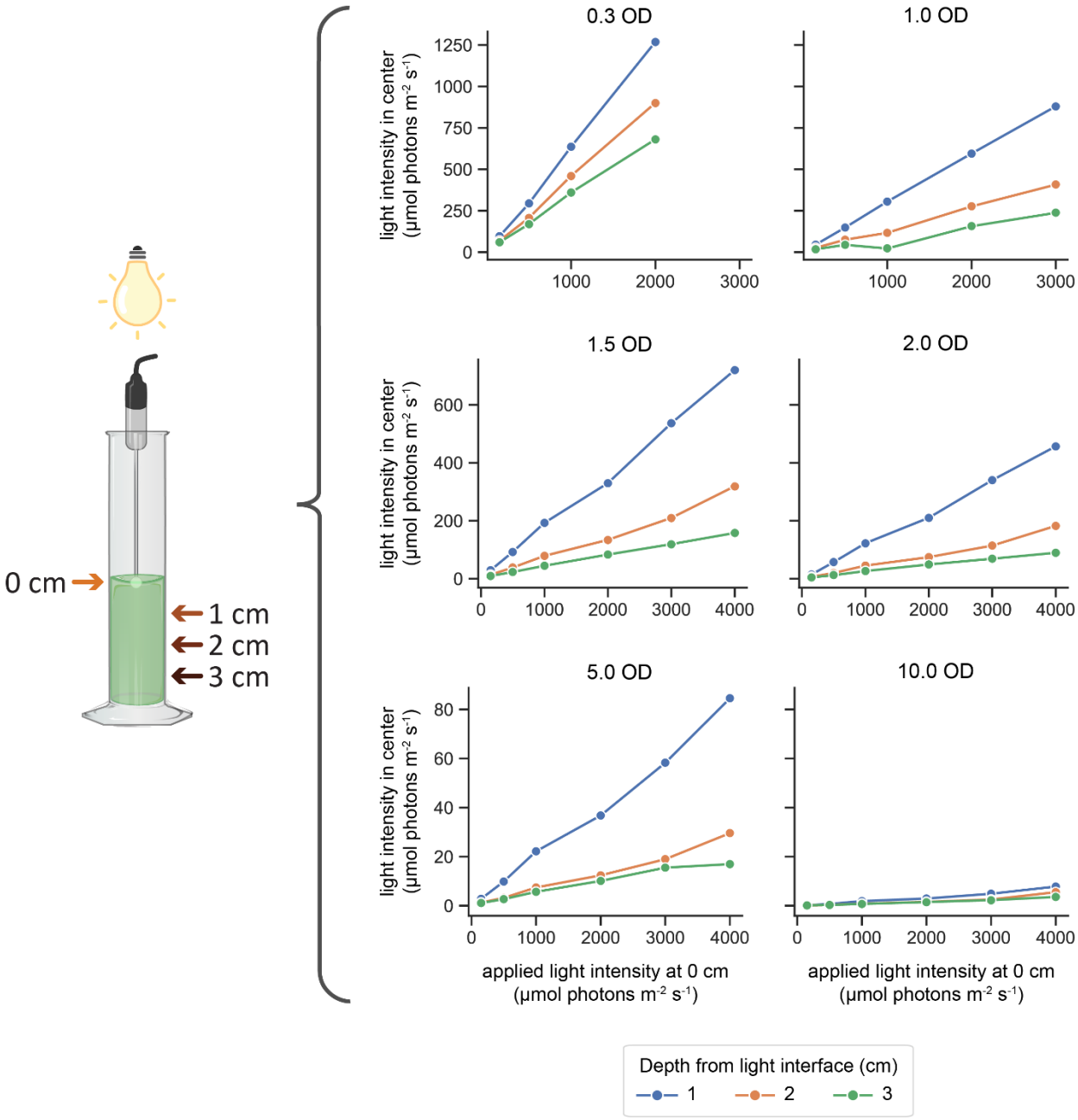

Figure S2.4. Light perceived in the center of a culture at varying OD_{750}, distance from the light interface, and irradiance. Measurements are averaged values from a 15-second interval.

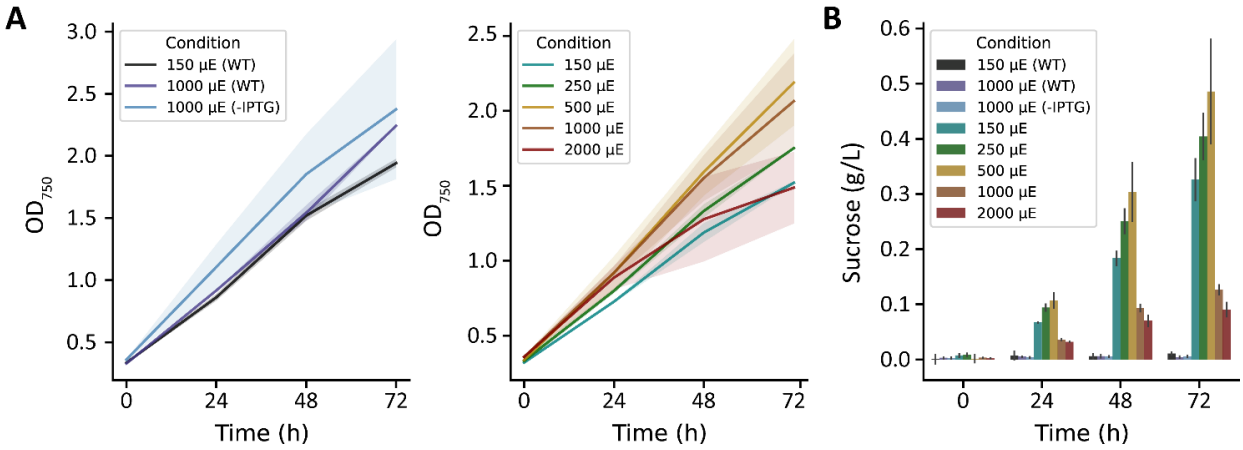

Figure S2.5. Growth and sucrose production of WT and c*scB/sps*-expressing *S. elongatus* grown in the MC-1000 under various light intensities and 0 mM HCO_3^-. **(A)** OD_{750} and **(B)** sucrose production of cultures. Error bars denote standard deviation.

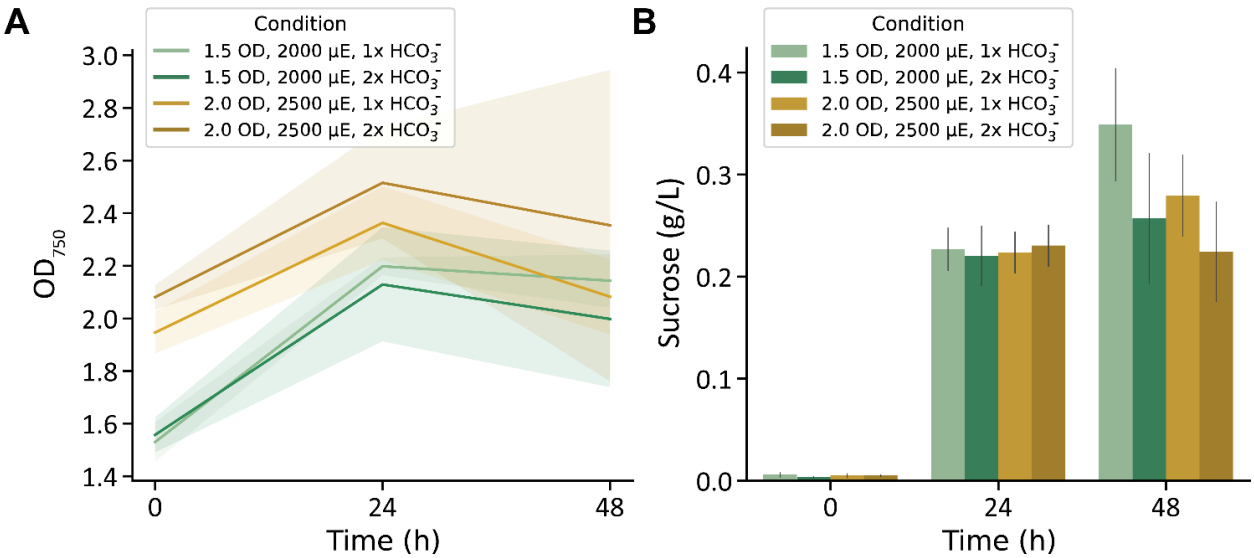

Figure S2.6. (A) Growth as OD_{750} and **(B)** sucrose production of *cscB*/*sps*-expressing *S. elongatus* of cultures started at high cell densities (1.5 and 2 OD_{750}). Error bars denote standard deviation.

CHAPTER 3:

UTILIZATION OF ENDOGENOUS AND HETEROLOGOUS OUTER-MEMBRANE PROTEINS FOR CYANOBACTERIAL SURFACE DISPLAY

This chapter was adapted from text originally published in:

Yun, L. Sakkos, J.K., and Ducat, D.C. (2024) Population-level heterogeneity complicates utilization of *Synechococcus elongatus* PCC 7942 surface display platforms. *microPub. Biol*. doi: 10.17912/micropub.biology.001097

Introduction

Surface display technologies offer a number of useful cellular properties that can be utilized for both academic research and biotechnological applications. However, these advancements have primarily been developed for only a few model heterotrophic microbes, leaving photosynthetic microbes, including cyanobacteria, with an underdeveloped molecular toolkit for surface display (Samuelson et al., 2002; Kondo and Ueda, 2004; Han et al., 2018). The ability to engineer cellular surface properties and to customize the binding of biologically derived and inorganic materials to the outermost cell membrane leaflet holds the potential to introduce innovative strategies to overcome the challenges of large-scale cultivation of photosynthetic microbes. For example, biomass recovery and dewatering represent a major barrier to achieving economically competitive cultivation of microalgae and cyanobacteria, and surface display could offer new options for inexpensive harvesting (Vandamme et al., 2013; Mathimani and Mallick, 2018) .

In the current study, I set out to broaden the applicability of recently developed surface display systems for cyanobacteria to accelerate the potential of this important class of biotechnology chassis species (Santos-Merino et al., 2019, 2023). Surface display of engineered epitope tags was reported in the model cyanobacterium, *Synechococcus elongatus* PCC 7942, to mediate binding to both biotic and abiotic targets (Chungjatupornchai and Fa-Aroonsawat, 2008; Chungjatupornchai and Fa-aroonsawat, 2009; Chungjatupornchai et al., 2011; Ferri et al., 2015; Fedeson and Ducat, 2017). The primary strategy of these studies was to encode an epitope within an extracellular-facing loop of the endogenous outer-membrane porin protein, SomA. Initial designs showed some reactivity of engineered epitope protein tags (*e.g.*, FLAG tag), but accessibility of the tags to appropriate antibodies was greatly improved by the genetic deletion of other factors likely occluding the cell surface, such as the O-antigen (OAg, *wzt*) and the putative surface layer (S-layer, *slpA*) proteins. Deletion strains (Δ*wzt*Δ*slpA*) exhibit more accessible tags that interacted with antibodies targeting this specific epitope (Fig. 1A) and a similar improved penetrance of immunostaining was observed in cells treated with chelating agents known to strip away cell surface components (Fedeson and Ducat, 2017).

To expand upon this toolkit, I evaluated multiple variants of the SomA outer-membrane porin and the heterologous adhesin, intimin, in a range of genetic backgrounds of *S. elongatus* PCC 7942. Importantly, we sought to improve the utility of this surface display system by removing the requirement for specialized mediating antibodies for binding and to allow for direct

adhesion. Towards this aim, we focused on two strategies: 1) inserting a SpyTag peptide for the covalent binding of its protein partner, SpyCatcher, into SomA at sites previously shown to allow for extracellular epitope tagging (Zakeri et al., 2012; Fedeson and Ducat, 2017), and 2) heterologous expression of intimin proteins that form an extended surface spike-like projection for the specific purpose of attaching to other cells such as *Escherichia coli,* and which have been modified with protein binding domains to mediate intercellular binding (Figure 3.1; Glass & Riedel-Kruse, 2018; Robledo et al., 2022). In each approach we attempted multiple designs while varying the peptide linker length between domains, linker type (*i.e.*, flexible vs. rigid), different binding motifs, and expressed these constructs in a wild-type (WT) or Δ*wzt*Δ*slpA* background of *S. elongatus* PCC 7942 to control for any impacts of surface-occluding factors, though this material will be relegated to the appendix of this chapter due to its preliminary nature.

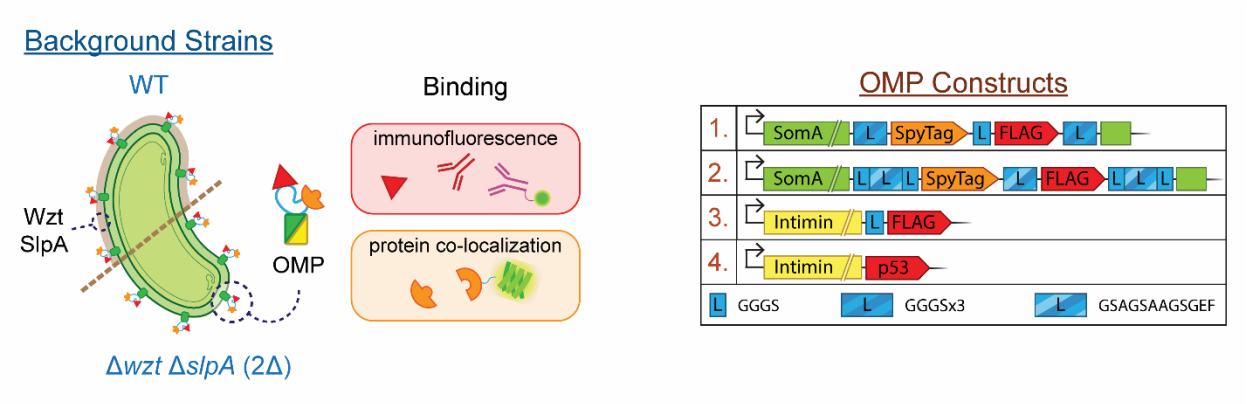

Figure 3.1. Schematic of background strains and engineered outer-membrane proteins. Diagram of WT and Δ*wzt*Δ*slpA* strains with outer-membrane occlusions and proteins (SomA or intimin) with engineered binding domains expressed on the surface of *S. elongatus* PCC 7942. Surface domains were detected by immunofluorescence or protein co-localization, as indicated. The table (right) summarizes the linker and epitope/peptide modifications for each outer -membrane protein construct displayed in this figure.

Results

Use of endogenous SomA for surface display

We evaluated expression, localization, and accessibility of the different surface display constructs using immunofluorescence and soluble reporter proteins fused to a compatible protein interaction domain. For surface display domains inserted in an extracellular facing loop of SomA (Figure 3.1, constructs 1 and 2), we first probed with α-FLAG antibodies in fixed cell populations. Immunostaining indicated a rise in the proportion of labeled cells following induced expression of the tagged SomA (Figure 3.2A). Furthermore, our results generally reinforced our prior

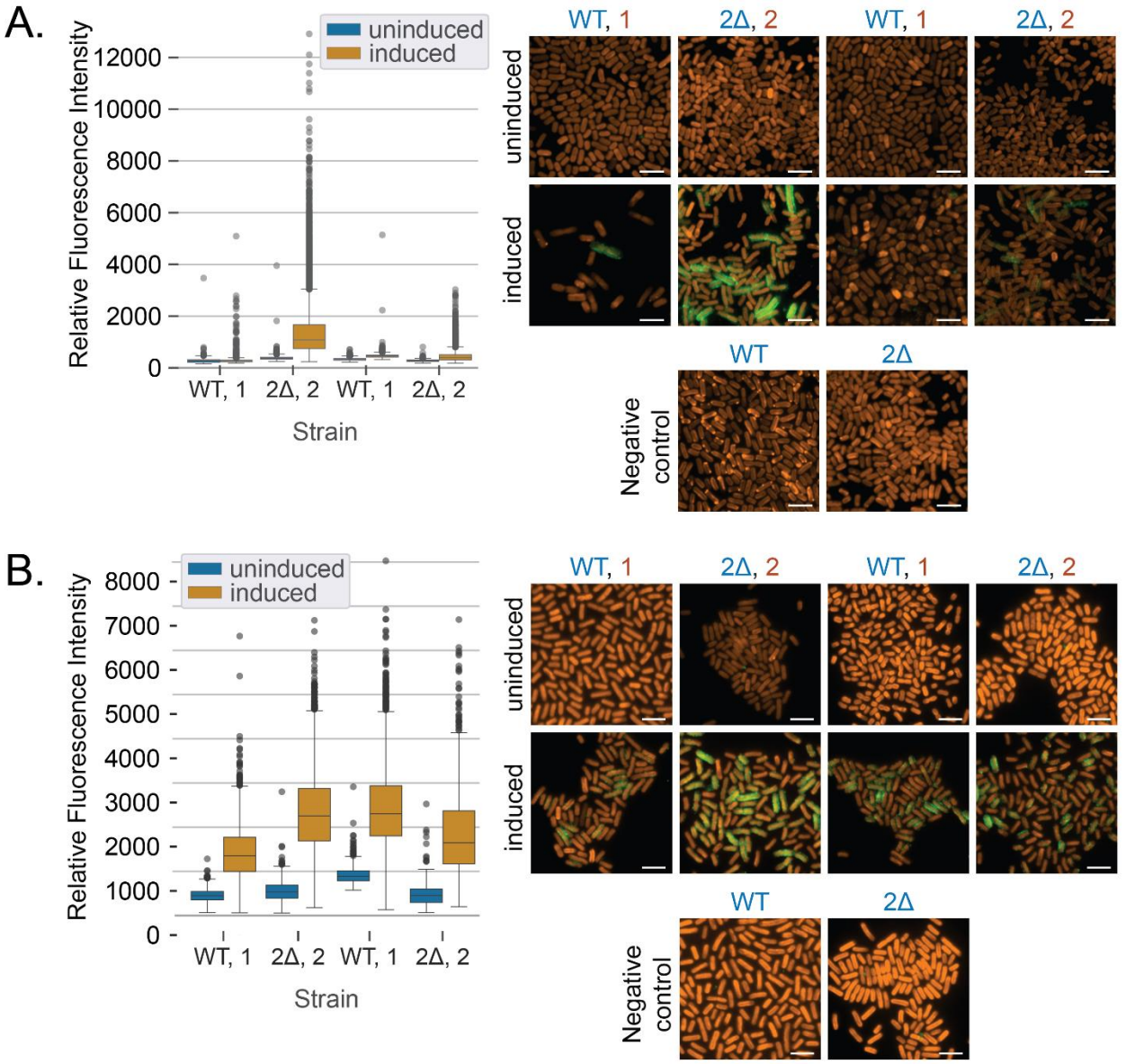

Figure 3.2. Immunofluorescence of fixed *S. elongatus* PCC 7942 cells with SomA. Background strains with constructs 1 and 2 labeled with **(A.)** α-FLAG and **(B.)** α-SpyTag antibodies in cells bearing SomA-SpyTag-FLAG fusions. All constructs appeared to localize to the surface of *S. elongatus* PCC 7942 when induced, albeit within a subset of the cell population that was dependent on strain background and the primary antibody used. All scale bars indicate 5 μm.

observations that the engineered epitope tag was more accessible on the surface of the Δ*wzt*Δ*slpA* mutant background, relative to paired controls expressing the same construct in a WT background (Figure 3.2). However, significant intercellular variation of immunolabeling was observed and a proportion of cells in the induced cultures stained poorly or did not exhibit fluorescence at higher levels than the uninduced controls. Generally, constructs with longer linker sequences (*e.g.*, GSAGSAAGSGEF) between introduced domains appeared to stain poorly with α-FLAG

antibodies relative to constructs with shorter, flexible linker sequences (Figure 3.2A). Hypothetically, longer linker sequences may increase the distance between the epitope and the cell surface, but an extended linker may instead impose difficulty in translocating to the outer-membrane. In our best-performing SomA designs (*i.e.*, GGGSx3 linker sequences in a Δ*wzt*Δ*slpA* background), the majority of fixed cells exhibited some staining localized to the cell periphery, although considerable variation in staining intensity was observed (Figure 3.2A). Due to the heterogenous staining, concerns regarding the integrity of the introduced SpyTag-FLAG epitope were raised, and we therefore conducted complementary immunostaining against SpyTag to validate if this epitope was localized to the cell surface. An extended incubation with α-SpyTag showed staining patterns similar to that of α-FLAG but with higher penetrance and average relative fluorescence intensity (Figure 3.2B). The majority of cells exhibited clear (albeit sometimes weak) staining with the α-SpyTag, with the exception of construct 2 in the WT background (Figure 3.2B). An overnight incubation with α-FLAG yielded a small handful of cells with puncta-like fluorescence on the cell periphery, whereas a 36-hour incubation with α-SpyTag reveals a spotty but more comprehensive labeling of the outer membrane (Figure 3.2B).

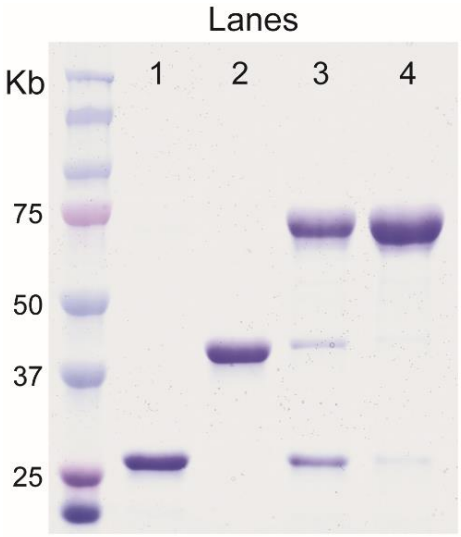

Figure 3.3. SDS-PAGE of purified SpyTag-GFP and SpyCatcher-mNG. SpyTag (32.5 kDa; lane 1) and SpyCatcher-mNG (43.2 kDa; lane 2) after 10 and 120 minutes of *in vitro* binding (lanes 3 and 4, respectively). Nearly all of the SpyCatcher and SpyTag proteins are competent to form covalent bonds, as exhibited under the longer incubation periods.

To evaluate if the neighboring SpyTag domains were functionally active and accessible in the SomA fusions, we incubated cells in the presence of soluble SpyCatcher-mNeonGreen (mNG) reporter proteins. The majority of purified SpyCatcher-mNG formed covalent bonds with purified compatible SpyTag-GFP protein within a 10-minute *in vitro* incubation; the reaction was driven to near-completion in 2 hours (Figure 3.3). When live cells bearing modified SomA-SpyTag constructs had their surfaces stripped with EDTA and incubated with the soluble SpyCatcher-mNG for 3 hours, a limited number of cells displayed a peripheral fluorescence signal consistent with successful binding between the SpyTag and SpyCatcher pair (Figure 3.4); this staining pattern was never observed in negative control experiments using *S. elongatus* PCC 7942 lacking an integrated SomA-SpyTag gene (Figure 3.4). However, the vast majority of cells did not exhibit any SpyCatcher-mNG staining. Furthermore, there was no consistent trend in the proportion of cells exhibiting SpyCatcher-mNG attachment when considering induction of gene expression, various linker combinations, or the parental background in which SomA-SpyTag variants were expressed (Figure 3.4). Nonetheless, the small fraction (<<1%) of labeled cells often displayed a clear localization pattern that could not be dismissed as a staining artifact (Figure 3.4; red arrowheads).

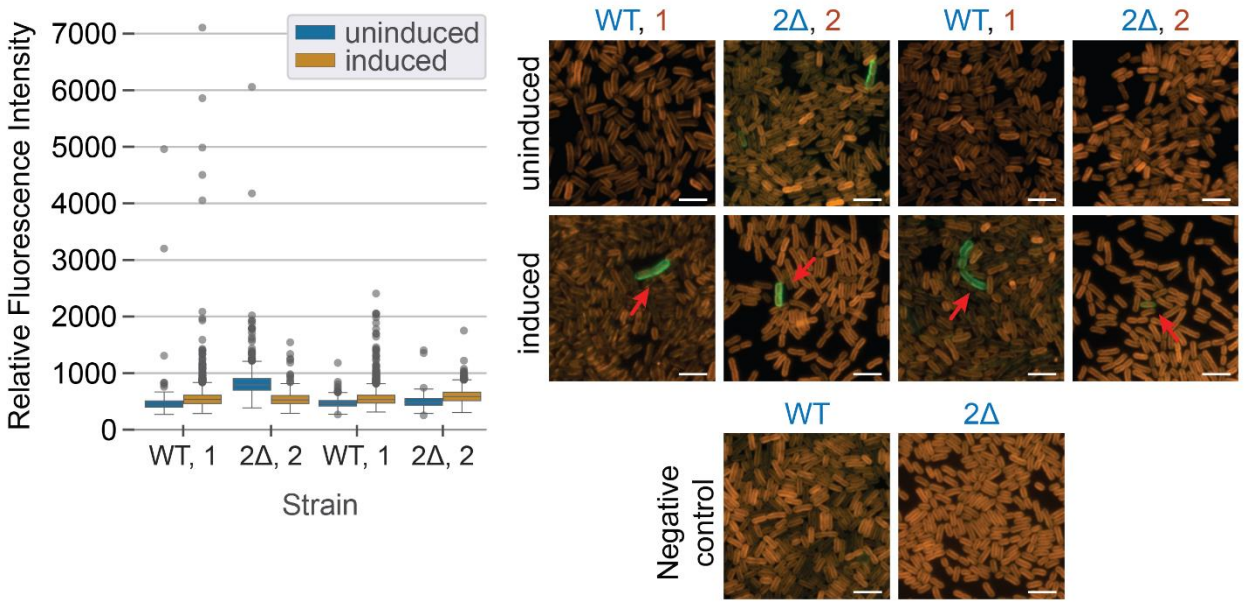

Figure 3.4. Protein co-localization of live *S. elongatus* PCC 7942 cells with SomA. Background strains with constructs 1 and 2 stripped with EDTA to remove surface-associated proteins and polysaccharides. Living cells were incubated with purified SpyCatcher-mNG and a small fraction of cells (generally <1%) exhibited localization patterns consistent with uniform binding of the reporter to SomA-SpyTag fusions (red arrows). All scale bars indicate 5 μm.

Intercellular variation in the level of expression, localization, and accessibility of surface-displayed domains was difficult to ascribe to any specific cellular feature or pattern. Relative to previously reported results (Fedeson and Ducat, 2017), the SpyTag epitope was accessible at a comparable penetrance to when probed with a prolonged α-SpyTag antibody incubation. By contrast, the FLAG epitope showed lower accessibility as assessed by an overnight incubation with α-FLAG antibodies. Overall, there appeared to be poor correlation between cell lines with higher penetrance of modified SomA (as observed by fixed cell immunofluorescence, Figure 3.2) and the proportion of living cells that reacted strongly with soluble SpyCatcher (Figure 3.4). The source of the intra-population variation in staining cells could not be explained as a merodiploid genetic insertion and was not resolved in separate control experiments using other engineered SomA variants, increased incubation times, or chemical protocols for 'stripping' the outer surface components with chelating agents (Sumper et al., 1990; Messner and Sleytr, 1992; Fedeson and Ducat, 2017). Furthermore, SpyCatcher-reactive cells of the population exhibited chlorophyll *a* fluorescence (Figure 3.4), and we were unable to find an association between cells exhibiting SpyCatcher-mNG staining and uptake of vital dyes; therefore, we cannot directly attribute the spurious staining with a subpopulation of dead cells. The nature of the variability remains largely unknown, although the most consistent explanation of our results is that other components (as yet, unknown) of the cell surface or extracellular matrix might contribute to epitope inaccessibility and the "all-or-nothing" staining patterns.

Use of heterologous intimin for surface display

To evaluate if a separate surface display system could resolve the inconsistency, I expressed intimin proteins that have been previously characterized to display a protein binding domain on an extended projection from the cell surface (Figure 3.1; constructs 3 and 4). When expressed, intimin-fusion proteins appeared to express poorly and/or primarily localize to the cytosol, as assessed by inclusion body-like immunofluorescence staining of fixed cell populations (Figure 3.5). Consistent with these results, we did not observe any reactivity of living cells with α-FLAG or α-p53 antibodies above the level of paired negative controls. Our results appear to suggest that intimins are not properly localized to the outer-membrane when expressed heterologously in *S. elongatus* PCC 7942.

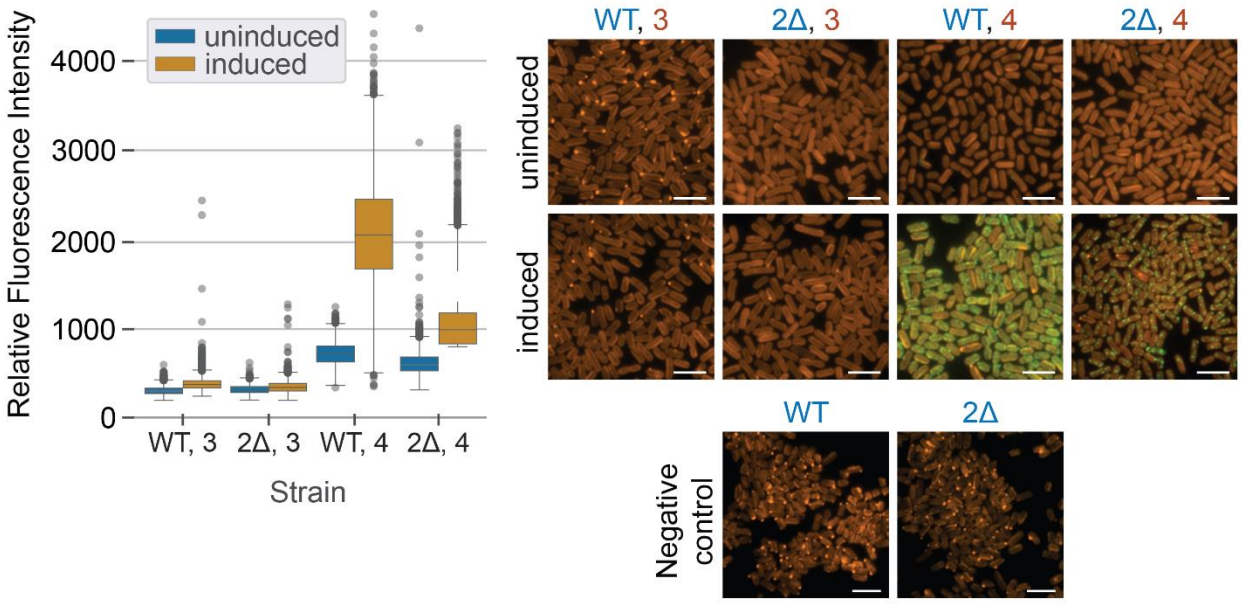

Figure 3.5. Immunofluorescence of fixed *S. elongatus* PCC 7942 cells with intimin. Background strains with constructs 3 (intimin-FLAG) and 4 (intimin-p53) labeled with α-FLAG or α-p53 antibodies, respectively. Cells exhibit limited expression (intimin-FLAG) or mis-localization of expressed protein (intimin-p53). All scale bars indicate 5 μm.

Discussion

In conclusion, while surface display technologies offer considerable biotechnological promise, our study highlights the complexities and challenges associated with achieving surface display of functional and accessible protein domains for direct adhesion in *S. elongatus* PCC 7942. There have been a limited number of successful reports of functional cyanobacterial surface display, such as the fusion of affibodies onto endogenous pili or S-layer proteins in *Synechocystis* sp. PCC 6803 and antibody-mediated adhesion in *S. elongatus* PCC 7942 (Fedeson and Ducat, 2017; Cengic et al., 2018). Strikingly, while some living cyanobacteria expressing SomA-SpyTag fusions reacted strongly with soluble SpyCatcher and displayed localization patterns that would be expected from a functional surface display system, the vast majority of cells in the clonal population were non-reactive even under prolonged incubation and/or chemical treatment to strip surface-associated proteins and polysaccharides (Figure 3.4). Despite genetic and chemical attempts to clear occlusions from the cell surface, expressing various linker types to extend further from the outer-membrane, and numerous variations to the binding procedures, we consistently observed low penetrance of binding to epitopes and SpyCatcher. One possible explanation is that the surface loops of SomA remain occluded by other endogenous cellular factors that project from the surface of *S. elongatus* PCC 7942, limiting accessibility even in surface-stripped cells.

Attempts to remedy this possible obstacle by mounting epitopes on intimins that project from the cell surface were unsuccessful, presumably due to a failure to correctly target these proteins to the outer-membrane (Figure 3.5). It is possible that rare mutations in a minority of cells give rise to phenotypes with surface features amenable to display: selective recovery and sequencing of these rare cells could be revealing of the mechanism(s) responsible in this case.

Our results suggest that future surface display efforts may be more effective if they are focused on engineering targets that project further from the surface of the cyanobacterial outer membrane. For example, type IV pili could represent a promising avenue for further engineering, as they have been successfully employed for surface display purposes in *Synechocystis* sp. PCC 6803, and cell-encapsulating S-layer proteins can be utilized as a scaffold for high-density surface display rather than be removed as occlusions (Cengic et al., 2018; Charrier et al., 2019). Ultimately, these results emphasize the need for further study into the outer-membrane of *S. elongatus* PCC 7942 for better design and application of surface display technologies.

Materials and Methods

Cell culture and strain generation

Cyanobacterial cultures were grown in baffled flasks in a Multitron Pro (Infors HT) incubator under constant illumination from fluorescent bulbs (150 μmol m^{-2} s^{-1}; 15W Gro-Lux; Sylvania) in 32°C, 2% CO_2, and with 125 rpm shaking. Cultures were routinely grown in liquid BG-11 medium supplemented with 1 g/L HEPES (H4034; Sigma-Aldrich) set to pH 8.3 with NaOH, with the appropriate antibiotic when needed (chloramphenicol, 25 μg/mL; kanamycin, 20 μg/mL; spectinomycin, 100 μg/mL). To improve consistency and maintain cultures in exponential rowth, cultures for immunostaining or protein co-localization were back-diluted to an OD_{750} of ~0.3 each day for three days before inducing with 1 mM isopropyl-β-D-1-thiogalactopyranoside (IPTG; I2481C25; Goldbio). Cultures were induced for 24 hours prior to any subsequent cell staining or analysis.

The knockout background strain (Δ*wzt*Δ*slpA*) was constructed by sequentially transforming with integration plasmids containing an antibiotic resistance selectable marker flanked by ~1 kilobase fragments upstream and downstream of the gene of interest on the 5' and 3' ends, respectively, as reported previously (Fedeson and Ducat, 2017). Surface display strains were constructed by combining synthesized gene fragments of adhesins (Glass & Riedel-Kruse, 2018; Integrated DNA Technologies) and PCR-linearized NS3 integration vector with the *S.*

elongatus PCC 7942 SomA with Gibson Assembly (Gibson et al., 2009; Fedeson and Ducat, 2017). Transformations were performed as outlined in Golden et al., 1987. Transformants were selected on BG-11 agar plates with appropriate antibiotics (chloramphenicol, 12.5 μg/mL; kanamycin, 16.7 μg/mL; and spectinomycin, 100 μg/mL), and verified by colony PCR and Sanger sequencing (RTSF Genomics Core, Michigan State University).

Fluorescent protein expression, purification, and in vitro binding

SpyCatcher-mNG and SpyTag-GFP plasmids were transformed into *E. coli* BL21(DE3) as is routine for protein purification, and transformants recovered on selective agar plates. Single colonies were cultured overnight at 37°C in 5 mL Lysogeny Broth (LB) with the appropriate antibiotic (ampicillin (50 μg/mL) for SpyCatcher-mNG, and kanamycin (50 μg/mL) for SpyTag-GFP). The following day, overnight cultures were back diluted 1:100 into fresh Terrific Broth (TB) with the appropriate antibiotic, and cultured at 37°C until a density of 0.4-0.6 OD_{600} was reached. At mid-exponential, cultures were chilled to approximately 23°C and induced with a final concentration of 400 μM IPTG for SpyCatcher-mNG and 500 μM anhydrous tetracycline (aTc) for SpyTag-GFP prior to culturing overnight at 23°C. Cell suspensions were chilled and transferred to a pre-weighed container to be pelleted, and the wet cell mass of the pellet was weighed before being resuspended with a minimal volume of lysis buffer and stored in -80°C until further processing. To prepare cells for lysing, frozen samples were thawed on ice and cold lysis buffer was added (final of 1:1 volume of lysis buffer to wet cell mass, w/w). During lysis, samples were kept on ice and a sonicator (Fisherbrand Model 120 Sonic Dismembrator; Fisher Scientific) equipped with a 1/8-inch probe microtip was used to disrupt cell integrity. Lysate was centrifuged 7,000 rpm for 25 minutes at 10°C on a Sorvall centrifuge equipped with the SS-34 fixed angle rotor (Sorvall) to pellet the cellular debris.

Expressed proteins (SpyTag-GFP and SpyCatcher-mNG) were recovered by affinity purification using encoded Hisx6 tags. To prepare the Ni-NTA agarose resin (Qiagen) for purification, 3 mL of the slurry was aliquoted into an empty gravity flow column (Poly-Prep Chromatography Columns; Bio-Rad) and the resin was washed 3 times with 3 mL lysis buffer. The cleared cell lysate was then loaded onto the column and the column was washed 4 times with 3 mL of the lysis buffer. Bound protein was eluted with the elution buffer. To remove the high concentration of imidazole from the elution buffer, the collected protein was transferred to an Amicon Ultra-15 Centrifugal Filter (Millipore) with the appropriate molecular weight cut off (20

kDa for SpyCatcher-mNG and 10 kDa for SpyTag-GFP). The filters were centrifuged at 10°C to remove the bulk of the liquid before adding the protein storage buffer to dilute the remaining amount of imidazole before being centrifuged again; there were two total additions of protein storage buffer before the protein was collected, quantified, aliquoted, and flash frozen with liquid nitrogen.

To ascertain functionality, *in vitro* binding assays were performed. Approximately 230 pM of each SpyCatcher-mNG and SpyTag-GFP were diluted in phosphate citrate buffer (pH 7.5) before combining at room temperature. To stop the reactions for time points (10 and 120 minutes), samples were mixed 1:1 with 2X Laemlli buffer (161-0737; Bio-Rad) and boiled at 95°C for 10 minutes. Samples were loaded onto 10% Mini-PROTEAN TGX Precast Protein Gels (Bio-Rad), and run with 75 V/10 mA for the first 10 minutes, and 120 V/30 mA for the remaining run time.

Immunostaining and protein co-localization

Cells were harvested (250 µL culture at ~1.5 OD_{750}), pelleted, and washed in PBS. For immunofluorescence, cells were fixed, permeabilized, blocked, labeled with α-FLAG, α-SpyTag, or α-p53 antibodies, and labeled against the primary antibody with a fluorescent secondary antibody. To fix cells, washed pellets were resuspended with 200 µL pre-chilled methanol and incubated at -20˚C for 10 minutes. Methanol was removed, and cells were washed with 500 µL PBS three times. To permeabilize, fixed cells were resuspended with 300 µL of lysozyme solution, and incubated in 37˚C for 30 minutes. Lysozyme solution was removed, and cells were washed with 500 µL PBS three times. Permeabilized cells were then incubated with blocking buffer for 30 minutes at room temperature. Blocking buffer was removed, and cells were resuspended with 300 µL of a diluted primary antibody in blocking buffer (1:1000 dilution for α-FLAG (DYKDDDDK) (LT0420; Lifetein) and α-p53 (DO-1) Alexa Fluor 488 (sc-126 AF488; Santa Cruz Biotechnology), 1:5000 dilution for α-SpyTag (HCA406; Bio-Rad)). Samples with α-FLAG and α-p53 were incubated in 4˚C overnight, and α-SpyTag samples were incubated in 4˚C for ~36 hours. The primary antibody was removed, and cells were washed with 500 µL PBS three times before being resuspended in 500 µL blocking buffer and incubated at room temperature for 15 minutes. The blocking buffer was removed, and the samples were protected from light in the following steps until imaging. Cells were resuspended with 300 µL of a diluted secondary antibody in blocking buffer (α-mouse goat IgG DyLight™ 488 (35502; Thermo Fisher Scientific), or α-rabbit goat IgG DyLight™ 488 (35552; Thermo Fisher Scientific)), and incubated in 30˚C for 1

hour. After labeling, cells were pelleted, the secondary antibody removed, and cells were washed with 500 µL PBS three times. For protein co-localization, washed cells had the cell surface stripped by resuspending pellets with 200 µL 150 mM EDTA and incubated for 30 minutes at room temperature with mixing. The EDTA solution was removed, and cells were washed with 500 µL phosphate citrate buffer three times.

To label living cells with the compatible soluble SpyCatcher-based reporter, cell pellets were collected as above, then resuspended with 300 µL phosphate citrate buffer with SpyCatcher-mNG (final molar ratio of ~1:20 SomA protein to SpyCatcher-mNG), and incubated for 3 hours with mixing at room temperature while protected from the light. After labeling, the protein solution was removed, and cells were washed with 500 µL phosphate citrate buffer three times prior to imaging.

Fluorescence microscopy and image analysis

To image, labeled cells were resuspended with 15-30 µL phosphate citrate buffer or PBS, spotted onto agarose pads (1.5% w/v agarose in distilled water), and mounted onto glass coverslips. Fluorescence images were collected using an Axio Observer.D1 microscope (ZEISS), Axiocam 503 camera (ZEISS), 63x1.3 NA objective, X-Cite 120Q (Lumen Dynamics), and the Zen Blue (ZEISS) software. The following filter sets were used: filter set 43 (000000-1114-101; ZEISS) for chlorophyll autofluorescence, filter set 38 (000000-1031-346; ZEISS) for DyLight 488 fluorescence, and filter set 46 (000000-1031-346; ZEISS) for mNG fluorescence. Exposure times were held constant for fluorescent antibodies and SpyCatcher reporter proteins, respectively, so that outcomes could be compared across experiments.

Image analysis was performed with Python 3. Cell segmentation was conducted using custom Python scripts that used the Unet segmentation architecture (Ronneberger et al., 2015) for deep learning and implementation by Pytorch (Paszke et al., 2019). Mean fluorescence intensity plots were generated by segmenting the cells using the chlorophyll autofluorescence channel, rotating the cells such that the medial axis was horizontal, and rescaling the dimensions to 500 × 200 pixels to ensure consistent boundaries. The pixel intensity of the DyLight 488 and SpyCatcher-mNG was averaged from the segmented cells in the collection of images from each respective strain.

ACKNOWLEDGEMENTS

We would like to thank our laboratory postdoctoral fellows Dr. María Santos-Merino and

Dr. Amit Singh, and our predoctoral fellows Emmanuel Kokarakis and Rees Rillema for helpful comments on this manuscript. We would also like to thank Dr. Bryan Ferlez for guidance in protein purification. The plasmid for SpyTag-GFP was kindly gifted to us by Dr. Cheryl Kerfeld.

This work was primarily supported by the National Science Foundation and the Division of Molecular and Cellular Bioscience (Grant: 1845463), and partially supported by a fellowship from the Plant Biotechnology for Health and Sustainability Training Program at Michigan State University (Grant: NIH T32-GM110523).

REFERENCES

Cengic, I., Uhlén, M., and Hudson, E. P. (2018). Surface display of small affinity proteins on *Synechocystis* sp. strain PCC 6803 mediated by fusion to the major type IV pilin PilA1. *J. Bacteriol.* 200, 10.1128/jb.00270-18. doi: 10.1128/jb.00270-18

Charrier, M., Li, D., Mann, V. R., Yun, L., Jani, S., Rad, B., et al. (2019). Engineering the S-layer of *Caulobacter crescentus* as a foundation for stable, high-density, 2D living materials. *ACS Synth. Biol.* 8, 181–190. doi: 10.1021/acssynbio.8b00448

Chungjatupornchai, W., and Fa-Aroonsawat, S. (2008). Biodegradation of organophosphate pesticide using recombinant cyanobacteria with surface- and intracellular-expressed organophosphorus hydrolase. *J. Microbiol. Biotechnol.* 18, 946–951.

Chungjatupornchai, W., and Fa-aroonsawat, S. (2009). Translocation of green fluorescent protein to cyanobacterial periplasm using ice nucleation protein. *J. Microbiol.* 47, 187–192. doi: 10.1007/s12275-008-0188-x

Chungjatupornchai, W., Kamlangdee, A., and Fa-aroonsawat, S. (2011). Display of organophosphorus hydrolase on the cyanobacterial cell surface using *Synechococcus* outer membrane protein A as an anchoring motif. *Appl. Biochem. Biotechnol.* 164, 1048–1057. doi: 10.1007/s12010-011-9193-3

Fedeson, D. T., and Ducat, D. C. (2017). Cyanobacterial surface display system mediates engineered interspecies and abiotic binding. *ACS Synth. Biol.* 6, 367–374. doi: 10.1021/acssynbio.6b00254

Ferri, S., Nakamura, M., Ito, A., Nakajima, M., Abe, K., Kojima, K., et al. (2015). Efficient surface-display of autotransporter proteins in cyanobacteria. *Algal Res.* 12, 337–340. doi: 10.1016/j.algal.2015.09.013

Gibson, D. G., Young, L., Chuang, R.-Y., Venter, J. C., Hutchison, C. A., and Smith, H. O. (2009). Enzymatic assembly of DNA molecules up to several hundred kilobases. *Nat. Methods* 6, 343–345. doi: 10.1038/nmeth.1318

Glass, D. S., and Riedel-Kruse, I. H. (2018). A synthetic bacterial cell-cell adhesion toolbox for programming multicellular morphologies and patterns. *Cell* 174, 649-658.e16. doi: 10.1016/j.cell.2018.06.041

Golden, S. S., Brusslan, J., and Haselkorn, R. (1987). "Genetic engineering of the cyanobacterial chromosome," in *Methods in Enzymolology*, eds. R. Wu, and L. Grossman (Academic Press), 153, 215–231.

Han, L., Zhao, Y., Cui, S., and Liang, B. (2018). Redesigning of microbial cell surface and its application to whole-cell biocatalysis and biosensors. *Appl. Biochem. Biotechnol.* 185, 396–418. doi: 10.1007/s12010-017-2662-6

Kondo, A., and Ueda, M. (2004). Yeast cell-surface display—applications of molecular display. *Appl. Microbiol. Biotechnol.* 64, 28–40. doi: 10.1007/s00253-003-1492-3

Mathimani, T., and Mallick, N. (2018). A comprehensive review on harvesting of microalgae for biodiesel – Key challenges and future directions. *Renew. Sustain. Energy Rev.* 91, 1103–1120. doi: 10.1016/j.rser.2018.04.083

Messner, P., and Sleytr, U. B. (1992). “Crystalline bacterial cell-surface layers,” in *Advances in Microbial Physiology*, ed. A. H. Rose (Academic Press), 213–275. doi: 10.1016/S0065-2911(08)60218-0

Paszke A, Gross S, Massa F, Lerer A, Bradbury J, Chanan G, et al., Chintala S. 2019. PyTorch: An imperative style, high-performance deep learning library. In *33rd Conference on Neural Information Processing Systems (NeurIPS 2019)*, Vancouver, Canada.

Robledo, M., Álvarez, B., Cuevas, A., González, S., Ruano-Gallego, D., Fernández, L. Á., et al. (2022). Targeted bacterial conjugation mediated by synthetic cell-to-cell adhesions. *Nucleic Acids Res.* 50, 12938–12950. doi: 10.1093/nar/gkac1164

Ronneberger, O., Fischer, P., and Brox, T. (2015). U-Net: Convolutional networks for biomedical image segmentation, in *Medical Image Computing and Computer-Assisted Intervention – MICCAI 2015*, eds. N. Navab, J. Hornegger, W. M. Wells, and A. F. Frangi (Cham: Springer International Publishing), 234–241. doi: 10.1007/978-3-319-24574-4_28

Samuelson, P., Gunneriusson, E., Nygren, P.-Å., and Ståhl, S. (2002). Display of proteins on bacteria. *J. Biotechnol.* 96, 129–154. doi: 10.1016/S0168-1656(02)00043-3

Santos-Merino, M., Singh, A. K., and Ducat, D. C. (2019). New applications of synthetic biology tools for cyanobacterial metabolic engineering. *Front. Bioeng. Biotechnol.* 7, 33. doi: 10.3389/fbioe.2019.00033

Santos-Merino, M., Yun, L., and Ducat, D. C. (2023). Cyanobacteria as cell factories for the photosynthetic production of sucrose. *Front. Microbiol.* 14, 1126032. doi: 10.3389/fmicb.2023.1126032

Sumper, M., Berg, E., Mengele, R., and Strobel, I. (1990). Primary structure and glycosylation of the S-layer protein of Haloferax volcanii. *J. Bacteriol.* 172, 7111–7118. doi: 10.1128/jb.172.12.7111-7118.1990

Vandamme, D., Foubert, I., and Muylaert, K. (2013). Flocculation as a low-cost method for harvesting microalgae for bulk biomass production. *Trends Biotechnol.* 31, 233–239. doi: 10.1016/j.tibtech.2012.12.005

Zakeri, B., Fierer, J. O., Celik, E., Chittock, E. C., Schwarz-Linek, U., Moy, V. T., et al. (2012). Peptide tag forming a rapid covalent bond to a protein, through engineering a bacterial adhesin. *Proc. Natl. Acad. Sci.* 109, E690–E697. doi: 10.1073/pnas.1115485109

APPENDIX

PRELIMINARY DATA FIGURES

The following datasets elaborate upon the information published in *µPublication Biology*. Due to the short format of the journal style, I was unable to include a number of additional pieces of data that detail other efforts to troubleshoot and use of additional controls. This information is provided here in a concise format for the reader who may have additional interest and/or wish to follow up on a related project.

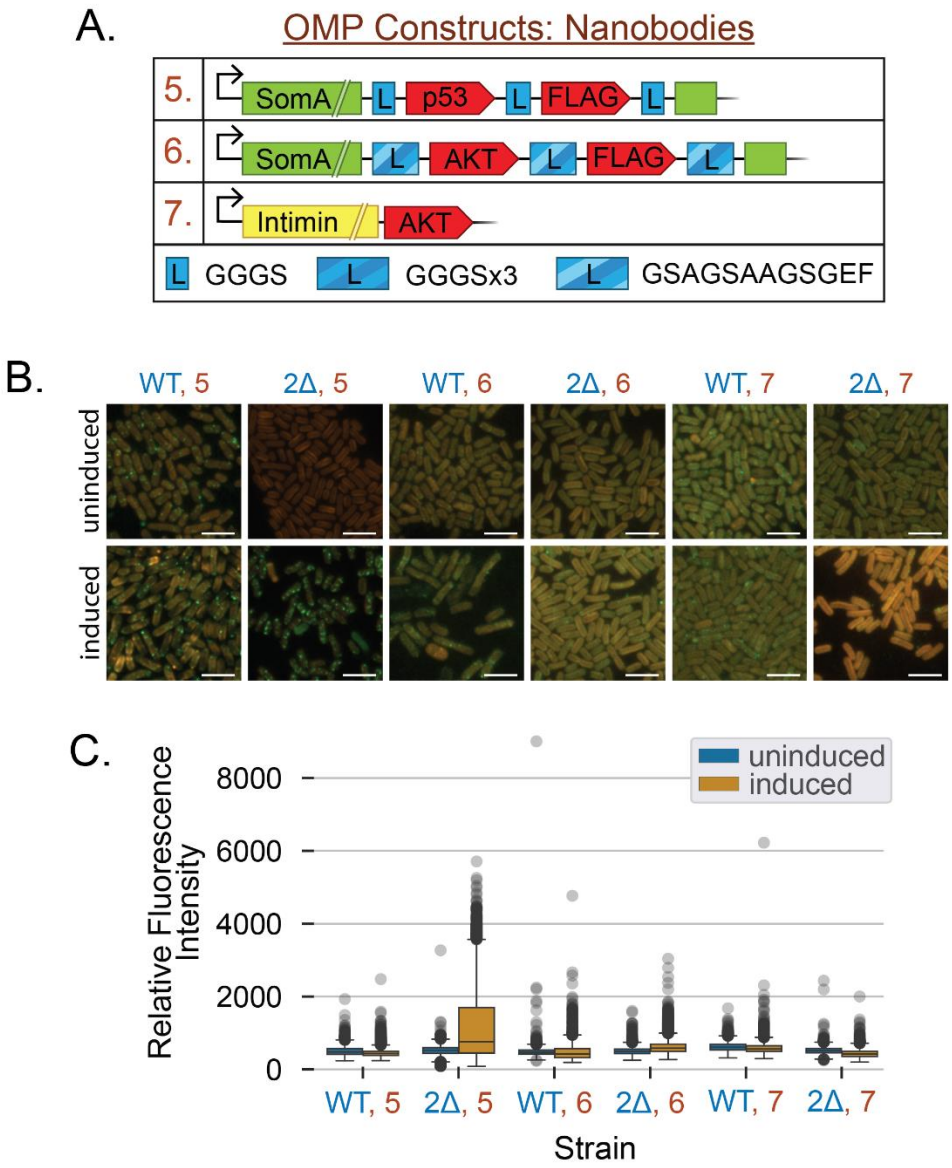

Figure S3.1. Immunofluorescence of fixed cells displaying nanobodies. (A) Table of constructs of SomA and intimin fusion proteins with p53 or AKT bound by various flexible linker types. **(B)** Immunofluorescence of fixed cells labeled with their respective antibodies (α-p53 or α-AKT). All images were taken with the same exposure as the figures in the main body text, but the brightness was adjusted for this figure due to the low fluorescence. The brightness adjustments remain the same for all images in this figure. All scale bars indicate 5 μm. **(C)** The relative fluorescence intensity of each strain and condition. Cells exhibit limited expression and/or mis-localization of expressed proteins. Nanobodies are markedly larger than FLAG (102 residues, p53; 118 residues, AKT; 24 residues, FLAG), suggesting their larger size prevents the protein from properly transporting to the outer-membrane. The best performing construct (construct 5) also had the shortest linkers, which may have aided their transport, but still formed inclusion bodies. Cells expressing intimin (construct 7) showed the least labeling, following the trend supporting poor transport of the heterologous outer-membrane protein.

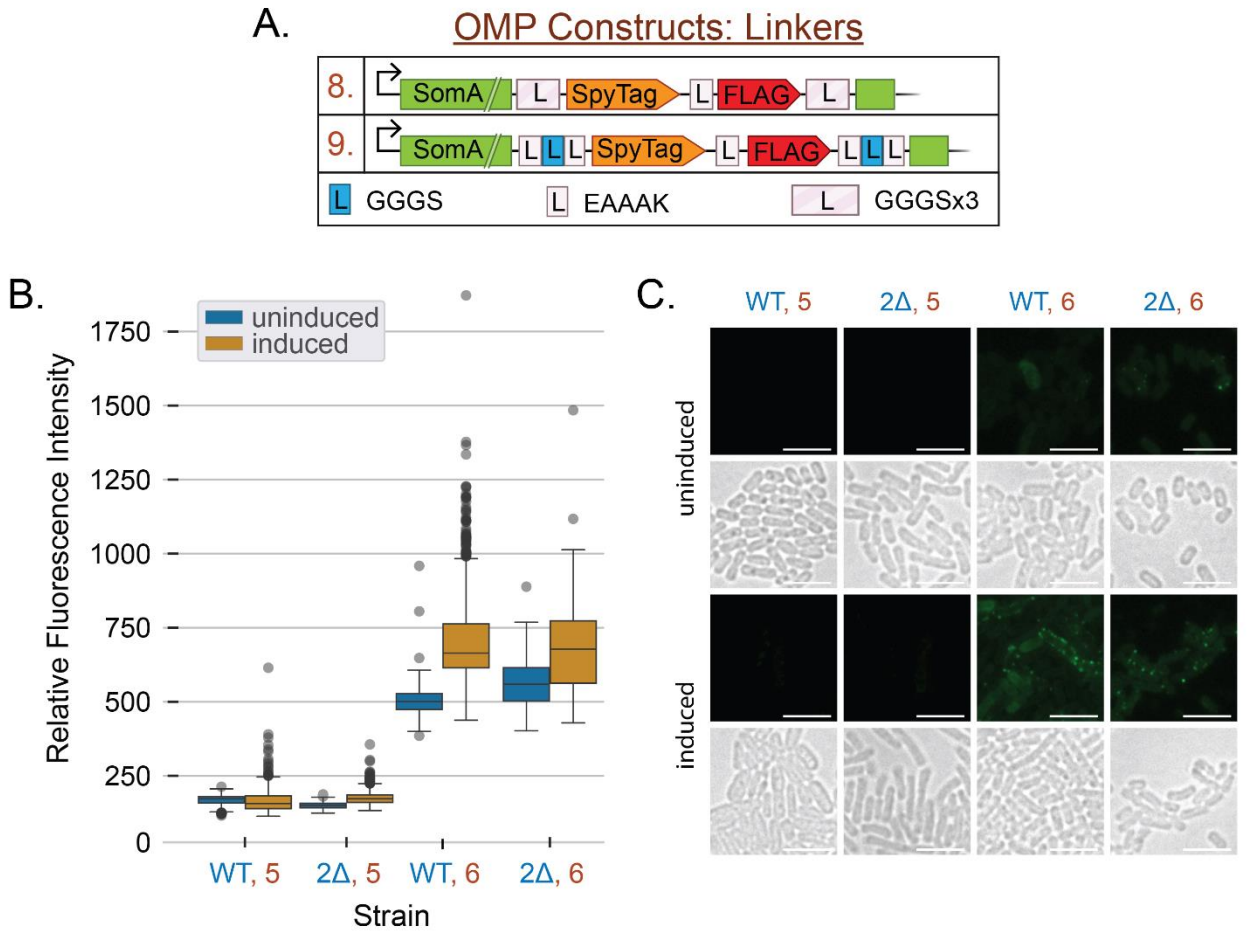

Figure S3.2. Immunofluorescence of fixed cells displaying rigid linkers. (A) Table of constructs of SomA-SpyTag-FLAG fusion proteins bound by all-rigid or rigid-flexible combination linkers. **(B)** Immunofluorescence and brightfield of fixed cells labeled with α-FLAG antibodies. All images were taken with the same exposure as the figures in the main body text, but the brightness was adjusted for this figure due to the low fluorescence. The brightness adjustments remain the same for all images in this figure. All scale bars indicate 5 μm. **(C)** The relative fluorescence intensity of each strain and condition. Cells exhibit limited expression (construct 8) and/or mis-localization of expressed proteins (construct 9). In anticipation of the distance the surface display may need to traverse to be accessible to binding targets, versions of rigid linkers were designed with the reasoning that their stiffness may help extend beyond extracellular polysaccharides that may occlude the cell surface. However, the strains expressing all-rigid linkers (construct 8) exhibit nearly no labeling and strains with combination linkers (construct 9) show partial labeling or inclusion bodies. Rigid linker-containing constructs were also the most difficult to obtain and culture, with many strains failing to be generated. Cells expressing surface display of all types outlined in this work undergo some degree of enlargement in size. Construct 5 in the Δ*wzt*Δ*slpA* background exhibited the most extreme of this phenotype with elongation that, at times, doubled their length **(**C, brightfield**)**. These data suggest that rigid linkers are not compatible with surface display in *S. elongatus* PCC 7942 in the approach undertaken in this dissertation.

CHAPTER 4:

CONCLUDING REMARKS AND FUTURE DIRECTIONS

Overview

With climate change and pollution worsening with current practices, the global economy will need to transition towards sustainable measures. Due to their metabolic flexibility, fast growth, and ability to fix CO_2 using light, non-potable water, and non-agricultural land, cyanobacteria are ideal candidates to contribute to a circular economy. The central theme of my dissertation was related to the capacity of cyanobacteria to produce sucrose as an alternative to terrestrial plant carbon feedstocks, which is economically and chemically expensive to harvest, and competes with resources required to grow food (Graham-Rowe, 2011; Lang et al., 2017). There has been much progress in the decade since the development of sucrose-secreting *Synechococcus elongatus* PCC 7942: the system has been expressed in various strains, has been made inducible without salt stress, and multiple enzymes up- and down-stream of the sucrose biosynthesis pathway have been engineered in an effort to increase productivity. However, there are still more gaps to fill in before cyanobacterial sucrose biosynthesis can reach the theoretical possibility of surpassing plant output. The work in this dissertation includes examples of directions that have not yet been fully tapped into by the broader research community. Genetic manipulation is often the go-to in biotechnology: while such strategies are the cornerstone of the field and will always be important, there are other parameters beyond interrogating metabolic pathways. While the genes (or lack thereof) are required for the production of novel compounds in a more efficient manner, cells are still dependent on the resources they are provided. Without adequate light to power photosynthetic machinery or nutrition to support biomass production, biosynthesis will suffer as cells will prioritize surviving before thriving.

In this dissertation, I explored the impact of light and CO_2 availability and have outlined several findings to improve the production of sucrose-secreting cyanobacteria which can be applied more broadly to bioproductive aquatic photoautotrophs. Photosynthesis, as the name implies, requires light, but I found that currently utilized irradiance (~150 µmol photons m^{-2} s^{-1}) is insufficient in the MC-1000, a bubble-stream style multicultivator. Growth and sucrose production of cultures with a starting density of 0.3 OD_{750} are light-limited until 500 µmol photons m^{-2} s^{-1}, but light intensities beyond this become detrimental (Figure 2.1A), as by Takatani et al., 2015. The difference in sucrose yield between 150 and 500 µmol photons m^{-2} s^{-1} cultures become evident within the first 24 h, suggesting that the higher irradiance is not damaging at a lower OD_{750}. After identifying 250 µmol photons m^{-2} s^{-1} as the optimal irradiance for low-starting density cultures

(0.3 OD_{750}), I transitioned to the HDC, a system consisting of cultivators with a gas permeable bottom and a bicarbonate buffer providing CO_2. The HDC can supply up to 8% CO_2 and showed the MC-1000 was CO_2-limited. Using the same irradiance and BG-11 medium, the HDC yielded 245% higher OD_{750} and 188% more sucrose (Figure 2.2A, B). Interestingly, the data showed that the commonly utilized 2% CO_2 in incubators (*e.g.*, Infors Multitron) is also carbon limiting. Normally, the growth of sucrose secreting strains is lower than those without the metabolic burden of exporting fixed carbon, but this pattern was not observed with the HDC. Furthermore, this indicates that sucrose production does not necessarily have to have a trade-off with growth if there is sufficient carbon to supply both the fixation of sucrose and cellular biomass.

With the increase in light and carbon availability, I was concerned that the standard BG-11 medium was not properly sustaining the stark increases I observed. Indeed, my suspicions were confirmed by replacing BG-11 with CD medium, a more nutrient-dense media recipe designed for high density photoautotrophic growth. The new medium increased sucrose yield by 139%, but also lead to a decrease in growth of induced sucrose-secreting strains, returning to the aforementioned pattern. I postulate this is due to the increased osmotic pressure the medium exerted on the endogenous and heterologous SPS, which is supported by the significant amounts of sucrose produced by strains not induced to export sucrose. Analysis of the proportions of total fixed carbon revealed that the stress response draws away a higher proportion of fixed carbon from growth to sucrose biosynthesis (Figure 2.2A, E). As cultures grow more dense, the light available to the cultures diminish due to self-shading; to address this, I further increased irradiances to 500 µmol photons m^{-2} s^{-1}. I observed another increase in growth and sucrose yield of 173% and 182%, respectively. Interestingly, the differences observed in the MC-1000 were not significant (Figure 2.1A, B), but were so in this instance with the difference being CO_2 availability – perhaps the carbon limitation inhibited the true potential of the tested light intensities. I revisited the idea of utilizing irradiances much higher than optimal for *S. elongatus* PCC 7942. Previously, I interrogated if high irradiances that may be damaging at low-starting densities may be beneficial for high-starting density cultures. However, after cultivating cultures of 1.5 and 2.0 OD_{750} with 2000 and 2500 µmol photons m^{-2} s^{-1}, I found that the growth of these cultures was not sustainable and sucrose titer was not improved relative to low-starting cultures (Figure 2.1C, D). This may have been because overnight cultures were concentrated to the desired OD_{750}. While experiments began with fresh media, the cells were “older”, and I have consistently observed sucrose

productivity decline with time. So, for my next foray into high light and high density, I began with a low-starting density of 0.3 OD_{750} with 500 µmol photons m^{-2} s^{-1} and increased the light intensity to 1000 µmol photons m^{-2} s^{-1} at 48 h once the cultures were on average 2.3 OD_{750}. Although 1000 µmol photons m^{-2} s^{-1} is considered to be detrimental to *S. elongatus* PCC 7942, it increased growth by 17% and sucrose titer by 15% in sucrose exporting strains (Figure 2.3 C, D). Additionally, uninduced strains produced 126% more sucrose in this condition than sucrose-exporting strains grown with 250 µmol photons m^{-2} s^{-1} – albeit with 618% higher OD_{750}. Unlike many genetic engineering attempts to increase sucrose production, enhancing light, CO_2, and nutrition increases sucrose titers without sacrificing cell health. In the end, our highest productivity was 47.8 mg L^{-1} h^{-1}; for reference, the highest productivity of *S. elongatus* PCC 7942 was achieved by a strain that forwent growth entirely to devote all fixed carbon had a productivity of 48 mg L^{-1} h^{-1} (Abramson et al., 2018). Previous attempts to improve sucrose yield relied heavily on genetic modification to increase the carbon flux towards sucrose, but this strategy came with the price of cell health. In the work outlined above, the cells remained resilient throughout: growth and sucrose continued to climb, despite prolonged incubation periods, high density, and high light. Interrogating long-standing common growth conditions is a promising avenue to improve the bioproductivity of existing strains while maintaining fitness, which will be required for cyanobacteria biotechnology to be commercially viable.

Of the many steps that are being taken to bridge the distance between lab research and "real-world" application are attempts to reduce the cost of harvesting biomass by eliminating extraneous costs and to improve productivity by utilizing co-cultures – both of which can be aided by the development of direct cyanobacterial surface display. For example, the cost of biomass harvesting can account for 20-30% of total costs when employing traditional methods (Christenson and Sims, 2011). Inducible intercellular adhesion could allow cyanobacteria to create flocs without the added costs or risks associated with added chemicals or centrifugation, while being more reliable than natural methods such as gravity sedimentation (Christenson and Sims, 2011). On another note, the use of engineered co-cultures are gaining traction as photoautotrophs can directly provide for the carbon requirements of bioproductive heterotrophs. Moreover, these engineered co-cultures show improved yields relative to their axenic counterparts (Cooper and Smith, 2015; Fedeson and Ducat, 2021). However, these novel systems do not have the advantage of shared evolutionary time (*i.e.*, most co-cultures characterized to date are from species that have not co-

evolved in a natural context), and are relatively unstable and difficult to maintain. Naturally occurring microbial communities often rely on spatial structure (*e.g.*, biofilms) (Flemming et al., 2016; Nadell et al., 2016), and experiments have revealed that this can also help stabilize engineered co-cultures. Microfluidic devices (Kim et al., 2008; Gupta et al., 2020), agar (Pande et al., 2016), and hydrogels (Smith and Francis, 2017) have been employed thus far with success, but these are limited to small-scale applications. Flocs created by intercellular adhesion can introduce spatial structure while still being in liquid culture, and thus be scalable. Previous works in cyanobacteria have engineered pili in *Synechocystis* sp. PCC 6803 (Cengic et al., 2018) and a porin in *S. elongatus* PCC 7942 (Fedeson and Ducat, 2017) with some success.

The work discussed in this dissertation continues to develop the porin, SomA, as well as utilizing a heterologous outer-membrane protein, intimin. The previous iteration of SomA for surface display required a mediating protein to assist in binding – likely due to occluding factors on the cell surface (Fedeson and Ducat, 2017). Anticipating the distance that may be required to bridge surface displayed components (FLAG, SpyTag, p-53) and targets of interest, I engineered linkers of various types and lengths in between SomA and adhesin domains (Figure 3.1). Likewise, intimin was employed due to its natural function of intercellular binding in *Escherichia coli* and a nanobody library developed for surface display (Glass and Riedel-Kruse, 2018). Our findings with immunofluorescence with α-FLAG initially agreed those outlined in Fedeson and Ducat (2017), that strains with genetically removed outer-membrane proteins (*e.g.*, *slpA*, *wzt*) had greater binding (Figure 3.2A), though my strains exhibited greater heterogeneity within the population. Additionally, I found that a shorter, flexible linker sequence (GGGSx3) performed better than strains with long flexible linkers (GSAGSAAGSGEF), which may be excessive rather than useful in traversing the outer-membrane. Due to the possibility of the epitopes cleaving away from the cell due to the introduced linkers, I performed an extended incubation with α-SpyTag to confirm both domains were available, which further validated my previous observations (Figure 3.2B). After confirming the presence and proper transport of the adhesins to the cell surface, I evaluated the accessibility of these functionalizing tags through the use of a protein co-localization study of surface displayed SpyTag to soluble SpyCatcher-mNG. The overall relative fluorescence intensities of all strains were markedly reduced compared to when strains were tagged with an antibody, and the penetrance remained low throughout the population (Figure 3.4). Intimin proteins did not fare better; rather, we observed inclusion body-like labeling suggesting that the

proteins did not transport to the outer-membrane properly (Figure 3.5). Clearly, more research is required to understand the environment of the *S. elongatus* PCC 7942 outer-membrane, and how to transport heterologous proteins to the outer-membrane if interest regarding intimin continues.

Future outlook and perspectives

Genetic engineering first drew me into the field of biotechnology – it is remarkable that we can introduce heterologous, modified, or even entirely novel genes to gain new functions. I was truly inspired by the microbial synthesis of bioplastics and biofuels as an impressionable undergraduate student. They still are incredible feats that open doors to what the future could be, but I have since learned to read more carefully and think more skeptically. Now, I seek less novelty and more applicability. *How* can we bring these advancements to the broader public? We must make them scalable, affordable, and accessible to replace the products that contribute to climate change and pollution. For this reason, I devoted my graduate career in search of how to make that possible, rather than the metabolic engineering I initially thought I would pursue. In the past six years of this journey, I have learned from personal experience that nothing in science is easy without luck, and that much of lab research has not transitioned into industry, not for a lack of effort. Still, I am not without hope. There is still so much to try and to learn from, which is an iterative process that forever betters itself, and that is what has kept me in science.

Regarding cyanobacterial biotechnology, I would like to see variations of my research topics to continue, though I admit I am biased. The idea of creating surface display for direct adhesion in cyanobacteria really stuck to me. My initial hopes were to create flocs in culture to use as a platform to investigate the impact of spatial structuring in safeguarding engineered mutualistic interactions, namely from "cheaters" which could easily arise in commercial applications by way of mutation or contamination. In the example outlined in Figure 4.1, *S. elongatus* PCC 7942 provides sucrose to the mutualistic *E. coli* in exchange for β-lactamase, which detoxifies the antibiotic in the medium. However, there is a low concentration of cheaters that benefit from the exchanged goods without bearing the metabolic burden of mutual contribution. This affords the cheater an advantage to out-grow the mutualistic bacteria (Figure 4.1B), rendering bioproductive cultures (axenic and co-cultures) useless. If mutualistic partners aggregate, the secreted public goods could localize to the floc, increasing their concentrations, thus improving the growth of the partners while effectively starving out the excluded cheater (Figure 4.1C). This approach could be a method to combat contaminants, but cheaters would also arise from *E. coli* losing the capacity

to provide β-lactamase while in the floc. In that case, the cheater would benefit from the localization of public goods and outgrow the mutualistic partners, but at its own demise because the cheater is dependent on both contributors to survive (Figure 4.1D). This could potentially lead to an interesting phenomenon called the Simpson's paradox in which the local population (*i.e.*, the aggregate) will be dominated by the cheater, but the global population (*i.e.*, the culture) will contain greater populations of the mutualistic partners. Individual flocs may be quickly overrun by cheaters, but they cannot continue to do so without the support of the mutualists it out-grew, keeping them relatively static, while flocs containing a majority of partners will continue to thrive. However, this is hypothetical. An ideal antibiotic concentration would be to only attenuate the growth of *S. elongatus* PCC 7942, but initial antibiotic screening with 15 different concentrations of chloramphenicol and hygromycin showed nearly binary responses: death or normal growth. For cellular aggregates to be used as a platform to study the stabilizing effects of spatial structuring, at

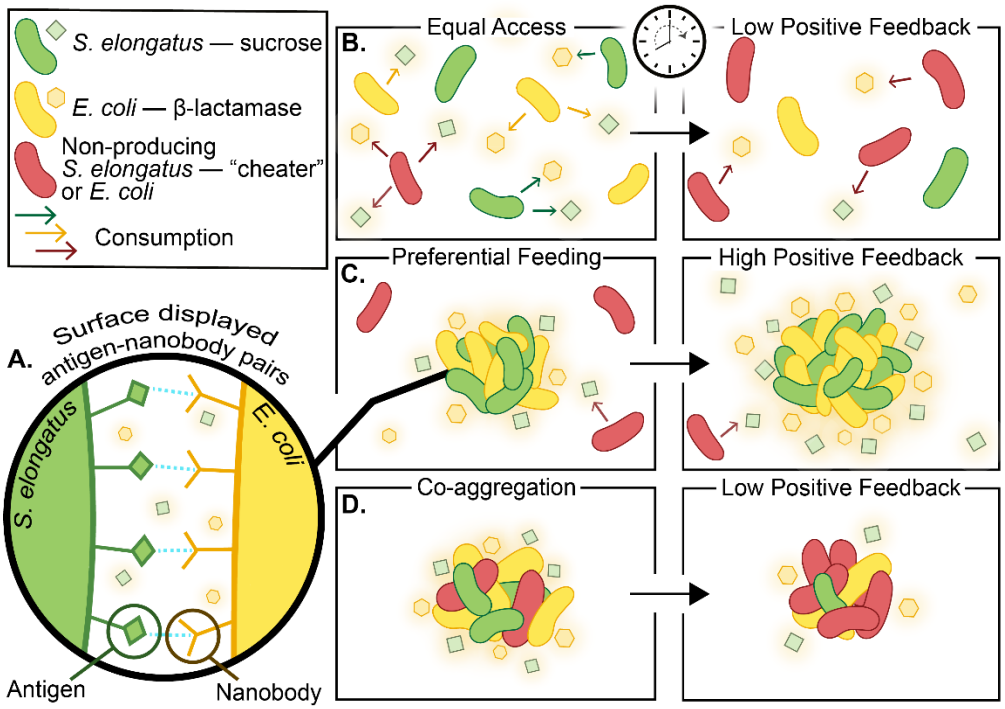

Figure 4.1. Co-culture of planktonic and attached *S. elongatus* PCC 7942 and *E. coli*. Cyanobacteria providing sucrose (green) in exchange for β-lactamase (yellow) from *E. coli* in the presence of a cheater (red) over time. **(A)** Surface display of an antigen-nanobody pair and localized metabolites. **(B)** A planktonic co-culture of collaborators and low concentration of cheaters that overrun the population. **(C)** Aggregated cooperators that exclude cheaters. **(D)** Co-aggregation of cooperators and cheaters.

least two obstacles must be overcome: 1) surface display in cyanobacteria and their heterotrophic partners need to be developed for specific intercellular adhesion; 2) a public good that is similarly detrimental to both the cyanobacteria and the cheater heterotroph needs to be identified. While the approach I outlined here for surface display was not successful, there have been at least two successful examples (Cengic et al., 2018; Lin et al., 2020), but have not been utilized for inter-species bindings. Some cyanobacteria, like *S. elongatus* PCC 7942, express S-layer proteins that could be engineered for surface display, but I am concerned about the extracellular polysaccharides and other occluding factors on the outer-membrane that may inhibit accessibility. There is limited literature characterizing the outer-membrane as most interest in cyanobacterial membranes often falls to those implicated in photosynthesis. Identifying a factor that is equally (or similarly) detrimental and recoverable to cyanobacteria and heterotrophs could prove difficult, but not impossible. From personal experience, *S. elongatus* PCC 7942 is more sensitive to antibiotics and environmental conditions than *E. coli*; a less robust heterotroph may need to be identified instead.

One of the reasons engineered microbial communities first began to gain traction was due to their simplicity relative to their natural counterparts, but our brief venture through their construction has revealed their own complexities. Even between only two species, there is much to understand and optimize as we take on the role evolution once played (though directed evolution is still an option). Still, I believe this is well worth the effort. The seemingly simple aggregation of bioproductive partners opens so many opportunities. Utilizing it as a platform to understand the rise of emergent properties (*e.g.*, robustness, division of labor) can not only guide engineering efforts to create more resilient co-cultures, but to also de-establish undesirable microbial communities for medical, commercial, and ecological applications.

Cyanobacteria have transformed the Earth to the lush and bountiful planet we know today, and with their help, we may be able to maintain it. The field of cyanobacteria is growing in every direction: ecology, genomics, biomedicine, biofuel, bioenergy, and endlessly more. In 1980, there were only 237 papers regarding cyanobacteria, but the numbers have jumped to 1634, 1584, and 1600 in 2016, 2017, and 2018, respectively (Konur, 2019). It is truly exciting to see the progress cyanobacterial research has made in the past decade.

REFERENCES

Abramson, B. W., Lensmire, J., Lin, Y. T., Jennings, E., and Ducat, D. C. (2018). Redirecting carbon to bioproduction via a growth arrest switch in a sucrose-secreting cyanobacterium. *Algal Res.* 33, 248–255. doi: 10.1016/j.algal.2018.05.013

Cengic, I., Uhlén, M., and Hudson, E. P. (2018). Surface display of small affinity proteins on *Synechocystis* sp. strain PCC 6803 mediated by fusion to the major type IV pilin PilA1. *J. Bacteriol.* 200, 10.1128/jb.00270-18. doi: 10.1128/jb.00270-18

Christenson, L., and Sims, R. (2011). Production and harvesting of microalgae for wastewater treatment, biofuels, and bioproducts. *Biotechnol. Adv.* 29, 686–702. doi: 10.1016/j.biotechadv.2011.05.015

Cooper, M. B., and Smith, A. G. (2015). Exploring mutualistic interactions between microalgae and bacteria in the omics age. *Curr. Opin. Plant Biol.* 26, 147–153. doi: 10.1016/j.pbi.2015.07.003

Fedeson, D. T., and Ducat, D. C. (2017). Cyanobacterial Surface Display System Mediates Engineered Interspecies and Abiotic Binding. *ACS Synth. Biol.* 6, 367–374. doi: 10.1021/acssynbio.6b00254

Fedeson, D. T., and Ducat, D. C. (2021). "Symbiotic Interactions of Phototrophic Microbes: Engineering Synthetic Consortia for Biotechnology," in *Role of Microbial Communities for Sustainability*, eds. G. Seneviratne and J. S. Zavahir (Singapore: Springer), 37–62. doi: 10.1007/978-981-15-9912-5_2

Flemming, H. C., Wingender, J., Szewzyk, U., Steinberg, P., Rice, S. A., and Kjelleberg, S. (2016). Biofilms: An emergent form of bacterial life. *Nat. Rev. Microbiol.* 14, 563–575. doi: 10.1038/nrmicro.2016.94

Glass, D. S., and Riedel-Kruse, I. H. (2018). A Synthetic bacterial cell-cell adhesion toolbox for programming multicellular morphologies and patterns. *Cell* 174, 649-658.e16. doi: 10.1016/j.cell.2018.06.041

Graham-Rowe, D. (2011). Agriculture: Beyond food versus fuel. *Nature* 474, S6–S8. doi: 10.1038/474S06a

Gupta, S., Ross, T. D., Gomez, M. M., Grant, J. L., Romero, P. A., and Venturelli, O. S. (2020). Investigating the dynamics of microbial consortia in spatially structured environments. *Nat. Commun.* 11. doi: 10.1038/s41467-020-16200-0

Kim, H. J., Boedicker, J. Q., Choi, J. W., and Ismagilov, R. F. (2008). Defined spatial structure stabilizes a synthetic multispecies bacterial community.

Konur, O. (2019). "Cyanobacterial bioenergy and biofuels science and technology: a scientometric overview," in *Cyanobacteria*, eds. A. K. Mishra, D. N. Tiwari, and A. N. Rai (Academic Press), 419–442. doi: 10.1016/B978-0-12-814667-5.00021-0

Lang, T., Schoen, V., Hashem, K., McDonald, L., Parker, J., and Savelyeva, A. (2017). "The Environmental, Social, and Market Sustainability of sugar," in *Advances in Food Security and Sustainability*, ed. D. Barling (Elsevier), 115–136. doi: 10.1016/bs.af2s.2017.09.002

Lin, T. Y., Wen, R. C., Shen, C. R., and Tsai, S. L. (2020). Biotransformation of 5-hydroxymethylfurfural to 2,5-furandicarboxylic acid by a syntrophic consortium of engineered *Synechococcus elongatus* and *Pseudomonas putida*. *Biotechnol J* 15, e1900357. doi: 10.1002/biot.201900357

Nadell, C. D., Drescher, K., and Foster, K. R. (2016). Spatial structure, cooperation and competition in biofilms. *Nat. Publ. Group* 14. doi: 10.1038/nrmicro2016.84

Pande, S., Kaftan, F., Lang, S., Svato, A., Germerodt, S., and Kost, C. (2016). Privatization of cooperative benefits stabilizes mutualistic cross-feeding interactions in spatially structured environments. *ISME J.* 10, 1413–1423. doi: 10.1038/ismej.2015.212

Smith, M. J., and Francis, M. B. (2017). Improving metabolite production in microbial co-cultures using a spatially constrained hydrogel. *Biotechnol Bioeng* 114, 1195–1200. doi: 10.1002/bit.26235

Takatani, N., Use, K., Kato, A., Ikeda, K., Kojima, K., Aichi, M., et al. (2015). Essential role of Acyl-ACP synthetase in acclimation of the cyanobacterium *Synechococcus elongatus* strain PCC 7942 to high-light conditions. *Plant Cell Physiol.* 56, 1608–1615. doi: 10.1093/pcp/pcv086